University of Windsor

[Scholarship at UWindsor](#)

1976

Analysis of ECG data, for data compression.

Mark Frederick. Stevens
University of Windsor

Follow this and additional works at: https://scholar.uwindsor.ca/etd

INFORMATION TO USERS

THIS DISSERTATION HAS BEEN
MICROFILMED EXACTLY AS RECEIVED

This copy was produced from a micro-
fiche copy of the original document.
The quality of the copy is heavily
dependent upon the quality of the
original thesis submitted for
microfilming. Every effort has
been made to ensure the highest
quality of reproduction possible.

PLEASE NOTE: Some pages may have
indistinct print. Filmed as
received.

Canadian Theses Division
Cataloguing Branch
National Library of Canada
Ottawa, Canada   K1A ON4

-AVIS AUX USAGERS

LA THESE A ETE MICROFILMEE
TELLE QUE NOUS L'AVONS RECUE

Cette copie a été faite à partir
d'une microfiche du document
original. La qualité de la copie
dépend grandement de la qualité
de la thèse soumise pour le
microfilmage. Nous avons tout
fait pour assurer une qualité
supérieure de reproduction.

NOTA BENE: La qualité d'impression
de certaines pages peut laisser à
désirer. Microfilmée telle que
nous l'avons reçue.

Division des thèses canadiennes
Direction du catalogage
Bibliothèque nationale du Canada
Ottawa, Canada   K1A ON4

,ANALYSIS OF ECG DATA, FOR DATA COMPRESSION

by

Mark Frederick Stevens

A Thesis
submitted to the Faculty of Graduate Studies
through the Department of
Electrical Engineering in Partial Fulfillment
of the requirements for the Degree
of Master of Applied Science at
The University of Windsor

Windsor, Ontario, Canada

1976

ABSTRACT

ANALYSIS OF ECG DATA, FOR DATA COMPRESSION

by

Mark Frederick Stevens

In this thesis the effects of quantization on
ECG data are analyzed, and techniques to improve data
reduction over those obtainable by direct quantization
are discussed. Basically, three data reduction techniques,
linear prediction, with differential pulse code modulation,
spectral analysis and slope change detection, are considered
and a relative assessment of their performance is presented.
The results of the investigation reveal that a reduction of
3:1 is obtainable if a slope change detection technique is
applied to prefiltered ECG data. This claim is based on
the number of bits/samples required for the slope technique
as compared to the number of bits/sample required when ECG
data is directly quantized. The maximum mean squared and
peak error in the reconstructed signals were 1% and 5%,
respectively.

ACKNOWLEDGEMENTS

At this time I would like to acknowledge with gratitude, the advice and guidance given me by my advisor Dr. M. Shridhar. I would also like to extend my thanks to the other faculty members and fellow graduate students who I confided in for advice pertaining to this research project.

I am also indebted to my wife Susan for her moral support and understanding during the course of this work.

I would like to acknowledge the financial support afforded me in the form of a scholarship by The National Research Council of Canada.

TABLE OF CONTENTS

TABLE OF CONTENTS cont'd

LIST OF TABLES

LIST OF FIGURES

LIST OF FIGURES cont'd

LIST OF FIGURES cont'd

CHAPTER I

INTRODUCTION

1.1 INTRODUCTION OF TOPIC

The number of electrocardiograms (ECG's) taken yearly has sharply increased, with the occurrence of more and more deaths due to heart disease. At one time, heart disease was mainly confined to the aged, and anyone under fifty years of age was not very aware of the problem. But today heart conditions of all kinds, are developing in middle age and young people at an ever increasing rate. Because of this fact, there is a growing concern for this problem among all age groups. Therefore, more and more people are having ECG's taken as part of a regular physical examination. This amounts to millions of ECG's taken yearly in Canada alone, thus putting a heavy burden on our physicians and cardiologists, who have to diagnose these ECG's by manual means.

Not long after the advent of digital computers, man began working towards automatic systems of monitoring, acquisition, storage and, in some cases, diagnosis of ECG information, using these digital machines. The work was started in the mid 1950's by people like Dr. H.V. Pipberger, Dr. E. Frank and Dr. O.H. Schmitt, who felt that digital computers could be used effectively to perform many of the tedious tasks involved with mass ECG analysis. It was felt that automatic systems would

1

have advantages over the conventional manual means. Some
of these are:

1. By combining the experience of top cardiac
specialists, one should be able to come up with a diagnos-
tic algorithm which can surpass the diagnostic speed,
accuracy and consistency of one cardiologist.

2. A computer can be used to continually monitor
coronary care patients that need around-the-clock
monitoring. While a human observer might miss a short
term cardiac phenomenon, or the start of a serious cardiac
condition, the computer would detect these sudden changes
and alarm an attendant and possibly store the abnormal
waveforms for later analysis by a cardiologist.

3. The computer would facilitate the retreival
of ECG data from various sources so that past and present
waveforms could be compared more effectively.

4. The speed of the computer would allow mass
ECG screening so that everyone could have ECG's taken
regularly, without overburdening the physicians.

5. ECG transmission over telephone lines could
be implemented so that heart patients can literally phone
in their ECG from any available telephone receiver, with
the appropriate equipment.
These are just a few of the areas in which computers can
be used to facilitate tedious duties and, in some cases,
accomplish duties that could not be handled by manual
methods in the past.

The first automatic system of ECG analysis was presented at a Conference in 1959, by Dr. H.V. Pipberger. The system made use of an analog-to-digital (A/D) convertor and a small digital computer, programmed to perform some fundamental ECG analysis. Later between 1960-61 Dr. Pipberger and associates developed a program for automatic waveform recognition which proved to be the basis for just about all the automatic ECG analysis programs up until now.

During the 1960's and the first part of the 1970's, a lot of research has been going on to develop better systems for automatic ECG analysis. Today there are a variety of systems in use and some of these are discussed by Chr. Zywietz and B. Schneider[1]. Even though these systems are in use today, the general consensus is that none of the existing systems are good enough and further research is needed to make these systems more reliable and less expensive.

Now, in order to keep the costs of these automatic ECG analysis systems down, one must find an efficient means of representing the ECG data in the digital machine. Normally these analog ECG signals are sampled, using an analog-to-digital convertor, and therefore, are represented by a set of discrete numbers, which sequentially vary with the magnitude of the original analog signal. Thus, if the sampling rate is 500 Hz then there will be 500 numbers representing every second of ECG data. Since a complete

ECG analysis makes use of twelve different ECG waveforms, recorded for possibly 5 to 10 seconds each, then the computer storage requirements will be large, if the ECG data is kept in its sampled form. Now by applying data reduction techniques to this data, one can come up with an ECG representation which significantly reduces the storage requirements, while maintaining an acceptable degree of fidelity in the representation. Thus, a reduction in data will mean savings in computer storage, thus reducing the cost of the system.

1.2.i PHYSIOLOGY OF THE HEART

The circulatory system is designed to deliver blood to and from the capillaries, where the blood gives up its oxygen and takes in carbon dioxide and other waste products. The centre of the circulatory system is the heart, a hollow, muscular contractile organ. The main function of the heart is to pump blood continuously throughout the body in a closed loop of vessels.

Figure 1 shows the main parts of the heart. The deoxygenated blood enters the right ventricle from the right atrium and the right ventricle in turn pumps the blood via the pulmonary arteries to the lungs. At the lungs the blood is oxygenated, the carbon dioxide is taken out and then the blood is returned to the left atrium via the pulmonary veins. The blood is then pumped into the left ventricle from the left atrium. From here
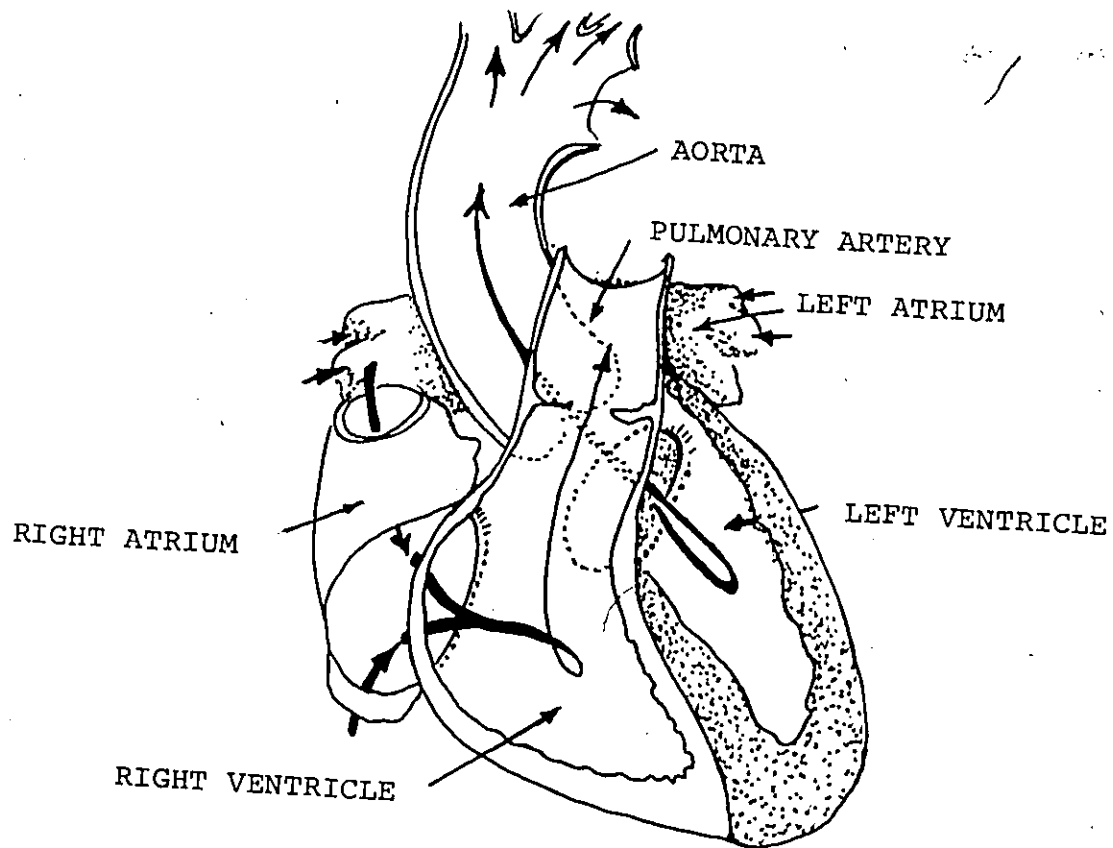
Figure 1. The Heart

the left ventricle pumps the oxygenated blood into the aortia artery, which in turn carries this oxygenated blood to all parts of the body through a complex artery system. After nuturing the body cells and picking up the carbon dioxide, the blood again returns to the right atrium and one cycle is complete. This cycle is repeated 60 to 120 times per minute throughout one's whole lifetime.

Stimulation of the heart is accomplished by electrical changes which spread throughout the heart and cause it to contract. Under rest conditions the heart cells are polarized, but when a proper electrical stimulus is applied the cells depolarize causing the muscle fibres to contract. Systole is the contraction of muscles of either the atriums or ventricles, to expel the blood from these chambers. Diastole is when a chamber is refilling with blood. While the ventricles are in systole the atriums are in diastole and vice versa.

All cardiac tissue has the property of rhythmicity (the ability to initiate its own beat). There is a specialized region of cells which exhibit the highest order of rhythmicity; this region is called the sinoatrial or sinus node. This node is the natural pace-maker of the heart, but other regions of the heart, or ectopic pacemakers, can initialize the beat under adverse heart conditions. In descending order of rhythmicity, the atrioventricular node, atriac myocardium, and the ventricular myocardium may serve as ectopic pacemakers.

The rate of depolarization of the ectopic pacemakers is slower than that of the sinus node, therefore, in order for them to become pacemakers 1) their own rythmicity must be enhanced, 2) the rythmicity of the higher order pacemakers must be depressed or, 3) all conduction pathways between the ectopic focus and those regions with higher degree of rythmicity become blocked. Thus, under normal conditions the sinus node initializes the depolarization of the heart muscle. Since the sinus node is located in the right atrium the depolarization spreads through the atriums first, then it proceeds to the ventricles so that one cardiac cycle is complete.

These electrical forces are conducted throughout the whole body and can be detected and recorded by the electrocardiograph machine. The shape and timing of the waveform being recorded depends on the anatomic make up of the structures being stimulated, the speed of conduction of the impulses through these structures, and the position of the electrodes in relation to the portions being activated. In the next section the electrocardiogram will be discussed from the standpoint of lead placement, diagnostic value and the physiological phenomena responsible for the deflections and intervals of the ECG tracing.

1.2.ii ELECTROCARDIOGRAM

Basically, an electrocardiogram is a plot, with time, of the differences of potential between pairs of points on the external surface of the body or between specific skin loci and a reference electrode. The standard electrocardiogram is made up of twelve waveforms using different lead configurations for each. Tables 1 and 2 list the six limb leads and six chest leads respectively, along with the electrodes used and potentials measured for each lead configuration.

TABLE 1

LEAD		POTENTIAL MEASURED	ELECTRODES USED FOR POTENTIAL MEASUREMENT	
I	(1)	left shoulder	(1)	left arm electrode
	(2)	right shoulder	(2)	right arm electrode
II	(1)	groin	(1)	average potential of R + L leg electrodes
	(2)	right shoulder	(2)	right arm electrode
III	(1)	groin	(1)	average potential of R + L leg electrodes
	(2)	left shoulder	(2)	left arm electrode
aVR	(1)	right shoulder	(1)	right arm electrodes
	(2)	lateral left lower rib cage	(2)	average potential of L leg + L arm electrodes
aVL	(1)	left shoulder	(1)	left arm electrode
	(2)	lateral right lower rib cage	(2)	average potential of R leg + R arm electrodes
aVF	(1)	groin	(1)	average potential of R + L leg electrodes
	(2)	neck	(2)	average potential of R + L arm electrodes

Limb (Frontal) Leads.

TABLE 2

LEAD	POSITION OF CHEST WALL ELECTRODES	VENTRICLE(S) USUALLY FACING THIS ELECTRODE
V1	4th right intercostal space at the right sternal border	right ventricle
V2	4th left intercostal space at the left sternal border	right ventricle
V3	5th left intercostal space between electrodes of V2 and V4	right ventricle (left ventricle)
V4	5th left intercostal space at the midclavicular line	left ventricle (right ventricle)
V5	5th intercostal space at anterior axillary line	left ventricle
V6	5th intercostal space at midaxillary line	left ventricle

Chest Leads.

Figure 2 shows the positive axis directions of the limb leads while Figure 3 shows the position of the chest lead electrodes. At any instant of time only one lead potential is being measured, therefore, there is no time relation between the different leads. Thus these are sometimes referred to as scalar leads since each lead represents the potential change in one direction only.

Figure 4 shows a typical lead II ECG with the important waves and intervals labelled. The heart depolarization is initiated by the sinus node in the upper left atrium so the P wave represents the depolarization spread through the atriums.
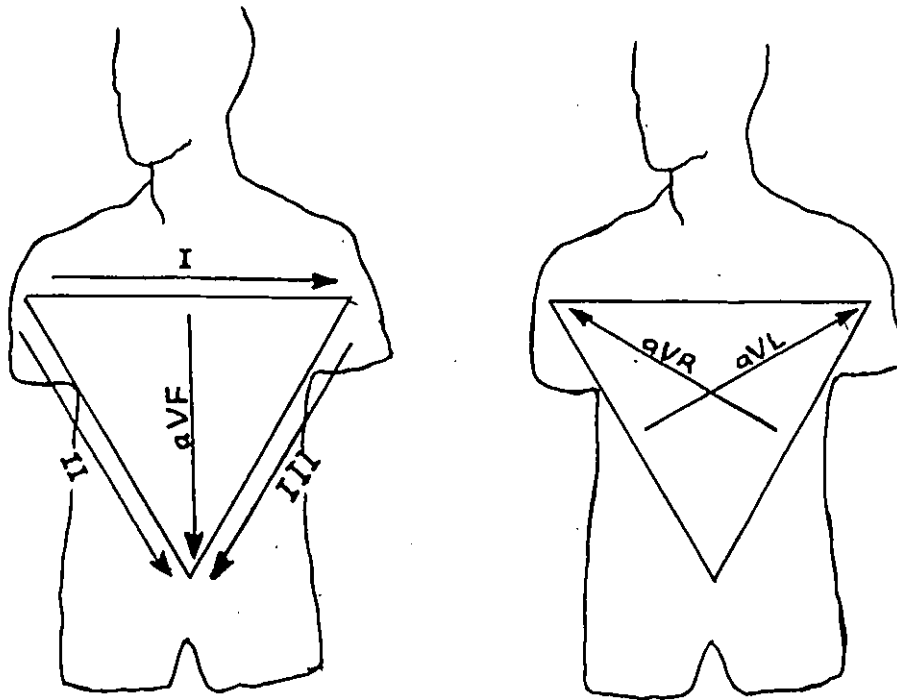
Figure 2. Positive axis directions of the limb (frontal)
leads
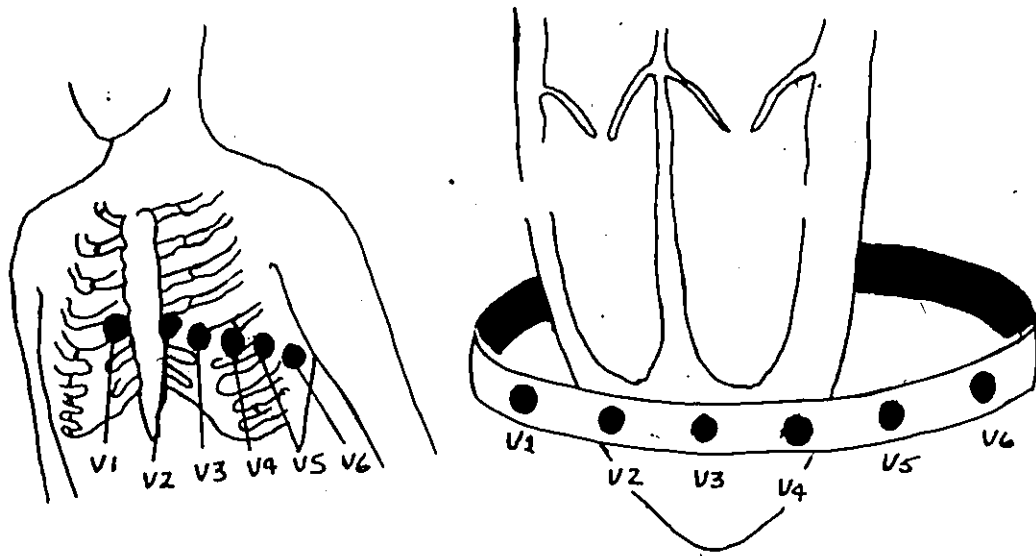
Figure 3. Position of chest lead electrodes
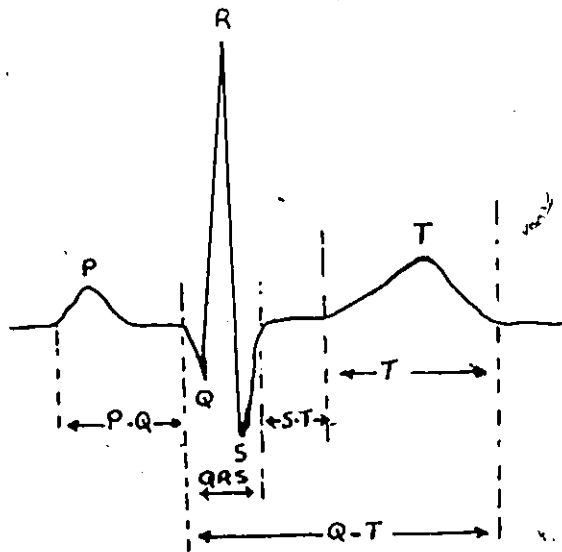
Figure 4. Lead II ECG signal.

The QRS waves represent two phenomena that normally occur during the same time span, these being the depolarization of the ventricles along with the repolarization of the atriums. The T-wave is caused by the repolarization process in the ventricles. The P-R interval is the time between the start of the depolarization of the atriums and the start of depolarization of the ventricles. This duration is usually between 0.12 to 0.20 seconds in a normal heart. The QRS interval is usually about 0.06 to 0.10 seconds and it represents the total time for depolarization of the ventricles. The S-T interval is the time between the depolarization and repolarization of the ventricles. This interval is felt to have no clinical significance. The Q-T interval is the period of electrical systole of the ventricles. Its duration is about 0.4 seconds, but varies inversely with the heart rate. The T duration is simply the time for ventricular repolarization.

By analyzing the details of these waveforms a cardiologist gains valuable insight concerning, 1) the anatomical orientation of the heart, 2) the relative size of the chambers, 3) a variety of disturbances of rhythm and of conduction, 4) the extent, location and progress of ischemic damage of the myocardium, 5) the effects of altering electrolyte concentrations, and 6) the influence of certain drugs (notably digitalis and its derivatives). .

A code known as the Minnesota Code was developed in the late 1950's to make ECG diagnosis systematic. The Minnesota Code gives a step-by-step method of checking the ECG's characteristics, to come up with consistent ECG evaluations. The author has included a copy of this code in Appendix A, to give the reader an idea of the complexity of manual ECG analysis.

1.3 LITERATURE SURVEY

Up until now the data reduction techniques that have been applied to ECG data, can be divided into three main categories, parameter extraction, transformation and direct data techniques. In the past, the parameter extraction techniques have been the most popular since the resultant parameters can be used directly in many automatic diagnostic schemes. The main disadvantage of this method is that the original signal cannot be reconstructed from the extracted parameters. Recently, authors have taken a close look at the transformation and direct data methods. These two techniques have the advantage that the original waveform can be reconstructed using the parameters of the model. C.A. Andrews, J.M. Davies and G.R. Schwarz[2] wrote a paper on data compression which outlines many of the traditional methods of data compression. They concluded that the direct data methods gave the best overall results of the techniques investigated. An ECG signal was used for the

reproduction comparisons.

1.3.i PARAMETER EXTRACTION TECHNIQUES[3][4]

The parameter extraction technique has been widely used in the area of automatic ECG analysis, for classification of different ECG waveforms. Basically, this technique attempts to extract a set of parameters which, in general, describe the ECG waveform. These parameters are made up of amplitudes, intervals, maximum slopes, phases, and a variety of other characteristics of the signal. In essence, the technique attempts to mimic the cardiologist in that it picks out those characteristics of the signal that are of diagnostic value. Figure 5 shows an ECG signal which is labelled to show some of the important parameters of the ECG signal. The subscript p stands for a peak amplitude, d stands for wave duration, a dot ($\cdot$) stands for the derivative or slope, while consecutive capital letters represent intervals. Some designers have used as many as 300 features to describe the ECG signals. The main difficulty with this sort of technique is in the actual extraction of these parameters. In practice the ECG waveforms have an infinite number of variations when talking about both normal and abnormal tracings. Because of this a lot of research has been carried out to develop reliable feature extraction routines.
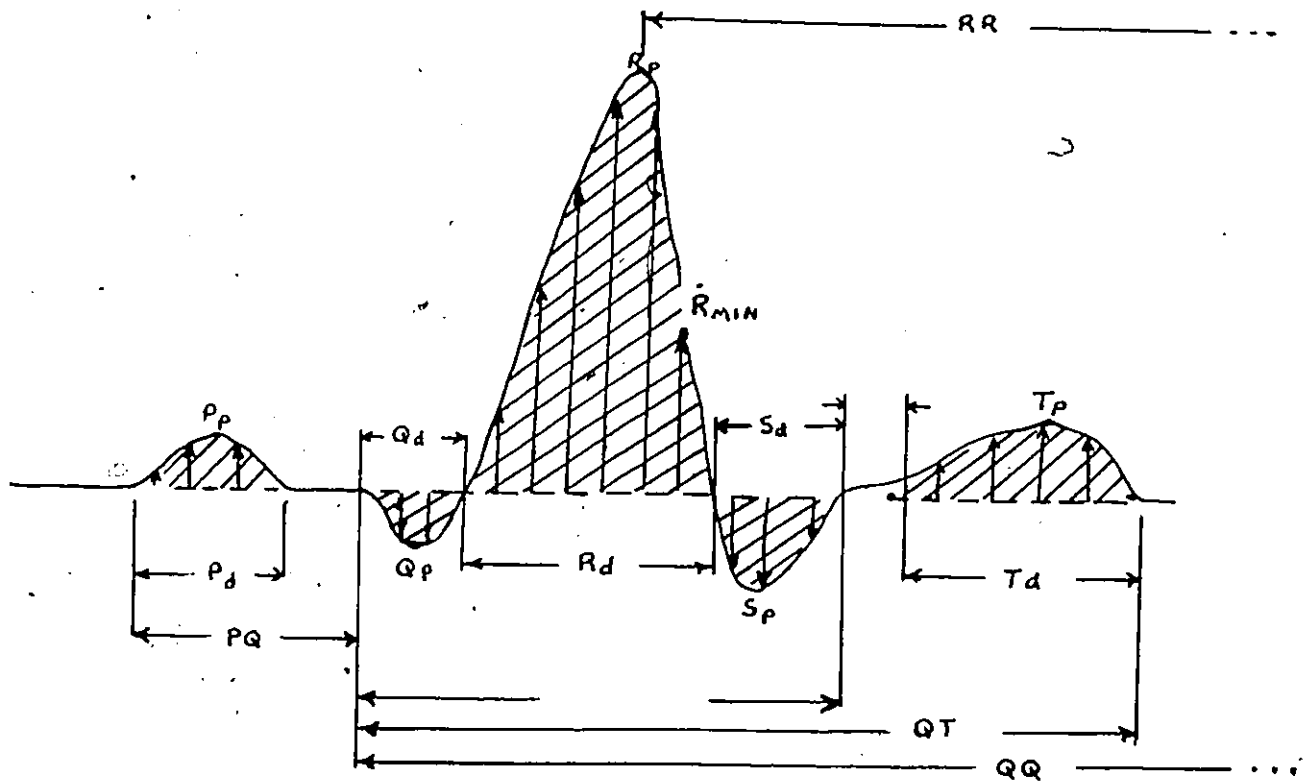
Figure 5. ECG signal with features labelled.

1.3.ii TRANSFORMATION TECHNIQUES[(5)(6)(7)]

The main objective of these transform techniques is to come up with a set of basis functions that will best represent the ECG data with the fewest number of basis functions. Letting the original time function be

$$g(t) \quad , \quad t_1 < t < t_2 \tag{1.1}$$

Now the estimate of the function g(t) is given by

$$\hat{g}(t) = \sum_{k=1}^{N} g_k \, \psi_k(t) \quad , \quad t_1 < t < t_2 \tag{1.2}$$

where $\hat{g}(t)$ is the estimate of g(t), g_k are the N coefficients and $\psi_k(t)$ represent the N basis functions. The g_k's depend on g(t) and the basis functions $\psi_k(t)$ are chosen to be independent of g(t). If g(t) is well behaved then $\hat{g}(t)$ will approach g(t) as N approaches ∞.

These basis functions $\psi_k(t)$ do not necessarily have to be orthogonal or normalized but when the $\psi_k(t)$'s are chosen to be orthonormal, the calculation of the g_k's is greatly simplified giving

$$g_k = \int_{t_1}^{t_2} g(t) \, \psi_k(t) \, dt \quad , \quad k = 1,2,3,\ldots,N \tag{1.3}$$

A variety of transform methods have been applied to ECG data in the past, for purposes of data reduction. Some of these being the Fourier, Karhunen-Loève, Discrete Cosine and Haar Transforms with sinusoidal, eigenvector,

sinusoidal and rectangular wave basis functions, rec-
pectively. The Karhunen-Loève transform is considered
the optimum (in the mean squared error sense) transform
since it's basis functions are uncorrelated, but this
transform is normally not used in practical situations
since there is no fast algorithm for calculating the
transform. Thus, authors in the past have used the
Karhunen-Loève transform as a basis for comparison of
other transform techniques.

The normal procedure followed is to calculate
the transform and then retain the M largest components,
where M is chosen according to the data reduction desired.
Then by setting the remaining components equal to zero
one can proceed to calculate the inverse transform using
only the M components. Of course M must be chosen so
that the resultant reconstruction is within an acceptable
tolerance.

It was observed that many of the authors making
use of the transform techniques did not reconstruct the
total ECG signal. Most authors did not include the
P-wave in their analysis, therefore, the evaluation of the
technique is difficult. This situation is evident in all
the papers referred to in this section.

1.3.iii DIRECT DATA TECHNIQUES[2][8]

There are a variety of data compression techniques
which fall into the category of direct data compressors.

C.A. Andrews[2] and C.M. Kortman[8] have investigated
some of these techniques. C.A. Andrews[2] found that the
polynomial predictors and interpolation compressors gave
the best results when applied to ECG data. These two
methods attempt to store only the sample points that best
characterize the shape of the signal, thus omitting any
redundant sample points. The signal can then be recon-
structed by using the stored information to estimate,
using some criterion, the intermediate sample points.

The two particular techniques which C.A. Andrews[2]
found most effective were the zero-order predictor with
floating aperature (ZOP-FA) and the first-order inter-
polator with two degrees of freedom (FOI-2DF). The ZOP-FA
technique estimates the signal by a set of constant
levels while the FOI-2DF technique estimates the signal
by straight line approximations. The ZOP-FA technique
was found to be inefficient in storing constant slope
information while the FOI-2DF was very sensitive to noise
in the signal.

These direct data techniques have been used in
conjunction with rhythm analysis algorithms to detect the
occurrence of certain ECG complexes within the ECG
waveform.

1.3.iv DISCUSSION

The main disadvantages of the parameter extraction
techniques is that the original signal cannot be re-

constructed from the parameters extracted from the signal. Once the specific information is retained, no more information can be obtained at a later date. The main purpose of these techniques is to categorize waveforms into different diagnostic categories for automatic ECG analysis rather than to store ECG data.

It was observed that most of the papers dealing with ECG data reduction did not take into account the effects of quantization, both on the original samples and on the model parameters. The data reduction ratios were calculated on a number per number basis so that no attempt was made to reduce the bit requirements for each parameter. Since a bit is the basic unit of computer storage, then it is only logical to compare a data reduction technique with the original sample signal on a bits basis. This gives a more realistic indication of the storage savings achieved when applying a data reduction technique, to sampled data.

It was also observed that a wide range of sampling frequencies were used by different authors. The sampling frequency will have a direct effect on the reduction factors. Therefore, it is felt that one must take the sampling frequency into account before passing judgement on a data reduction technique. By sampling the data at a high rate one can claim very high reduction ratios but they have introduced signal redundancy which shows up in the inflated reduction ratios.

1.4   PROBLEM STATEMENT

The objectives of this work are as follows:

1. To investigate three data reduction techniques, linear prediction, with differential pulse code modulation (DPCM), spectral analysis and slope change detection, as applied to ECG data, and present a relative assessment of their effectiveness in reducing data. These techniques are compared on a mean squared error, peak error and visual reproduction basis versus reduction ratio. For these cases the reduction ratio is calculated as the total number of original sample points versus the total number of model parameters, without taking into account quantization.

2. To carry out a quantization study of the original ECG sample points in order to come up with the minimum number of bits/sample required to represent these samples points without significant distortion in the quantized version. Refer to Appendix C for the bits/sample criterion.

3. To apply a quantization method to the best technique of the three studied and determine how many bits/sample are needed to represent the original data. This technique is then compared to the quantized original data on a bits/sample basis, rather than on a number per number basis which is used by many authors.

1.5   THESIS OUTLINE

The first chapter of the thesis discusses the importance of data reduction for automatic ECG analysis system along with a brief summary of techniques that have been applied in the past. There is also a short section on the electrocardiogram from the standpoint of electrode placement, diagnostic value and physiological phenomenon responsible for these electrical signals.

In Chapter II the acquisition and preprocessing of the ECG data is discussed. Included is a system block diagram and a bandwidth discussion.

The three main data reduction techniques are presented in Chapter III. The theory involved with each technique is discussed along with problems faced and modifications made on each of these methods. Finally, an original waveform along with reproductions using each technique are presented at the end of each subsection of the chapter.

In Chapter IV the results of each technique are discussed, from the standpoint of mean squared and peak errors, as well as the visual fidelity in the reconstructions. The techniques are compared for different levels of reduction, where the reduction is based simply on a number per number basis. Conclusions are reached as to which technique gives the best reduction while maintaining an acceptable representation of the ECG data.

In Chapter V a quantization study is carried out on both the original data and the slope change detection technique parameters. It is found that the original data can be represented by 6 bits/sample without significant distortion in the reconstruction. By quantizing the parameters of the slope change detection technique, as applied to prefiltered data, one can represent this same data using 2 bits/sample while maintaining the mean squared and peak errors below 1% and 5%, respectively.

In Chapter VI the conclusions of the work are presented.

CHAPTER II

ACQUISITION AND PREPROCESSING OF THE ECG DATA

2.1 EQUIPMENT DESCRIPTION

Figure 6 shows a block diagram of the equipment
used for the sampling and analysis of the ECG data. The
Lead II configuration was used to obtain the ECG signals.
For this configuration three electrodes are used, one for
the right shoulder and one for each of the legs of the
subject. The potential is measured between the right
shoulder with respect to the average of the two legs.
All the waves, P, Q, R, S and T are normally well defined
in the Lead II configuration, mainly because the
potential is being measured in the general direction of
the depolarization and repolarization spread through the
heart. Thus, this lead is quite often used for ECG
analysis systems.

Before any sampling was done, two visits were
made to the Coronary Care Unit of Grace Hospital,
Windsor, Ontario, in order to become familiar with the
procedures for taking good electrocardiograms. These
two days were spent observing the ECG technicians as
they took the ECG's and discussing the problems that can
arise when the ECG is not taken properly. The ECG
machines used at the hospital were almost identical to
the one used for this analysis.

24
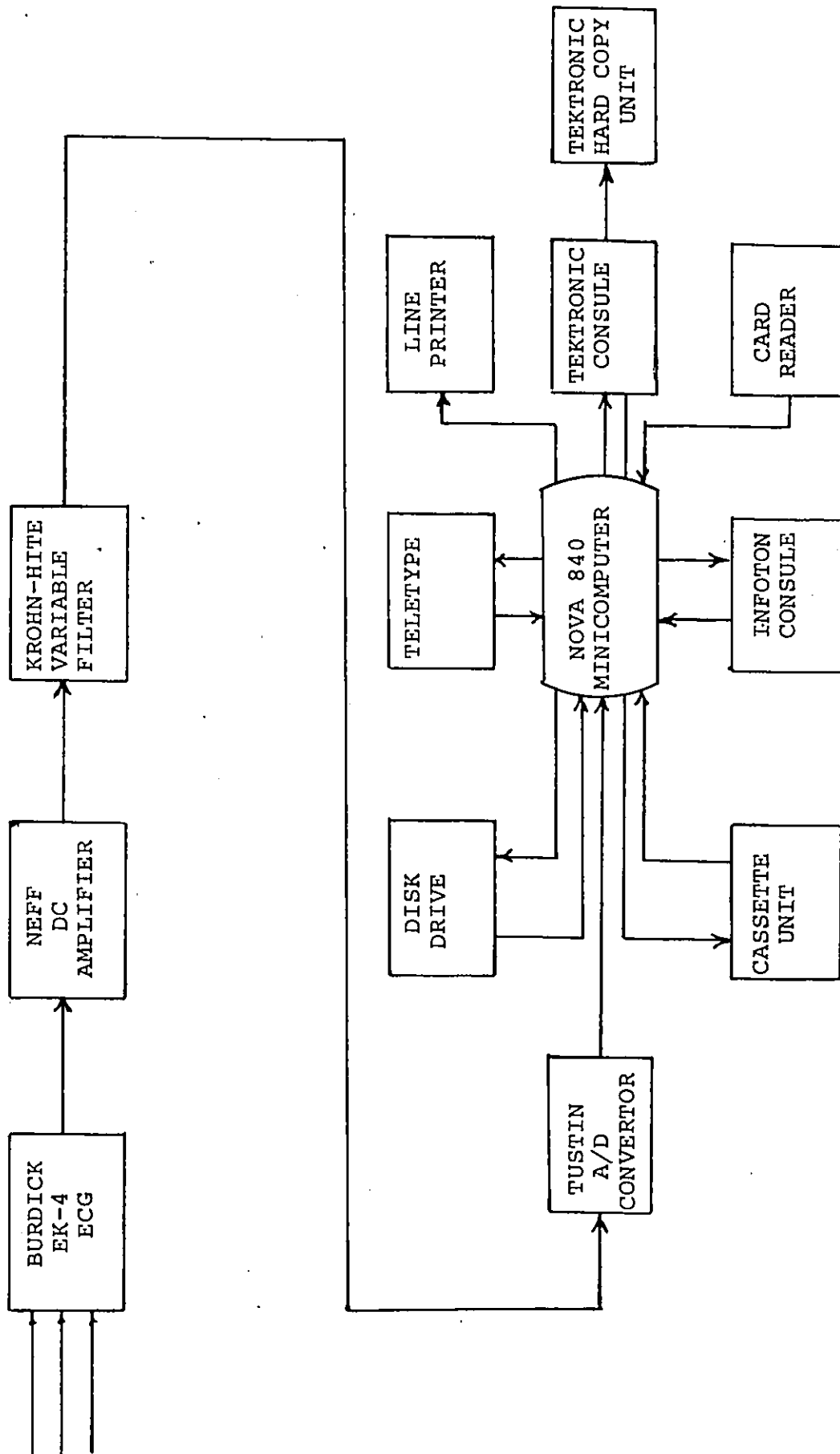
Figure 6. Block diagram of the equipment used in the analysis.

2.1.i BURDICK EK-4 ELECTROCARDIOGRAPH

This ECG machine is fitted with an output terminal
for oscilloscope monitoring of the signals being recorded
on the paper chart. The monitoring terminal gives an
output of 1 volt per centimeter deflection of the record-
ing needle. Thus, by adjusting the sensitivity one can
control the signal output level. The output impedance
is approximately 100 Ω with maximum output currents of
about 0.1 milliamperes.

All the ECG's were taken from male subjects
between the ages of 24 to 35 years of age. The subjects
were lying quietly on their backs while the ECG's were
taken, thus reducing the possibilities of muscle noise in
the tracings. For a couple of cases, the ECG signals
were sampled, immediately after the subject had done
some running on the spot.

2.1.ii NEFF MODEL 122 DC AMPLIFIER

The DC amplifier was used to amplify the ECG
signals so that the full range of the analog to digital
(A/D) convertor could be utilized. This particular
amplifier is a wideband differential DC amplifier which
is designed for low level signal amplification in
conjunction with data systems. The unit has a built-in
variable 2nd order filter with 3dB points ranging from
10 Hz to 100 KHz, stepped by factors of 10. The gain
of this amplifier is variable from 0 to 1000. The input

impedance is 100 megohms, minimum, shunted by 100 pf, while the output impedance is approximately 0.1 ohms in series with a 10 µH inductance.

2.1.iii KROHN-HITE MODEL 3750 VARIABLE FILTER

This filter was used to low pass filter the ECG data for A/D conversion. The filter is a variable electronic filter which covers the frequency range from 0.02 Hz to 20 KHz. The unit is made up of high pass and low pass sections which can be used independently or in series to accomplish all four filter configurations; high-pass, low-pass, band-pass and band-reject. The pass-band gain can be set to either unity (0dB) or 10 (20dB) by simply pushing a switch. The out of band attenuations are 6, 12, 18 or 24 dB per octave. Thus this filter can be used throughout the frequency range from 0.02 Hz to 20 KHz for all four configurations and with variable gain and attenuation. One has the choice of either a Butterworth (maximum flat response) for frequency domain operation or low Q (damped response) for transient-free time domain operation. The input can vary between $\pm$ 15 volts for a gain of 0 dB and $\pm$ 1.5 volts for a gain of 20 dB. The input impedance is 10 megohms in parallel with 200 pf and the output impedance is 50 ohms.

For this analysis the filter was used as a low pass filter with a Butterworth response and the maximum

out of band attenuation, 24dB/octave.

2.1.iv   TUSTIN X-1500 A/D CONVERTOR

The Tustin analog-to-digital (A/D) convertor is a 13 bit plus one sign bit convertor. The full scale input voltage range is $\pm$ 10 volts where + 10 volts corresponds to + 2^{13} and - 10 volts corresponds to - 2^{-13} + 1. There are 16 channels available, made up of 4 buffered and 12 unbuffered channels. The input impedance is greater than 20 megohms in parallel with 200 pf. The conversion time is 15 μsec with an accuracy of 0.005% of full scale, $\pm$ ½ LSB. The actual conversion is done using a method known as the successive approximation method, which is the most widely used technique for A/D conversion.

In the successive approximation A/D convertor, a feedback voltage $-V_F$ is made to approximate the input voltage V_X in a sequence of successive steps, where during each step, $-V_F$ is changed in accordance with the result of the previous comparison between V_X and $-V_F$. The amount by which $-V_F$ is increased or decreased is $V_R/2^i$ where i defines the ith step in the operation and V_R is the reference voltage which is 10 volts in this case. A simple example will best demonstrate the operation of this type of convertor. Let V_R = 10 volts and V_X = 7.9 volts which represents the value of an analog signal at a particular instant of time.

1. V_F is set equal to $V_R/2^1 = 10/2 = 5$ volts and is compared with V_X to get the error voltage V_E, $(V_X - V_F = V_E)$. Since V_E is positive then the most significant bit (MSB) is set equal to a logical '1'.

2. Now V_F is set equal to $5 + 10/4 = 7.5$ volts, thus V_E is now negative so the next MSB is set equal to a logical '0'.

3. Since V_E was negative, then V_F is now set equal to $7.5 - 10/8 = 6.25$ volts, which gives a positive V_E, therefore, the next MSB is set equal to a logical '1'.

4. Now V_F is set equal to $6.25 + 10/16 = 6.875$ volts which again gives a positive V_E, thus the next MSB is equal to a logical '1'. Therefore, the first four MSB's of the generated digital output are 1011. This procedure is repeated N times for an N bit convertor. For this case N was equal to 13.

2.1.v DATAGEN NOVA 840 MINICOMPUTER AND PERIPHERAL EQUIPMENT

The Nova 840 is a general purpose minicomputer which operates using 16 bit word lengths. The core memory size at the time of this work was 32K, with disk storage capabilities of approximately 1.25 million words. The Nova system used is equipped with a variety of peripheral equipment, which can be used for different input/output purposes. The peripheral devices are shown in Figure 6.

Infoton Consule: This consule is made up of a full key-
board with a cathode ray tube (CRT) display. Its main
purpose is for inputing instruction to the Nova and
outputing instructions or computational results via the
CRT display.

Data General Cassette Unit: This unit allows the user
to store material on a cassette tape and read material
from stored tapes.

Diablo Disk Drives: This unit allows individual users
to store up to 1.25 million words of data or actual
programs on digital tapes. By keying in the appropriate
statements the user has access to all the files on the
mounted disk.

Teletype: It is used for inputing and outputing instruc-
tions or data to the Nova. It also allows the user to
input or output information using a paper tape.

Centronics 101 Line Printer: Used mainly for outputing
information from the Nova.

Tektronix 4013 Terminal: Made up of a keyboard and CRT
display. For this analysis the unit was used primarily
as a means of displaying data and plotting waveforms,
although it is set up to be used in place of the Infoton
console.

Textronix 4610 Hard Copy Unit: This is used to get a
hard copy of what ever is displayed on the Tektronic CRT
display.

Documentation D150 Card Reader: Simply used to read information into the Nova using standard computer cards.

2.2 BANDWIDTH REQUIREMENTS

In order to sample the analog ECG signal, one must decide on a bandwidth for the signal. Normally the bandwidth is chosen to be as small as possible without excluding any important frequency components. Once the bandwidth of the signal has been established, by the sampling theorem, one can sample at a frequency which is twice the value of the bandwidth frequency, as long as the signal is band limited at this frequency. Ideally, a signal is considered band limited if the spectral components are zero beyond the band limit frequency. For practical situations one wants the out of band frequency components to be insignificant in magnitude so that the aliasing will be kept to a minimum. Usually the signal is low pass filtered in order to attenuate the higher frequency components. Therefore, by low pass filtering and by sampling at a frequency a little higher than twice the bandwidth, one can be relatively sure that any aliasing affects will be insignificant.

It was found that a wide range of bandwidths have been proposed by various authors, ranging from 5Hz to 40Hz, C.A. Swenne[9], to DC to 1477Hz, C.E. Burton[5]. In the former case the author was dealing with the QRS portion of the ECG signal only, while in the latter case

the author was using Fourier coefficients in order to
detect ECG waveform changes. The choice of bandwidth is
very important because it can significantly affect one's
reduction factor, since the number of samples needed to
represent a set amount of data is directly proportional
to the sampling rate.

Many of the problems associated with computer
analysis of ECG's, including bandwidth of the ECG signal,
were discussed at a conference on computer application on
ECG and VCG analysis. Most of the pioneers of this field
were present and the conference papers and discussions
were published by Chr. Zywietz and B. Schneider[1].
The bandwidth of the ECG signal was discussed and the
participants were unable to agree on the bandwidth
requirements of the ECG signal. Their ECG analysis
systems assumed bandwidths with upper bounds ranging from
100 Hz to 500 Hz. A spectral analysis was carried out on
ECG data by D.P. Golden and Associates[10] and their
conclusion was that ECG amplitude information is contained
within a bandwidth DC to 200 Hz, while a bandwidth up to
500 Hz is needed to retain certain high frequency
notching information.

Because of the wide range of bandwidths presently
being used, it was decided to do a preliminary bandwidth
analysis on some ECG signals. First some ECG data was
low pass filtered to 1000 Hz and sampled at a rate of
2000 Hz. Now the sampled signal was low pass filtered

at a variety of frequencies and comparisons were made
with the 1000 Hz bandwidth signal. The filtering was
accomplished by taking the Fourier transform of the sample
sequence and truncating the spectrum at the appropriate
frequencies. Now by taking the inverse Fourier transform
with the higher frequency components set equal to zero,
one gets the filtered time signal representation. For
this part of the analysis there was no apparent distor-
tion in the filtered waveform due to Gibb's phenomenon
when the spectrum was truncated, using a rectangular
window. For this analysis a fast Fourier transform (FFT)
algorithm was used to attain computational efficiency.

It was observed that there was no apparent visual
distortion in the signals analyzed, when the bandwidth
was reduced to 100 Hz. This comparison was done by
superimposing the 100 Hz bandwidth signal on the I000 Hz
bandwidth signal. The paper by D.P. Golden[10] found
that the peak errors were below 0.5% when the bandwidth
of the signal was reduced to 100 Hz. This 0.5% error
would be almost impossible to detect on a visual basis.
Thus the paper[10] also concluded that the ECG signal
bandwidth can be set to 100 Hz if the high frequency
components prove to be unimportant as far as diagnostics
are concerned. The diagnostic value of these high
frequency components has been questionable up until now
so most authors have chosen to ignore them in their
analysis.

It was then decided to investigate the effects of reducing the bandwidth below 100 Hz. For this part of the analysis the spectrum was multiplied by a hamming window to reduce the possibility of Gibb's phenomenon, although this did not prove to be necessary in the previous analysis. The Hamming window used is given by

$$w(n) = 0.54 + 0.46 \cos \frac{n\pi}{N} \quad , \quad n = 1,2,3,\ldots,N \qquad (2.1)$$

This Hamming window was applied to the last 20 points of the spectrum (N = 20) before the frequency cutoff. It was found that the bandwidth had to be reduced below 50 Hz before there was any significant visual distortion in the waveform. The only noticeable distortions caused by reducing the bandwidth from 100 Hz through 50 Hz was the rounding of sharp peaks. Even though the overall representations for bandwidths between 50 Hz and 100 Hz appeared acceptable, it was found that the maximum error was in excess of 5% for some ECG data, for bandwidths up to about 80 Hz. H.V. Pipberger and Associates[11] stated that the maximum deviation from the original signal cannot exceed 5%. Therefore, if this criterion is applied then the signal bandwidth must be at least 80 Hz for ECG signal sampling.

It was finally decided to set the bandwidth to 100 Hz, and sample the signals at 250 Hz in order to reduce any aliasing effects.

2.3 COMMENTS

Once the ECG data was sampled, it was displayed on the Tektronix display to make sure the tracing was acceptable before being stored. The discrete data points were shown on the display as analog waveforms. The digital-to-analog (D/A) conversion was accomplished by simply linearly interpolating between sample points. This is known as a first order hold system of D/A conversion. This method of D/A conversion was used for all the waveforms shown in subsequent chapters.

CHAPTER III

DATA REDUCTION TECHNIQUES INVESTIGATED

3.1 LINEAR PREDICTION TECHNIQUE

Let the sample sequence of the ECG signal be given by

$$S_i \quad , \quad i = 1,2,3,\ldots,N \tag{3.1}$$

where N is the total number of points in the sequence. Linear prediction attempts to estimate the present sample point by a linear combination of past samples. Therefore, the linear prediction estimate is of the form

$$\hat{S}_i = \sum_{j=1}^{P} a_j \, S_{i-j} \tag{3.2}$$

where a_j, $j = 1,2,3,\ldots,P$ are the prediction parameters and $\hat{S}i$ represents the estimate of S_i. The system is represented by an all pole model which has a transfer function in the z-domain as follows

$$H(z) = \frac{1}{1 + \sum_{j=1}^{P} a_j \, z^{-j}} \tag{3.3}$$

where a_o has been normalized to unity. Usually Equation (3.2) has an extra term y_i on the right side of the equation. This y_i represents the excitation function of the system. Since the proper choice of y_i is sometimes

36

difficult, it was decided to implement the linear pre-
diction model using the first P samples as starting
values, thus $\bar{y}_i$ drops out of the equation giving (3.2).
Therefore,

$$\hat{S}_1 = S_1$$

$$\hat{S}_2 = S_2 \tag{3.4}$$

$$\vdots$$

$$\hat{S}_P = S_P$$

Now in order to calculate the a_j's in (3.2), one
must minimize the mean squared error between the samples
S_i and the estimate $\hat{S}_i$. Therefore,

$$e_i = S_i - \hat{S}_i$$

giving

$$e_i = S_i - \sum_{j=1}^{P} a_j \, S_{i-j} \tag{3.5}$$

Now the sum of the squared error is given by

$$E = e_i^2$$

$$= \sum_{i=1}^{N} \left(S_i - \sum_{j=1}^{P} a_j \, S_{i-j} \right)^2 \tag{3.6}$$

Now one can calculate the a_j's by differentiating with
respect to the a_j's and setting the resultant equation
equal to zero, giving

$$\frac{\delta E}{\delta a_k} = -2 \sum_{i=1}^{N} (S_i - \sum_{j=1}^{P} a_j S_{i-j}) S_{i-k} = 0 \quad , \quad k = 1,2,3,\ldots,P$$

$$(3.7)$$

Therefore,

$$\sum_{i=1}^{N} \sum_{j=1}^{P} a_j S_{i-j} S_{i-k} = \sum_{i=1}^{N} S_i S_{i-k} \quad , \quad k = 1,2,3,\ldots,P$$

$$(3.8)$$

Letting

$$\phi_{jk} = \sum_{i=1}^{N} S_{i-j} S_{i-k}$$

$$(3.9)$$

$$\psi_k = \sum_{i=1}^{N} S_i S_{i-k}$$

Therefore, in matrix form

$$
\begin{bmatrix}
\phi_{11} & \phi_{12} & - & - & - & \phi_{1P} \\
\phi_{21} & \phi_{22} & - & - & - & \phi_{2P} \\
| & | & & & & | \\
| & | & & & & | \\
| & | & & & & | \\
\phi_{P1} & \phi_{P2} & - & - & - & \phi_{PP}
\end{bmatrix}
\begin{bmatrix}
a_1 \\
a_2 \\
| \\
| \\
| \\
a_P
\end{bmatrix}
=
\begin{bmatrix}
\psi_1 \\
\psi_2 \\
| \\
| \\
| \\
\psi_P
\end{bmatrix}
\qquad (3.10)
$$

giving,

$$\phi a = \psi \qquad (3.11)$$

The solution of the set of linear equations (3.11) yields
the optimum (in the mean squared error sense) prediction
parameters, a_j, $j = 1,2,3,\ldots,P$.

There are some problems that can arise when using this linear prediction model for synthesis. Instability problems in the model can arise because of the mean squared error criterion used along with the finite precision of the sample points. These problems may cause the poles of the model to be outside the unit circle thus giving an unstable system.

3.1.i PREDICTION PARAMETER DETERMINATION

The prediction parameters are determined by solving for the a_j's, $j = 1,2,3,...,P$ in the linear Equations (3.10). One finds that the matrix ϕ is a symmetric matrix since

$$\sum_{i=1}^{N} S_{i-j} S_{i-k} = \sum_{i=1}^{N} S_{i-k} S_{i-j}$$

Therefore,   (3.12)

$$\phi_{jk} = \phi_{kj}$$

Thus one only needs to calculate the leading diagonal and upper triangle elements of the matrix ϕ and the remaining elements will follow directly from (3.12).

Further computational time can be saved if the signal is assumed to be stationary in the analysis interval. If this is assumed then

$$\phi_{j+1,k+1} = \phi_{jk} \qquad (3.13)$$

When equation (3.13) holds then the matrix is known as a Toeplitz matrix which simply means the diagonal elements are equal. Therefore, assuming the matrix is Toeplitz and since (3.12) holds, then the ϕ matrix can be determined by calculating the first row elements only and then use Equations (3.12) and (3.13) to obtain the remaining elements. Therefore, the final ϕ matrix is as follows

$$
\phi = \begin{bmatrix}
\phi_{11} & \phi_{12} & \phi_{13} & - - - & \phi_{1P} \\
\phi_{12} & \phi_{11} & \phi_{12} & - - - & \phi_{1P-1} \\
\vdots & \vdots & \vdots & & \vdots \\
\vdots & \vdots & \vdots & & \vdots \\
\vdots & \vdots & \vdots & & \vdots \\
\phi_{1P} & \phi_{1P-1} & \phi_{1P-2} & - - & \phi_{11}
\end{bmatrix} \tag{3.14}
$$

N. Levinson has developed a recursive procedure for solving a system of simultaneous linear equations assuming the ϕ matrix has the above mentioned characteristics. This method of solution is outlined in E.A. Robinson's book[12].

3.1.ii PREDICTIVE CODING

In order to improve the linear prediction model, one can encode the error signal

$$
e_i = (S_i - \hat{S}_i) \tag{3.15}
$$

Now, if the estimate using linear prediction is accurate, one can expect that the error e_i, can be encoded using fewer bits than the original sample points. Suppose that

the original sample sequence S_i, i = 1,2,3,....,N must

be represented by J bits for the required fidelity.

Therefore, J·N bits are needed to represent the N sample

points. Now by applying the linear prediction model along

with error coding, one hopes that the total number of bits

needed to represent the N sample points is significantly

reduced. If the error values e_i can be quantized to M

bits and the K model parameters can be quantized to L bits

then,

$$M \cdot N + K \cdot L < J \cdot N \qquad (3.16)$$

must be true in order to obtain a savings of storage.

This method of data compression has been found to provide

significant improvements in picture transmission, speech

transmission and transmissions of a variety of other

telemetry signals.

3.1.iia   OPEN LOOP PREDICTIVE CODING

By implementing this model directly in an open

loop scheme, one finds that the estimate is subject to

error build up which may cause unacceptable reconstructions

on the output. Figure 7 shows an open loop predictive

coding scheme, where the $\wedge$ represent the linear prediction

estimates and the $\sim$ represents the quantized versions.

Therefore,

$$\hat{S}_i = \sum_{j=1}^{P} a_j \, S_{i-j} \qquad (3.17)$$
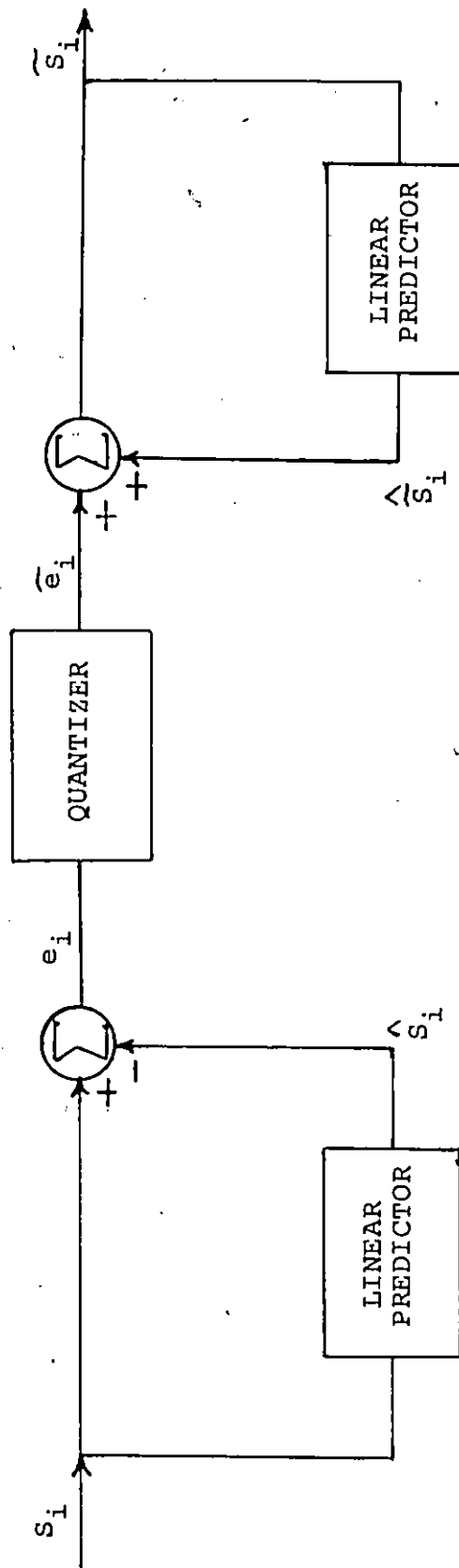
Figure 7. Open loop coding scheme.

and the error in the estimate is given by

$$e_i = S_i - \hat{S}_i \qquad (3.18)$$

with $\tilde{e}_i = e_i$ (quantized).

Now the final estimate of S_i is given by

$$\tilde{S}_i = \hat{\hat{S}}_i + \tilde{e}_n \qquad (3.19)$$

$$= \hat{\hat{S}}_i + (S_i - \hat{S}_i) - (e_i - \tilde{e}_i) \qquad (3.20)$$

The final error in the estimate can now be calculated as

$$S_i - \tilde{S}_i = (\hat{S}_i - \hat{\hat{S}}_i) + (e_i - \tilde{e}_i) \qquad (3.21)$$

From this equation one observes that the final error is made up of two different error terms, the quantization error of the error term $(e_i - \tilde{e}_i)$ and the quantization error of the estimate $(\hat{S}_i - \hat{\hat{S}}_i)$. Since,

$$\hat{\hat{S}}_i = \sum_{j=1}^{P} a_j \tilde{S}_{i-j} \qquad (3.22)$$

Then the overall error will accumulate which can cause the model to be unacceptable.

In order to improve this situation a differential pulse code modulation (DPCM) scheme was developed which uses feedback to prevent the accumulation of error, due to the first term of Equation (3.21).

3.1.iib DIFFERENTIAL PULSE CODE MODULATION (DPCM)

Figure 8 shows the DPCM scheme. It can be shown that the error in the final estimate is equal to the quantization noise in the error term alone. The final estimate is given by

$$\widetilde{S}_i = \hat{\widetilde{S}}_i + \widetilde{e}_i \qquad\qquad (3.23)$$

where

$$\hat{\widetilde{S}}_i = \sum_{j=1}^{P} a_j \widetilde{S}_{i-j} \qquad\qquad (3.24)$$

and

$$\widetilde{e}_i = e_i \text{ (quantized)} \qquad\qquad (3.25)$$

By expanding Equation (3.23) one gets

$$\widetilde{S}_i = \hat{\widetilde{S}}_i + (S_i - \hat{\widetilde{S}}_i) - (e_i - \widetilde{e}_i) \qquad (3.26)$$

Therefore, the final error in the estimate is given by

$$S_i - \widetilde{S}_i = e_i - \widetilde{e}_i \qquad\qquad (3.27)$$

which is simply the quantization error in the error term. Therefore, by (3.27), it is observed that the error no longer accumulates.

The quantizer used for this analysis was a one bit quantizer although higher bit quantizers could have been used. B. Cirjanic[13] has discussed a variety of linear quantizers which could be implemented in this sort of scheme. Figure 9 shows the input-output relationships
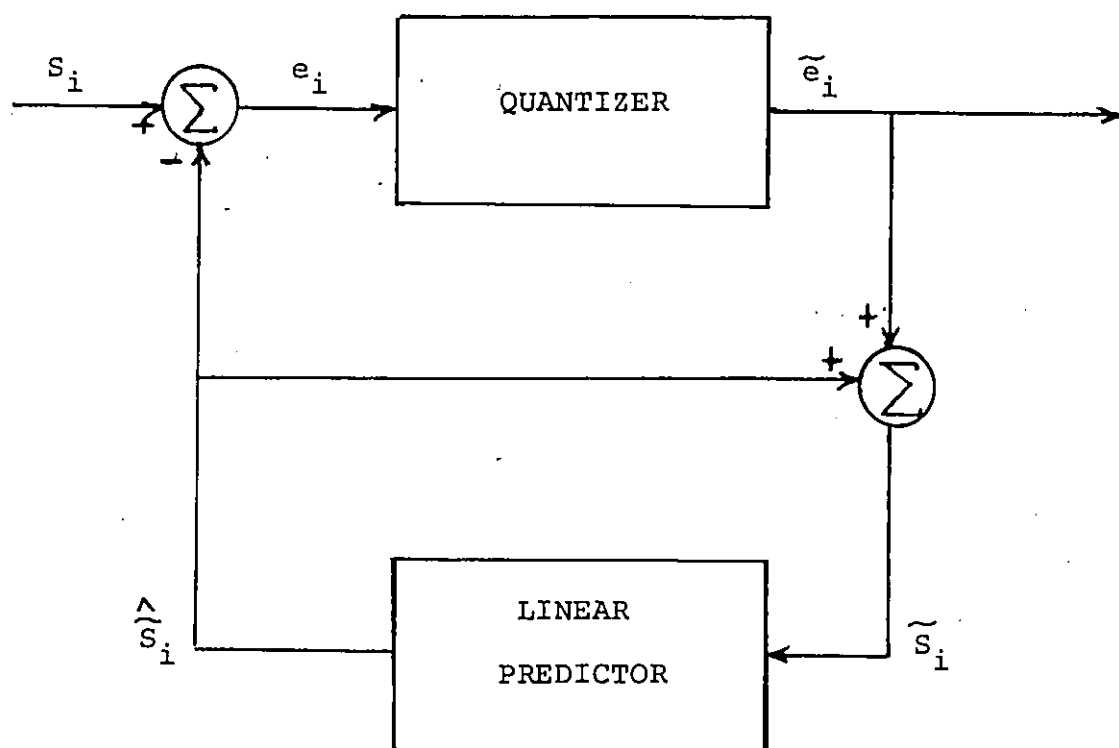
Figure 8. Differential pulse code modulation (DPCM) scheme.
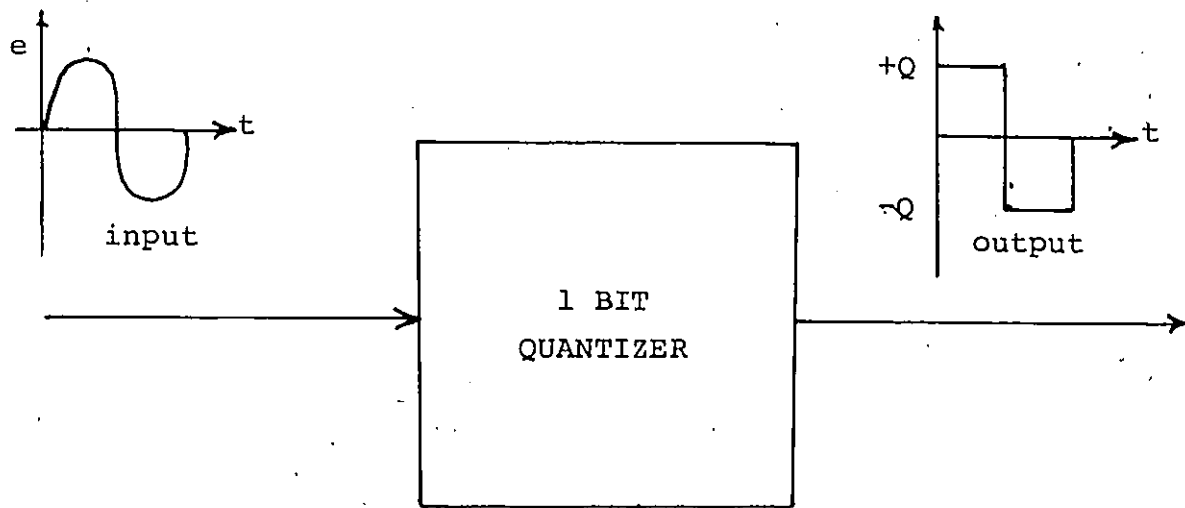
Figure 9. Input/output relationship of a 1 bit quantizer.
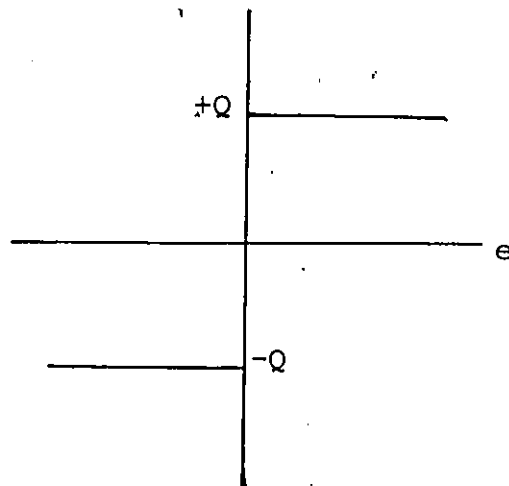
Figure 10. Quantizer level (Q) versus the error.

of a two level (1 bit) quantization scheme while Figure 10 shows the quantization levels versus the error plot of the two level quantizer. The final estimate is given by

$$\widetilde{S}_i = \sum_{j=1}^{P} a_j \widetilde{S}_{i-j} + Q \text{ sgn } e_i \qquad (3.28)$$

where

$$e_i = S_i - \sum_{j=1}^{P} a_j \widetilde{S}_{i-j}$$

and

$$\begin{aligned} \text{sgn}(e_i) &= +1 \quad , \quad e_i \geq 0 \\ &= -1 \quad , \quad e_i < 0 \end{aligned}$$

and Q is the quantizer level. The main disadvantage of the DPCM scheme, as shown in Figure 8, is that the determination of an optimum quantizer level Q is very difficult. This difficulty arises because of the non-linear characteristics of the quantizer and because of the closed loop around the quantizer.

The original sample sequence can be represented by

$$S_i = \sum_{j=1}^{P} a_j S_{i-j} + \left[S_i - \sum_{j=1}^{P} a_j S_{i-j} \right] \qquad (3.29)$$

Now the estimate is given by,

$$\widetilde{S}_i = \sum_{j=1}^{P} a_j \widetilde{S}_{i-j} + Q \text{ sgn } e_i \qquad (3.30)$$

Now, if $Q \ \text{sgn} \ e_i$ can be calculated to be a good approxi-
mation of $Si - \sum\limits_{j=1}^{P} a_j S_{i-j}$ then $\widetilde{S}_i$, $i = 1,2,3,\ldots,N$ will
be close to S_i, $i = 1,2,3,\ldots,N$. Since $\text{sgn}(e_i) = \pm 1$, then
Q must be chosen to be an optimum estimate of the magnitude
of $S_i - \sum\limits_{j=1}^{P} a_j S_{i-j}$ in the analysis interval. Therefore,
Q is chosen to be

$$Q = \frac{1}{M} \sum\limits_{i=1}^{M} \left| S_i - \sum\limits_{j=1}^{P} a_j S_{i-j} \right| \qquad (3.1.31)$$

where M is the number of samples over which Q is con-
sidered constant. This quantizer level Q is updated every
M samples where the value of M is found empirically.

3.1.iii IMPLEMENTATION OF THE LINEAR PREDICTION MODEL WITH DPCM (LP-DPCM)

It was found that the model was sensitive to the
starting location on the ECG waveform. Thus a preliminary
investigation was carried out in order to come up with the
best starting point. It was concluded after several
locations were tried, that the model gave the best
results when the analysis was started at the Q-wave.
Therefore, the first Q-wave had to be detected before the
linear prediction model could be applied to any of the
ECG sample sets.

The next step in the analysis was to come up with
the best number of prediction parameters P. Thus, the
linear prediction model was implemented, without any
error coding, in an attempt to come up with an optimum

value of P. It was observed that the reconstructions did
not significantly improve when the number of prediction
parameters were increased above 16. Thus it was decided
to implement the linear prediction model letting P = 16.
It was also found that the prediction parameters had to
be updated every cycle for the best reconstructions.
This was due to the non-stationary characteristics of the
ECG signal. Therefore, the analysis was carried out on a
cycle per cycle basis with the starting location at the
Q-wave for each cycle.

Therefore, for each cycle of ECG sampled data,
one has to specify –

16   prediction parameters

16   initial sample points

Q_i , i=1,2,$\cdots$,NQ   Quantizer levels
'1' or '0'   for each sample point

3.1.iv SIMULATED ECG SIGNALS

Figures 11a,b,c and Figures 12a,b,c show an
original ECG signal along with two reconstructed wave-
forms using the linear prediction model with DPCM.
Figures 11a and 12a are the original waveforms. Figures
11b and 12b are the reconstructed waveforms with
approximately 2:1 reduction in data while Figures 11c
and 12c show the reconstructions with a data reduction of
about 3:1.
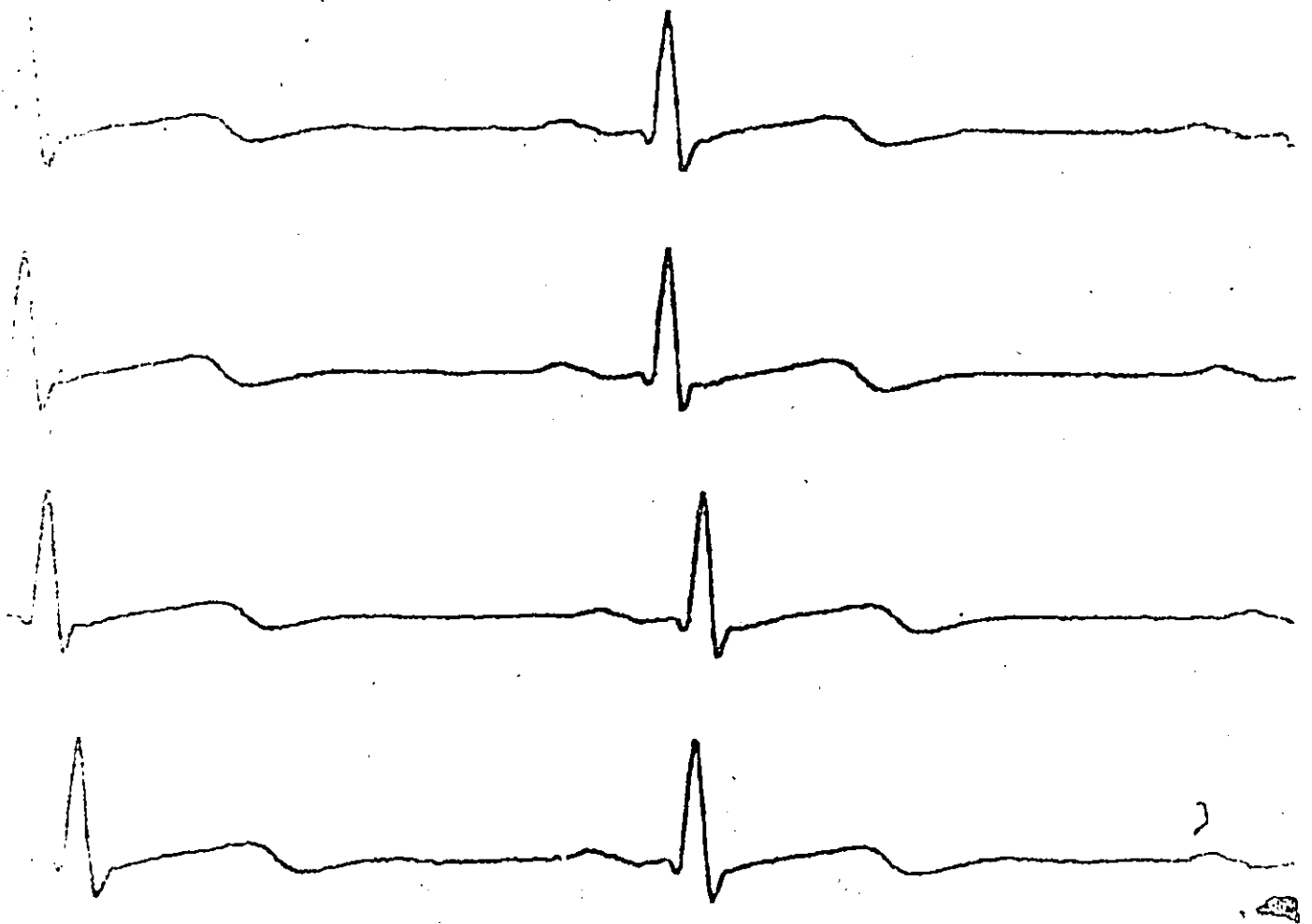
Figure 11a. Original ECG signal (1).
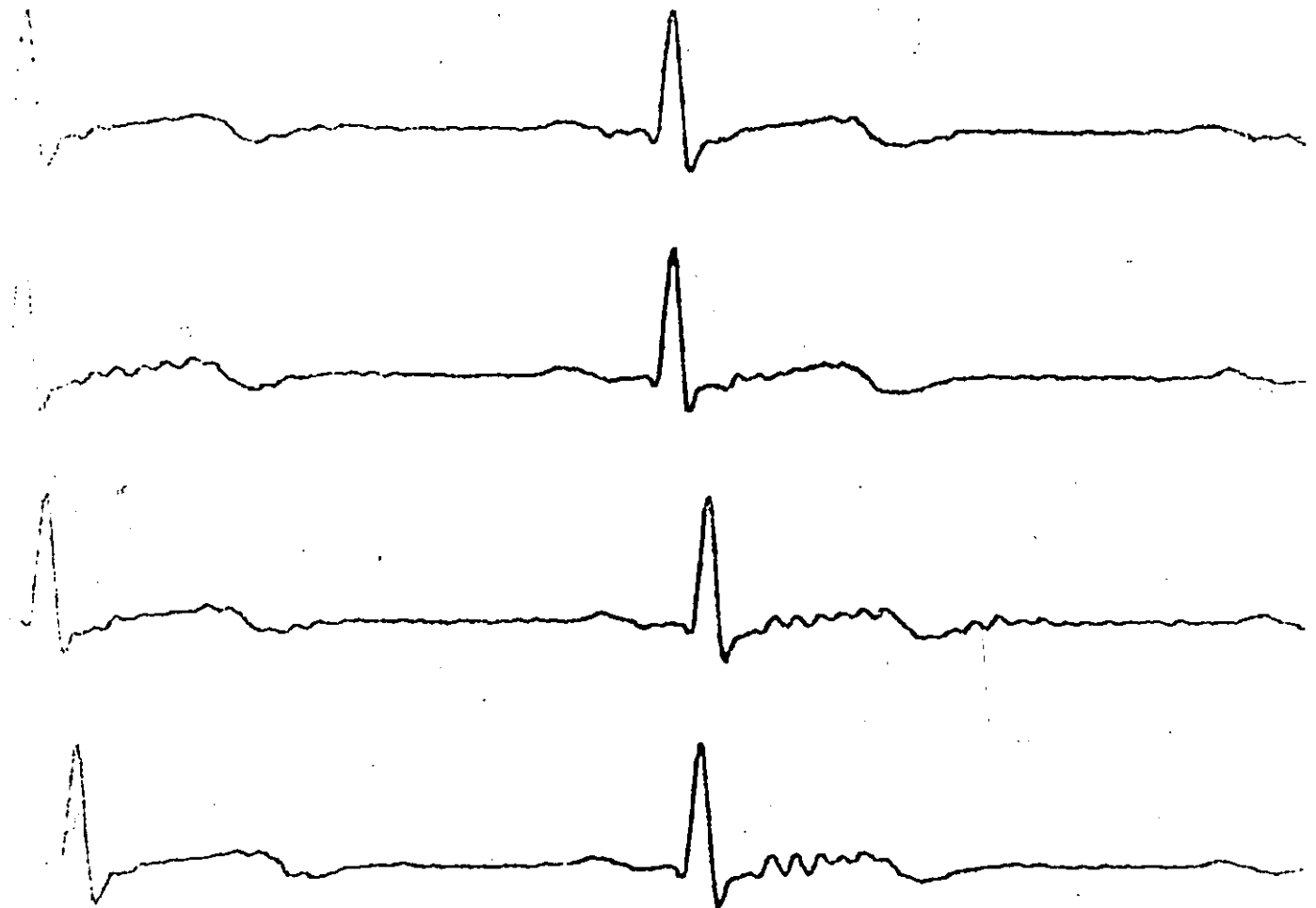
Figure 11b. Reconstruction with 2:1 data reduction (LP-DPCM).
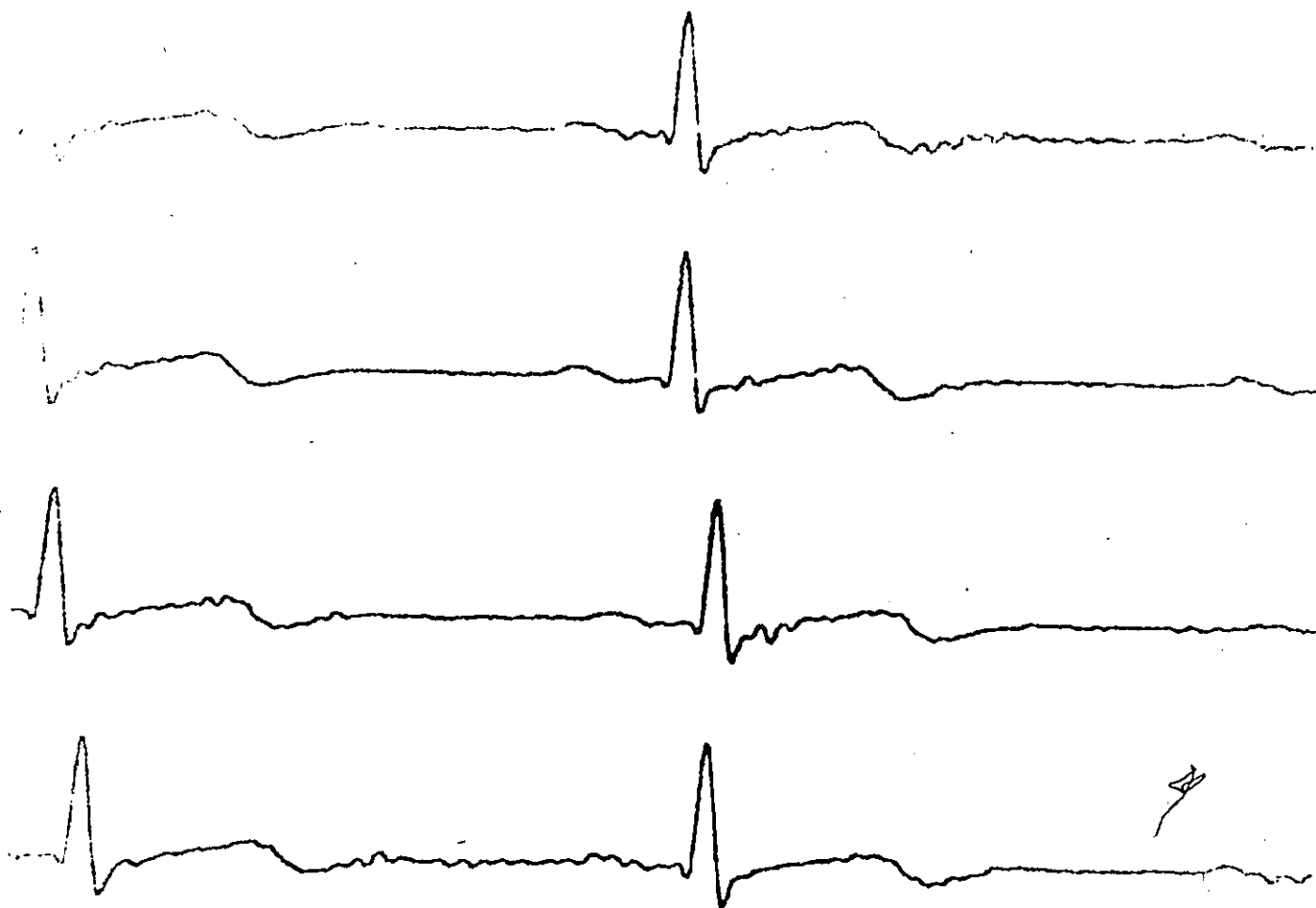
Figure 11c. Reconstruction with 3:1 data reduction (LP-DPCM).
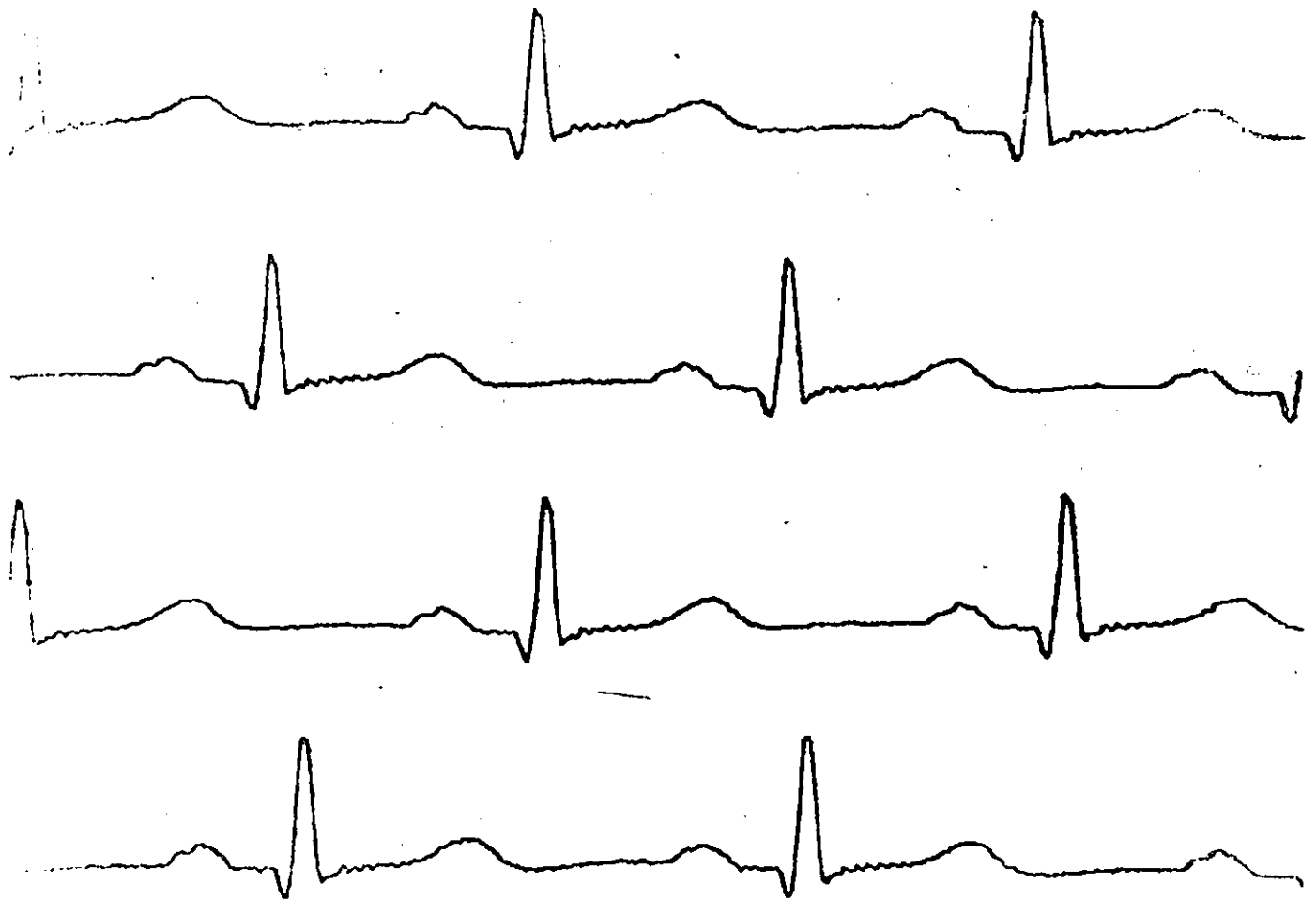
Figure 12a. Original ECG signal (2).

Figure 12b. Reconstruction with 2:1 data reduction (LP-DPCM).

Figure 12c. Reconstruction with 3:1 data reduction (LP-DPCM).

3.2 SPECTRAL TECHNIQUE

This technique attempts to make use of the ECG signals spectral information in order to achieve a reduction of data. By removing the redundant spectral information, one can reconstruct the time signal using only the nonredundant components, thus a reduction of data may be accomplished.

Since the spectrum is estimated using the Fourier transform, this method of data reduction can be categorized as a transform technique. Authors in the past have made use of the Fourier transform for the purpose of data compression, as mentioned in the introduction. Two basic approaches have been followed in the past.

1. First, the frequency spectrum is estimated using the Fourier transform. The spectrum is then truncated at various frequencies and the inverse transform is taken to come up with time signal representation. By truncating the spectrum, one is, in reality, low pass filtering the data at the truncation frequency. Therefore, this method, in essence, is removing the signal redundancy, due to an improper choice of bandwidth. It is felt that if the signal bandwidth is chosen properly, then this approach should not give a significant reduction of data.

2. The other approach taken is to calculate the spectrum and proceed to pick out the M largest frequency

components, set the remaining components, equal to zero and then take the inverse transform. Therefore, M can be chosen so that a given data reduction is achieved. Of course, as M is decreased, the distortion in the reconstruction will increase so that M must be chosen so that the reconstruction is acceptable.

3.2.i   SPECTRAL BAND MODEL

The main objective of this model is to divide the spectrum into predetermined bands and proceed to pick out the important frequency components from each of these bands. Therefore, an attempt is made to retain the important low frequency and high frequency information. It was hoped that the important, relatively low magnitude, high frequency components would be represented in this band model.

Now the frequency spectrum is estimated using the discrete Fourier transform. The discrete Fourier transform (DFT) and the inverse discrete Fourier transform (IDFT) are defined by

$$F(k\Omega) = \sum_{n=0}^{N-1} f(nT) \, e^{-j\Omega Tnk} \quad \text{DFT} \qquad (3.32)$$

where k = 0,1,2,...,N-1

f(nt) = n = 0,1,2,...,N-1   Sample Sequence

$\Omega = 2\pi/NT$

T = sampling period

and $e^{-j\Omega Tnk}$, n = 0,1,2,...N-1 the N basis functions.

$$f(nT) = \frac{1}{N} \sum_{k=0}^{N-1} F(k\Omega) \, e^{jTkn\Omega} \qquad \text{IDFT} \qquad (3.33)$$

where $n = 0,1,2,\ldots,N-1$.

Therefore, the basis functions $e^{-j\Omega Tnk}$, $n = 0,1,2,\ldots,N-1$

of the discrete Fourier transform are sampled complex

sinusoids.

The direct computation of the DFT, using

Equation (3.32) and the IDFT, using Equation (3.33), is

very impractical so fast Fourier transform (FFT)

algorithms were developed to greatly reduce the computa-

tions needed to make these transformations. Bergland[14]

has described the basic principals behind the FFT

algorithm.

Once the Fourier transform is taken using the

FFT algorithm, one can calculate the frequency spectrum

by taking the $\log_{10}$ magnitude of the complex coefficients

$F(k\Omega)$, $k = 0,1,2,\ldots,N-1$, giving

$$S(k\Omega) = 10 \, \log_{10} \, |F(k\Omega)| \quad , \quad k = 0,1,2,\ldots,N-1 \qquad (3.34)$$

Now once the nonredundant spectral information is picked

out of the predetermined bands, the model parameters are

·made up of complex Fourier coefficients and the corres-

ponding frequency information. Let the parameters be

defined as Z_i and F_i where the Z_i's are the complex

Fourier coefficients and F_i's are the corresponding

frequency values. Therefore, Z_i and F_i are defined as

$$Z_i = \dot{F}(L\Omega)$$

$$\text{(3.35)}$$

$$F_i = L\Omega$$

where L represents the values of K for which a complex
Fourier coefficient is retained. Figure 13 shows a block
diagram of the procedure followed for this sort of model.
Now the time signal is reconstructed from the Z_i and F_i
parameters in the following manner.

$$\hat{f}(nT) = \sum_{i=1}^{P} R_e(Z_i) \cos(F_i nT) + \sum_{i=1}^{P} I_m(Z_i) \sin(F_i nT) \quad \text{(3.36)}$$

where $n = 0,1,2,\ldots,N-1$

$R_e(Z_i)$ = real part of Z_i

$I_m(Z_i)$ = imaginary part of Z_i

and

$\hat{f}(nT)$ represents the estimate of $f(nT)$ while P repre-
sents the number of Fourier coefficients used in the
estimate, $\hat{f}(nT)$.

3.2.ia SPECTRAL BAND MODEL IMPLEMENTATION

The frequency spectrum was calculated using a
1024 point FFT. Four complete cycles of ECG data were
used for this spectral estimation. Since the four
cycles of ECG data represented less than 1024 sample
points, the difference was made up by adding zeros to
the sample sequence. Since the sampling frequency
used was 250 Hz, then the frequency resolution in the
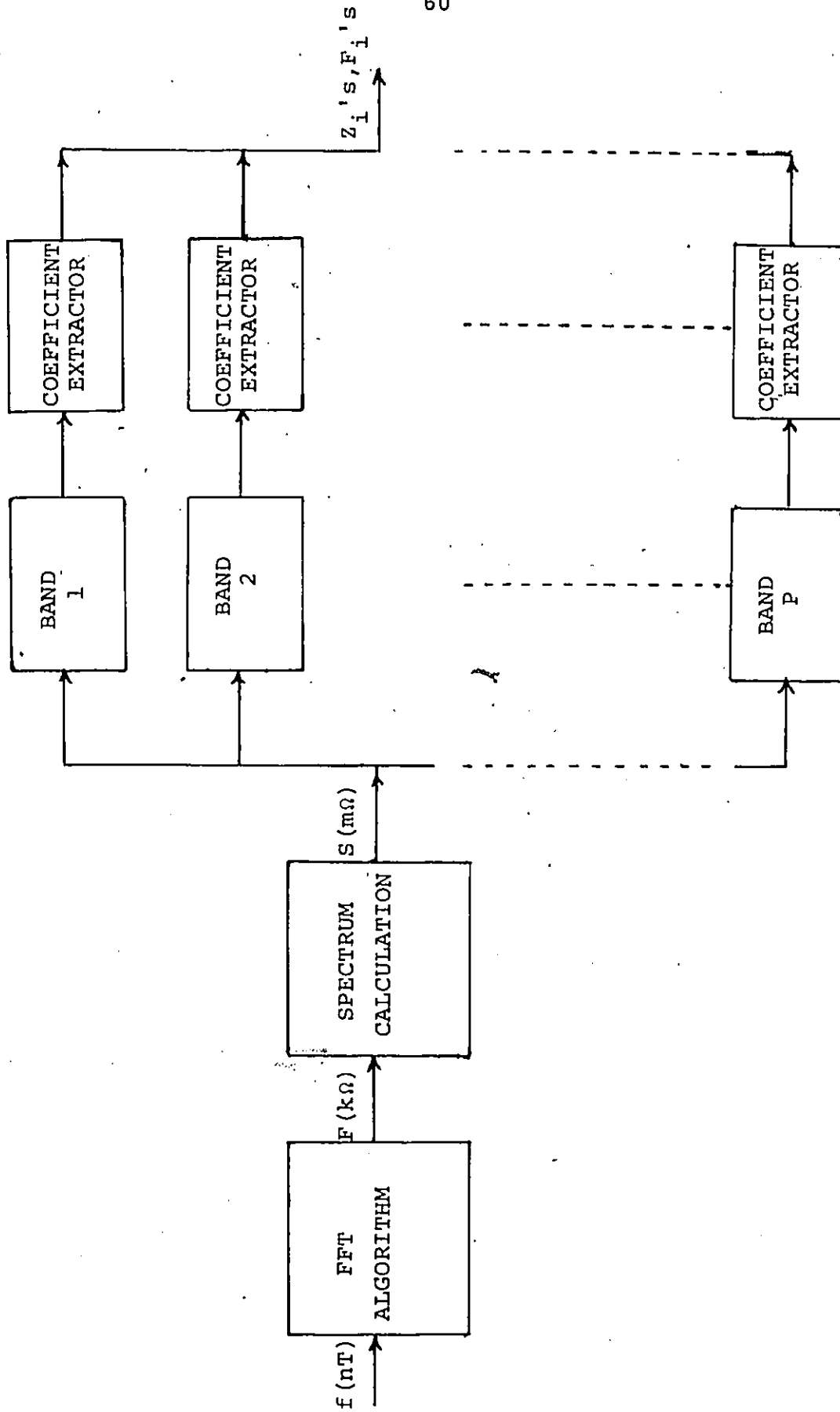
Figure 13. The specral band model.

spectrum was

$$\Delta f = \frac{1}{NT} \simeq 0.25 \text{ Hz} \qquad\qquad (3.37)$$

where N = 1024

      T = sampling interval 1/250 = 0.004 sec.

      Because of the quasi-periodic nature of the ECG signals, it was felt that the ECG spectrum might exhibit some Fourier series characteristics in that the spectrum would have harmonically related spectral peaks. If this were the case, then one could reconstruct the time signal using only the peak coefficients in the inverse transformation. This approach was investigated and it was found that the time signal representation was very oscillatory due to the absence of important frequency components, making this approach unacceptable.

      The spectral band model was then implemented as shown in Figure 13. Now one must decide on the frequency bands to be used in the model. Since the sampling rate was set at 250 Hz, the spectrum had magnitudes up to 125 Hz. Therefore, because the bandwidth of the ECG signal was chosen to be 0 to 100 Hz, it was decided to truncate the spectrum at 100 Hz. Table 3 shows the bands used in the analysis. This choice of bands was based on observations of the ECG spectrum, as well as on an experimental study carried out.

TABLE 3

BAND	BAND FREQUENCY RANGE (Hz)
1	DC to 30
2	30^+ to 50
3	50^+ to 100

Frequency Bands Used in
Spectral Model.

Now, in order to pick out the predominant co-
efficients within each of these bands, threshold levels
were set up within each band. Frequency, components
with magnitudes greater than the threshold were retained
while components with magnitudes less than the threshold
were set equal to zero. Now by adjusting the threshold
level within each band, one can vary the frequency
content of the signal. The parameters of this spectral
model are made up of predominant complex Fourier co-
efficients along with the corresponding frequency infor-
mation, from each of the frequency bands. Now the time
signal is reconstructed by taking the inverse Fourier
transform, using the predominant coefficients and setting
the remaining coefficients equal to zero.

The reconstructed time signal was passed through
a digital smoothing filter to improve the representation.
The input/output relationship of the filter is given by

$$g(nT) = \frac{[a\ f(n-1)T + b\ f(nT) + c\ f(n+1)T]}{a + b + c} \qquad (3.38)$$

where a, b and c are the weighting functions. For this analysis a = 1, b = 4 and c = 1, therefore giving most of the weight to the sample being estimated.

After going through some analysis using this particular spectral model, it was observed that the frequency band from DC to 30 Hz was very sensitive to the omission of frequency information, from this particular band. Furthermore, it was found that in order to get a good reconstruction of the ECG signal, one had to store most of the frequency components from DC to 30 Hz. Therefore, it was decided to retain all the spectral components from DC to 30 Hz. Now since all the spectral components are being retained from DC to 30 Hz, then no frequency information has to be stored for this range. Therefore, the model parameters are made up of complex Fourier coefficients from DC to 30 Hz along with the complex Fourier coefficients and frequency information from the other two bands. This new approach significantly improved the amount of data reduction over that of the previous approach.

Figure 14 shows a block diagram of the steps involved in implementating this final spectral model. The spectrum was normalized for this model so that overall threshold levels could be established for all the data analyzed.
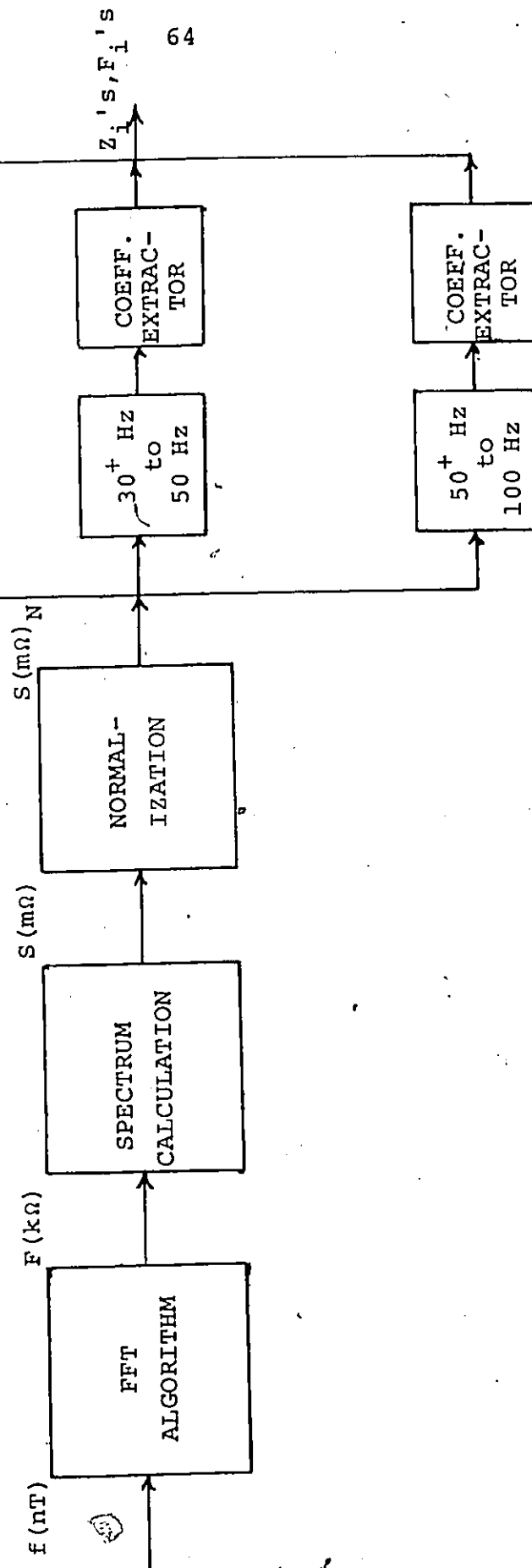
Figure 14. Implemented spectral band model.
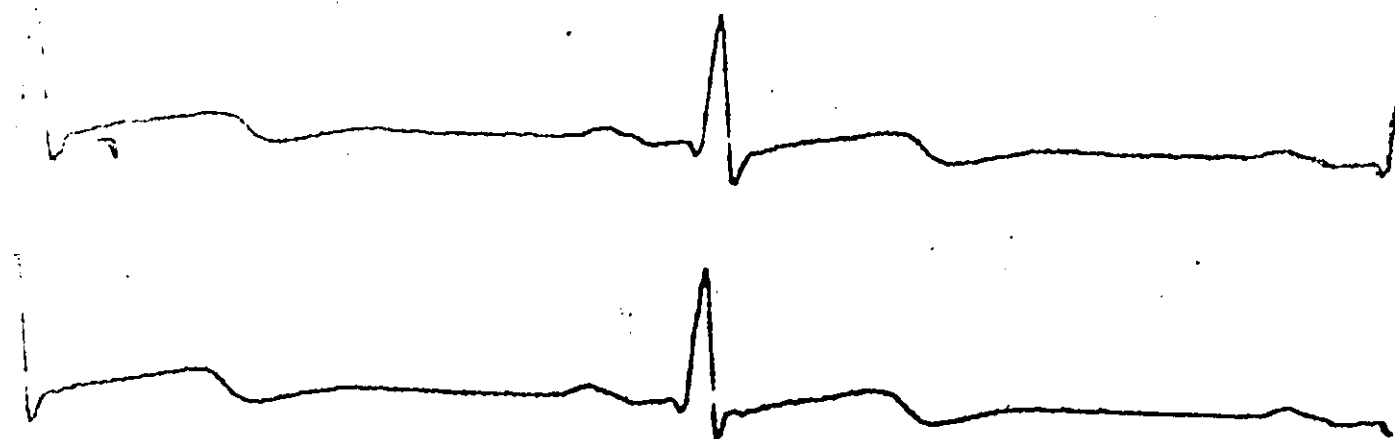
Figure 15a. Original ECG signal (1).
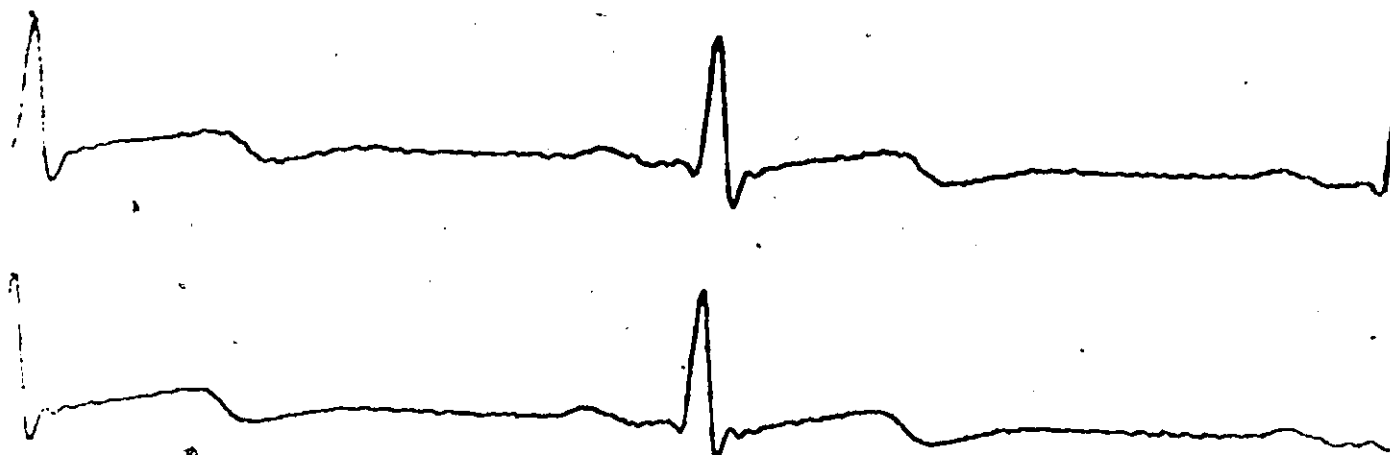
Figure 15b. Reconstruction with 2:1 data reduction (SPECTRAL-
TECHNIQUE).
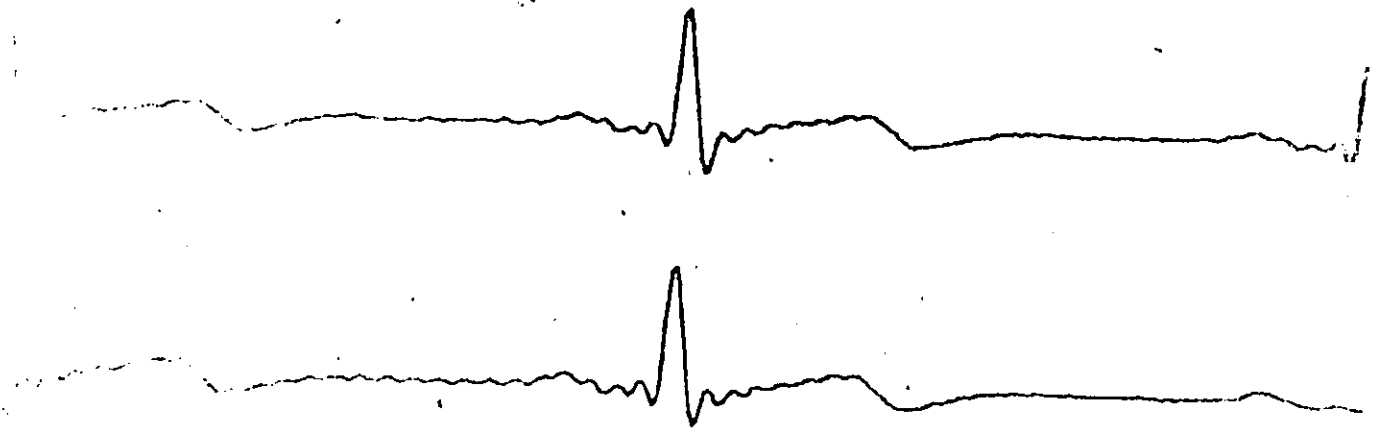
Figure 15c. Reconstruction with 3:1 data reduction (SPECTRAL-
          TECHNIQUE).
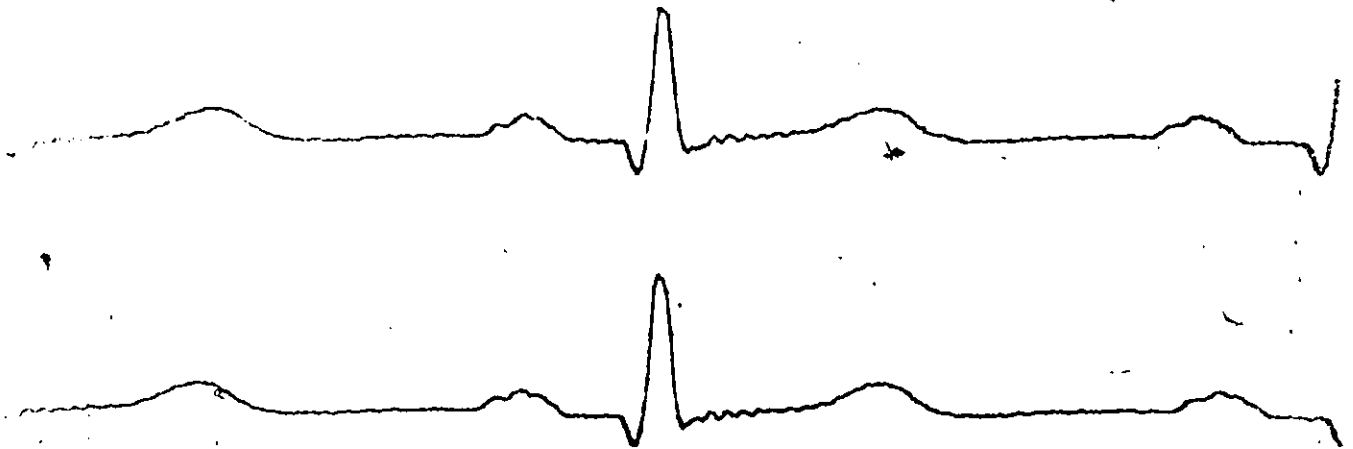
Figure 16a. Original ECG signal (2)
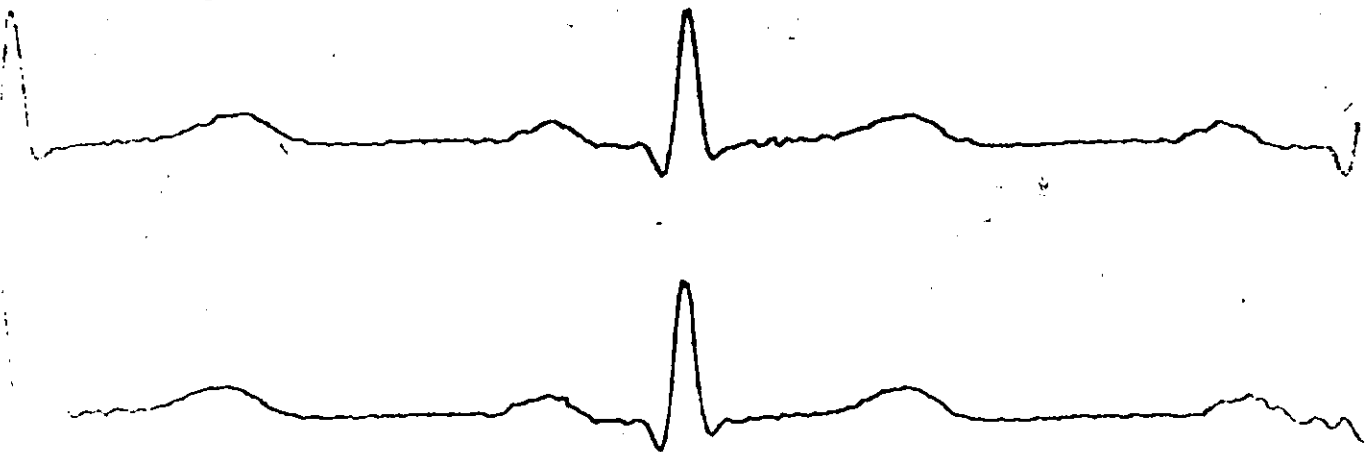
Figure 16b. Reconstruction with 2:1 data reduction (SPECTRAL-
            TECHNIQUE).
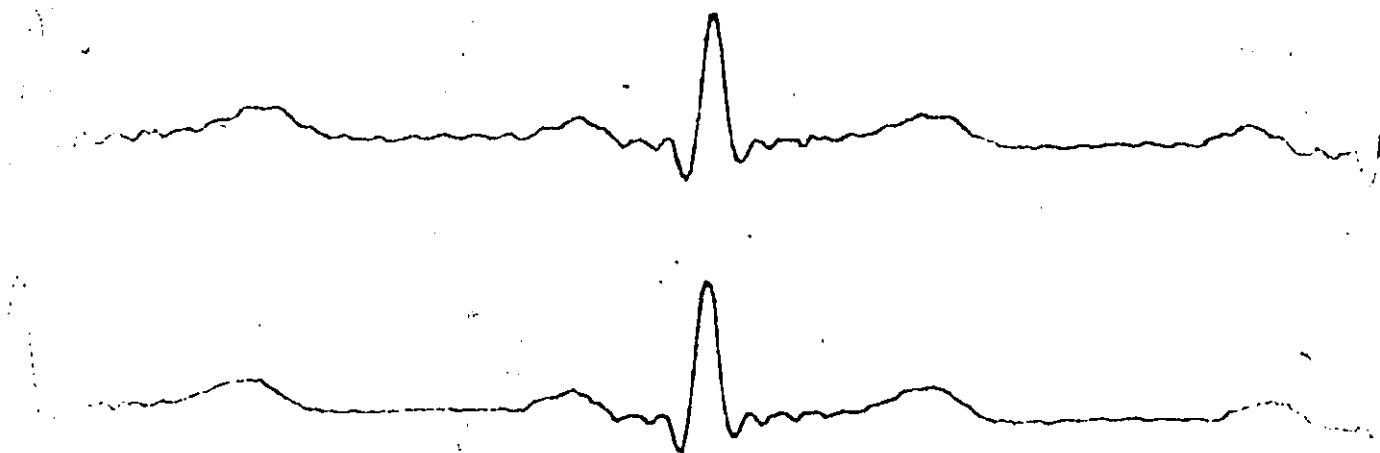
Figure 16c. Reconstruction with 3:1 data reduction (SPECTRAL-
TECHNIQUE).

3.2.ii SIMULATED ECG SIGNALS

Figures 15a,b,c and Figures 16a,b,c show an original ECG signal along with two reconstructions using the spectral technique. Figures 15a and 16a show the original ECG signals. Figures 15b and 16b show the reconstruction with a data reduction of approximately 2:1, while Figures 15c and 16c show the reconstruction with a data reduction of about 3:1.

3.3 SLOPE CHANGE DETECTION TECHNIQUE (SCD-ORG)

The slope change detection technique attempts to approximate a signal by storing only the sample points and corresponding times at which a significant slope change occurs. This technique is similar to a group of techniques known as interpolation compressors, discussed by C.A. Andrews[2] and C.M. Kortman[8].

Let the sample sequence be

$$f_n \quad , \quad n = 1,2,3,\ldots,N \quad\quad\quad (3.39)$$

where the period T has been set to unity to simplify the analysis. The first sample point f_1 is stored to start off the procedure. The following steps outline the procedure.

1. First a reference slope is calculated using the first two sample points giving

$$S_R = f_2 - f_1/\Delta n = f_2 - f_1$$

for $T = 1$ and $\Delta n = 1$.

    2. Now the following slope is calculated using the next two sample points as follows

$$S_L = f_3 - f_2$$

    3. S_L is compared with the reference slope S_R to see if S_L differs by more than a predetermined tolerance level ε. Let the slope change be given by

$$\Delta S_P = |S_R - S_L| \qquad (3.40)$$

    4. If $\Delta S_P < \varepsilon$ then the next slope is calculated giving

$$S_L = f_4 - f_3$$

and ΔS_P is again calculated according to Equation (3.40). Now as long as $\Delta S_P < \varepsilon$, then there is no information stored.

    5. This procedure is continued until the slope change ΔS_P is greater than ε for a particular point $(n = M)$. Now the values $f_m - 1$ and $M - 1$ are stored as parameters. -

    6. Now a new reference slope S_R is calculated using the last stored value and the next sample value giving

$$S_R = f(n) - f(n-1)$$

where $N = M$.

7.   Now consecutive slopes are again checked
against the new reference to see if the slope change
exceeds the tolerance level ε.   The only time sample
points are stored is·when the slope change exceeds the
value ε.

Figure 17 shows the algorithm for the slope
change detection technique. Portions of signal with
slowly varying slopes will be represented by a few stored
values. Figure 18 shows an arbitrary waveform along with
the reconstructed waveform using the slope change
detection technique. Since the stored sample points will
not occur at regular intervals of time, the corresponding
time information must also be stored. Therefore, in order
to get an effective reduction of data, the algorithm must
retain less than one half of the sample points along with
the time values.

3.3.i SIGNAL RECONSTRUCTION

Now the signal can be reconstructed by using the
stored sample points and time information to estimate the
intermediate points. For this analysis, linear
interpolation was used between stored sample points.
Therefore, the intermediate points are estimated as
follows.

Let S_j , $j = 1,2,3,...,M$ Stored Sample Points

And T_j , $j = 1,2,3,...,M$ Stored Time Values

Figure 17. Slope change detection algorithm.
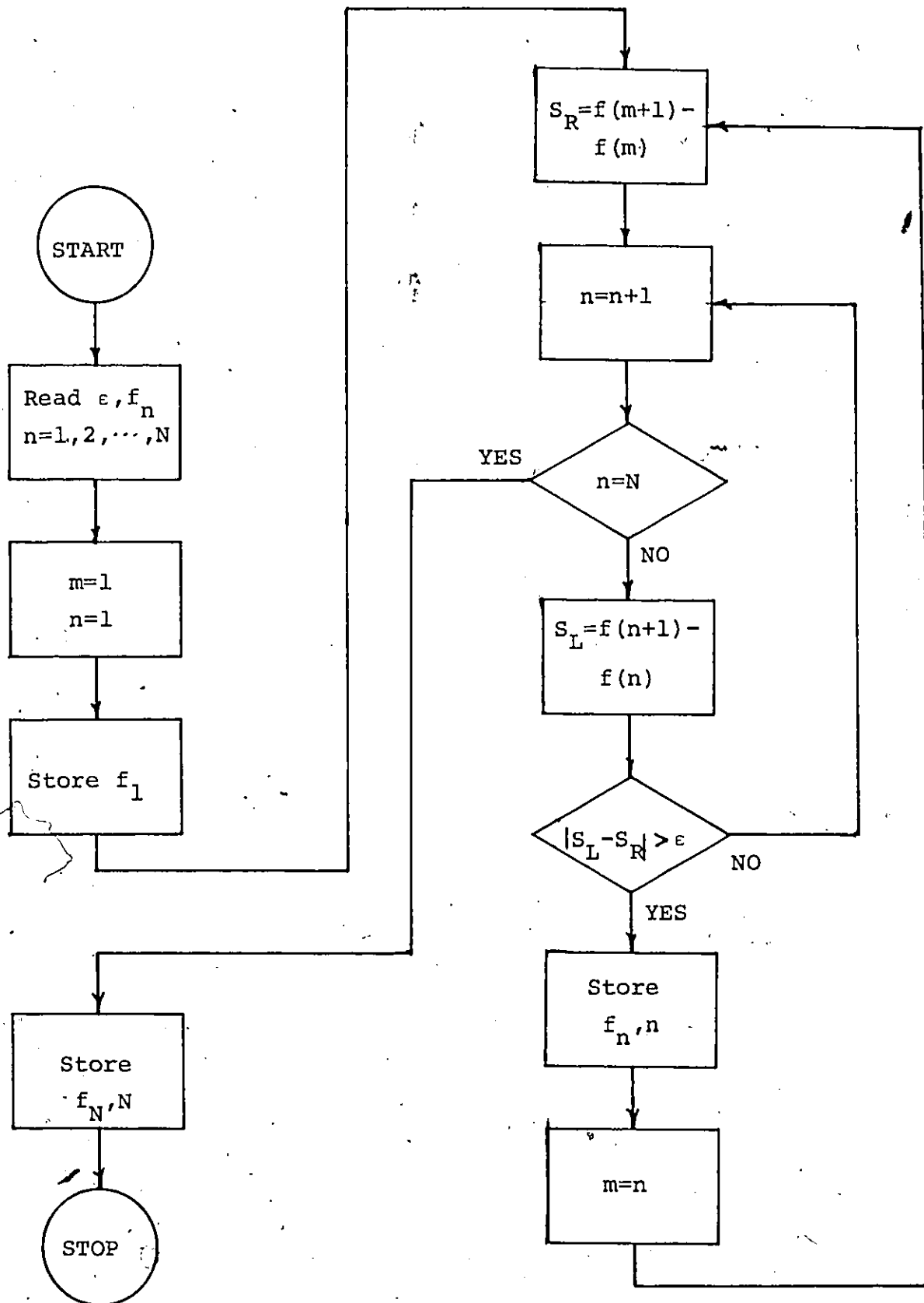
ORIGINAL
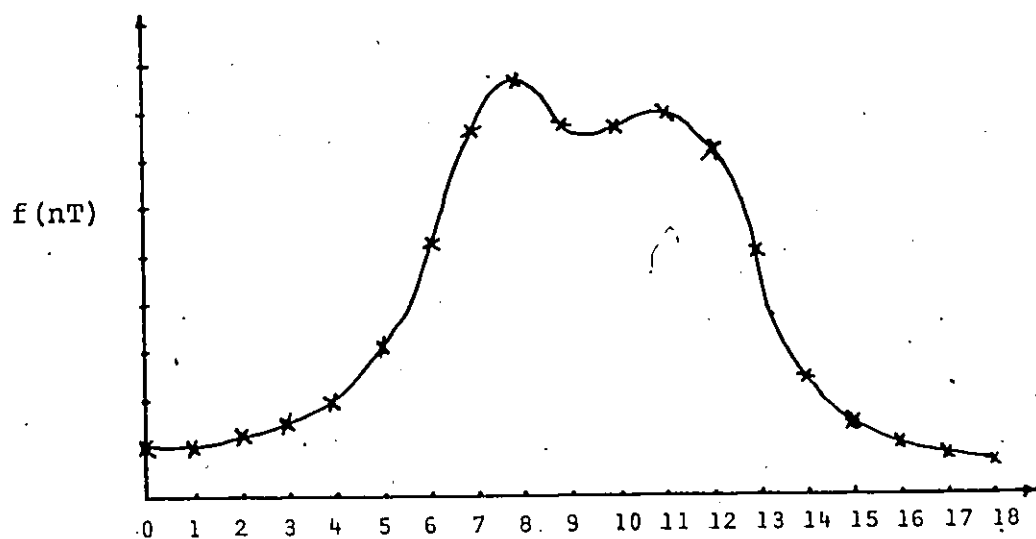
RECONSTRUCTION
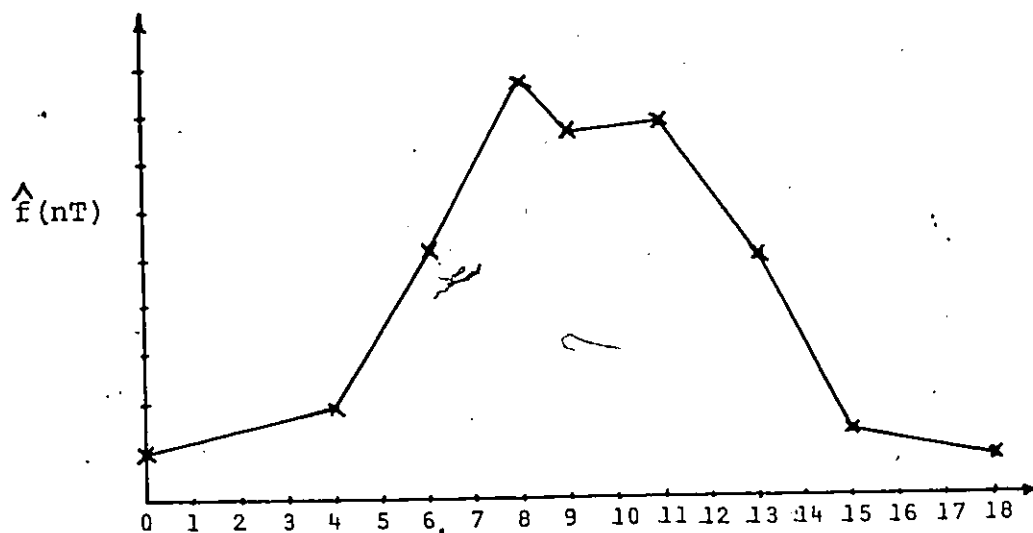
Figure 18. Original waveform and reconstruction using
the slope change detection algorithm.

$$f_n = f_{n-1} + \text{delta} \qquad (3.41)$$

where delta = $S_{j+1} - S_j / T_{j+1} - T_j$, and the number of inter-plated values is equal to $T_{j+1} - T_j$.

It was found that this method was very sensitive to sudden changes in slope and noise components present in the waveform. The former situation causes degradation in the reproduction of the P-wave, which can be seen in Figures 21b,c and 22b,c. The noise components in the waveform cause the algorithm to store many unnecessary sample points, because of the many slope changes. This is evident in the reconstructions of the ECG waveforms shown in Figure 22b,c.

3.3.ii SLOPE CHANGE DETECTION WITH PREFILTERING (SCD-P)

In order to overcome the problems mentioned above, it was decided to apply the slope change detection technique to prefiltered ECG data. The prefiltering in this case was accomplished by passing the ECG signal through a numerical integrator. The integral of the ECG signal is shown in Figure 19 as a slowly varying waveform. Now this waveform is more suited for the slope change detection method.

The integration routine used for the prefiltering was a three-point version of Simpson's rule given by

$$Y_i = \frac{f_{i-1} + 4f_i + f_{i+1}}{3} \qquad (3.42)$$
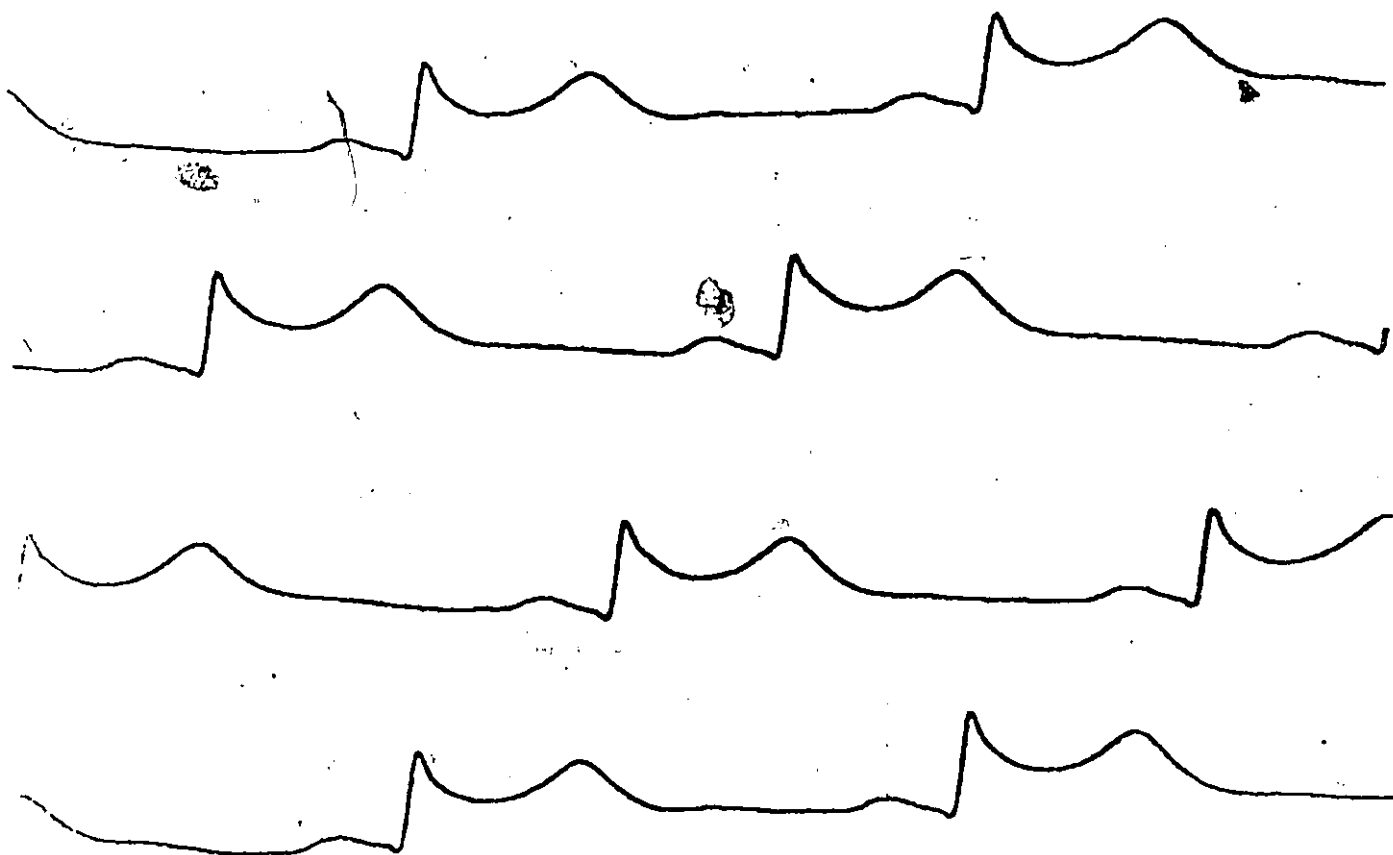
Figure 19. Integral of an ECG signal.

for $\quad f_i, \quad i = 1,2,3,\ldots,N \quad$ Sample Sequence

where Y_i = integrated sample point, and

$\quad Y_1 = 0.0.$

Because the integration Equations (3.42) is a three-point scheme, it was decided to upsample the data by a factor of 2 so that the number of integrated points could equal the number of original points. This up-sampling was accomplished by simply linearly inter-polating between sample points. For more accuracy the original data could have been sampled at twice the established sampling frequency. By doing this the error involved in integrating the signal could have been reduced.

3.3.iia DIGITAL IMPLEMENTATION

Figure 20 shows a block diagram of the steps involved in implementing the slope change detection technique as applied to prefiltered data. Once the data is sampled, the energy of the signal is equalized to some standard so that general threshold levels can be established. One particular set of data was used to equalize the energy in the signals analyzed. The equalization of energy was done in the following manner.

Let $\quad X_i \quad, \quad i = 1,2,3,\ldots,N \quad$ Signal to be Equalized

$\quad Y_i \quad, \quad i = 1,2,3,\ldots,N \quad$ Standard Equalization Signal

First the DC levels are set to zero,
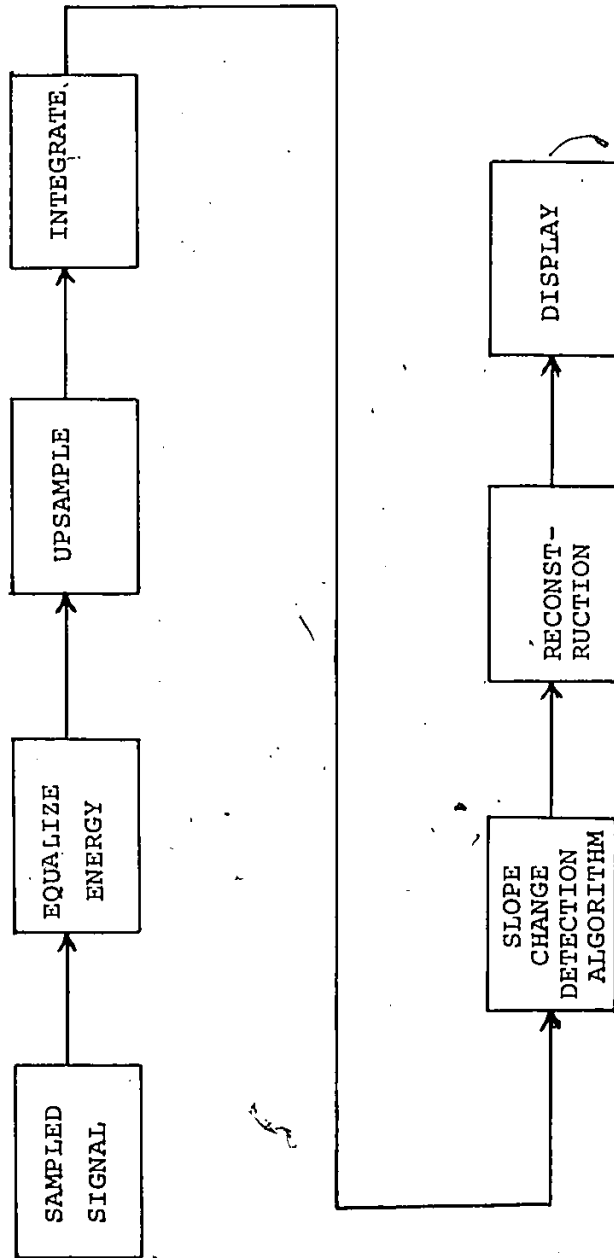
Figure 20. Block diagram outlining the slope change detection technique, with prefiltering.

$$X_i' = X_i - AV1 \quad , \quad i = 1,2,3,\ldots,N \tag{3.43}$$

where $AV1 = \dfrac{1}{N} \sum\limits_{n=1}^{N} X_n$

and $Y_i' = Y_i - AV2 \quad , \quad i = 1,2,3,\ldots,N \tag{3.44}$

where $AV2 = \dfrac{1}{N} \sum\limits_{n=1}^{N} Y_n$.

Now the energy of X_i is equalized to that of Y_i as follows

$$X_i'' = X_i' \cdot \text{ratio} \tag{3.45}$$

where

$$\text{ratio} = \text{SQRT} \left[\frac{\sum\limits_{n=1}^{N} Y_n'^2}{\sum\limits_{N=1}^{N} X_n'^2} \right]$$

The signal is then upsampled to 500 Hz and integrated using Equation (3.42). Since the slope change detection algorithm estimates the signal by constant slopes, one finds that these constant slopes represent constant values on the reconstructed signal. Therefore, the slopes rather than sample points, are stored along with the time information. The slope value at the intersection of two slopes is estimated as the average of the two slope values on either side. Therefore, the reconstructed signal is made up of constant levels corresponding to the constant slopes and the level transition values are estimated as the average of the

two consistent levels. Therefore, the final parameters
of the model are made up of constant level values and
the time information.

3.3.iii SIMULATED ECG SIGNALS

Figures 21a,b,c and 22a,b,c, show the original
signal along with the reconstruction using the slope
change detection technique, as applied to the time signal.
Figures 23a,b and 24a,b show the reconstructions using the
slope change detection technique as applied to the pre-
filtered data. The figures with subscripted b are re-
constructions with 2:1 reduction of data, while the
figures with subscripted c are the reconstructions with
a 3:1 reduction of data.
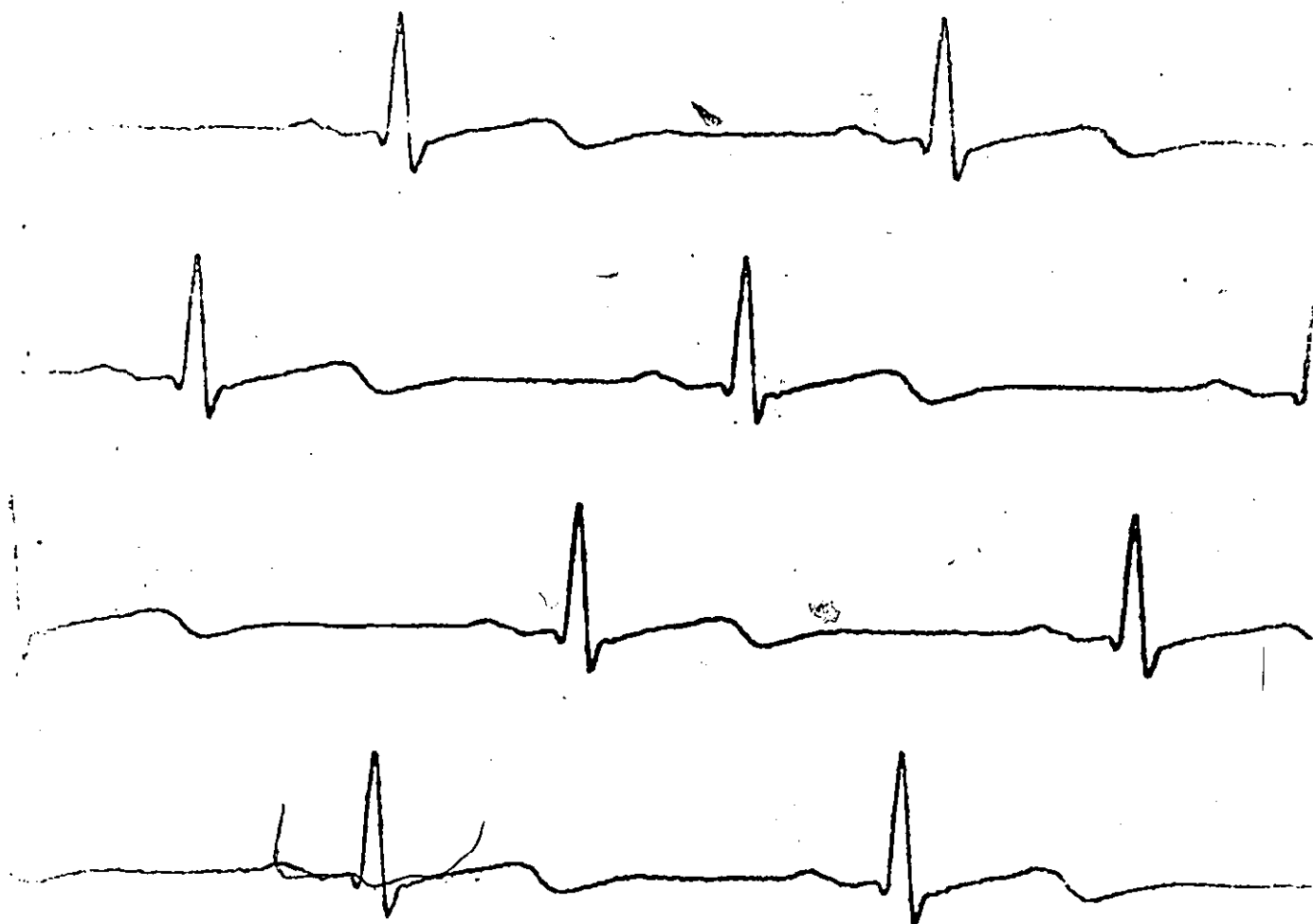
Figure 21a. Original ECG signal (1).
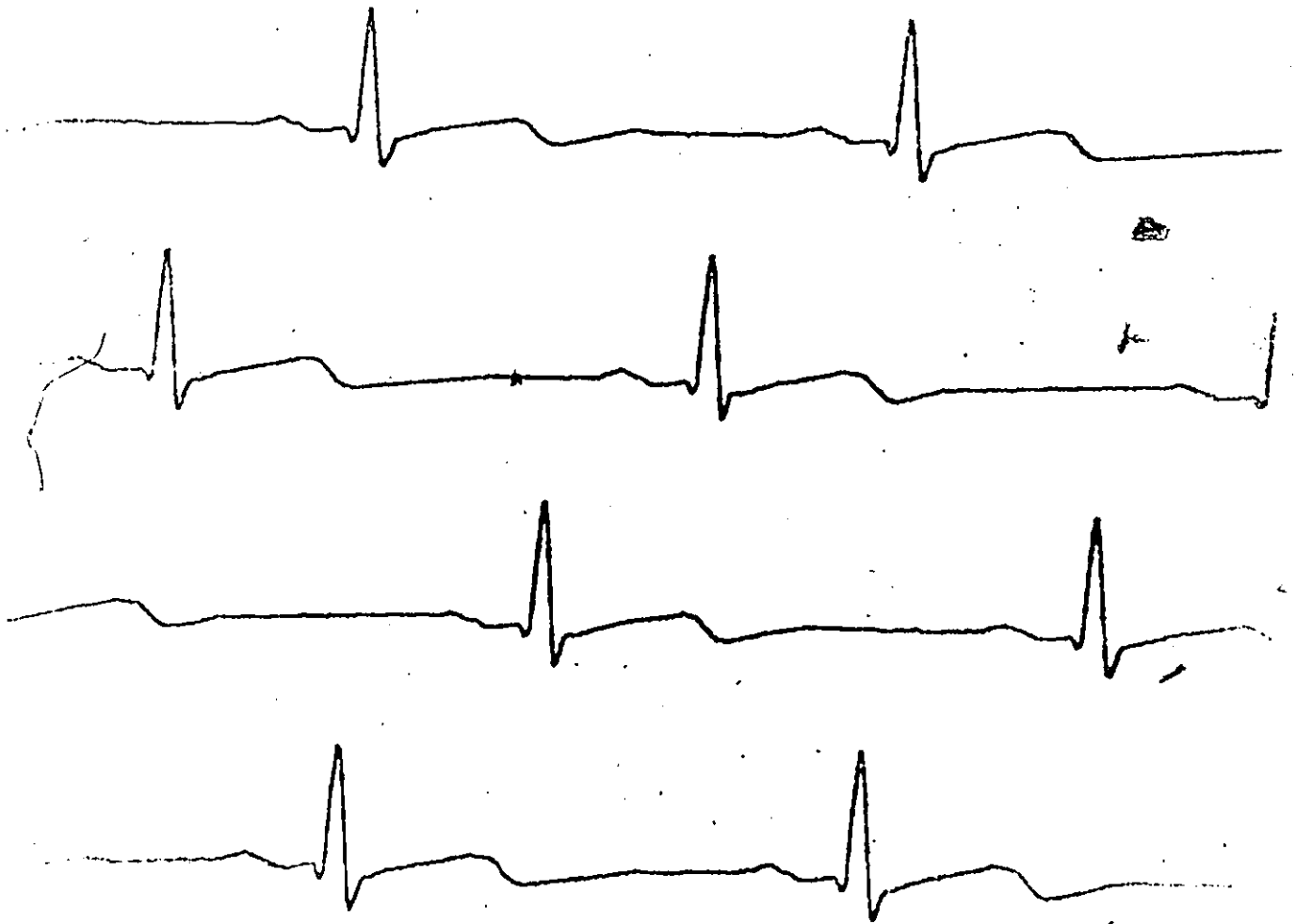
Figure 21b. Reconstruction with 2:1 data reduction (SCD-ORG).
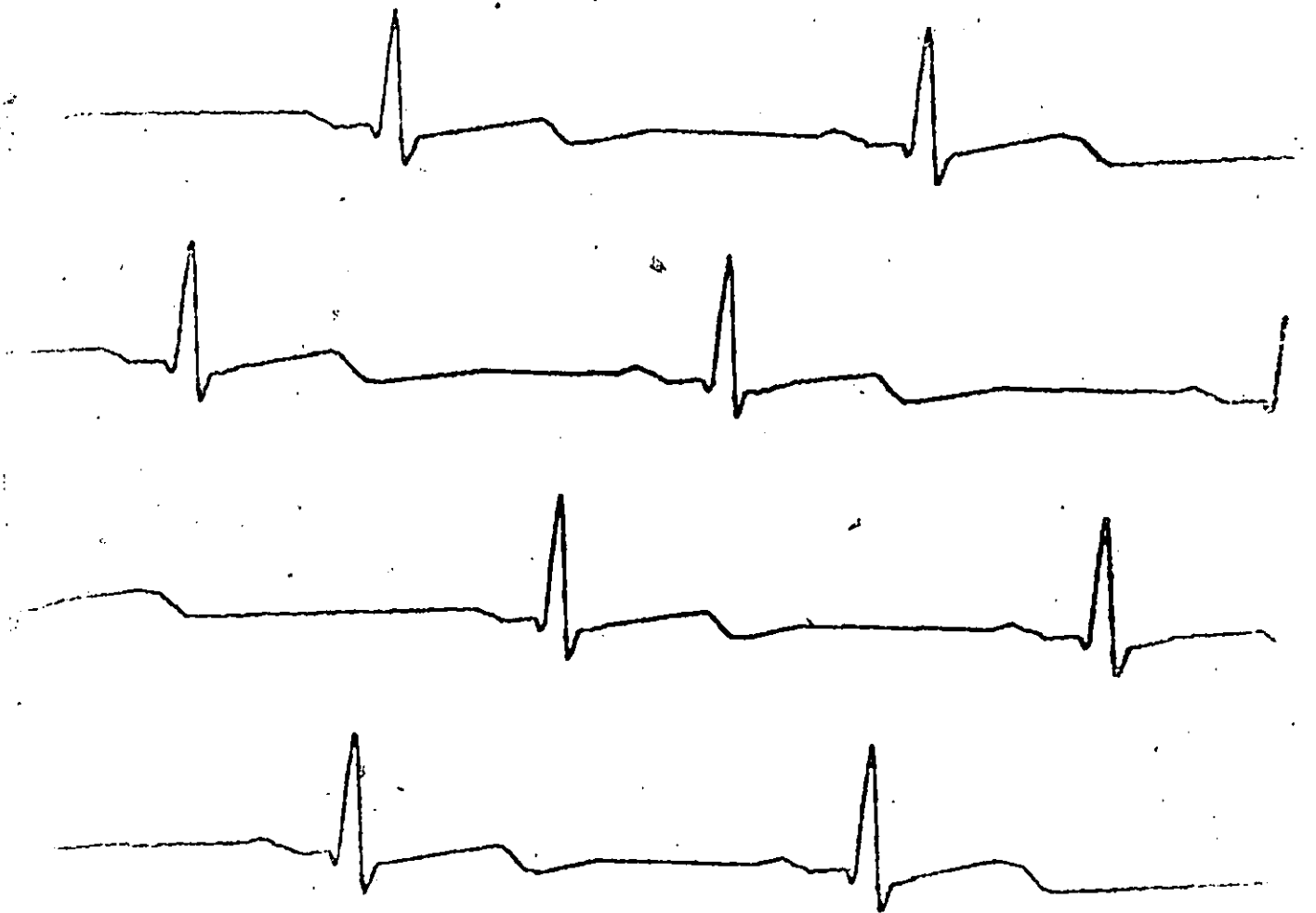
Figure 21c. Reconstruction with 3:1 data reduction (SCD-ORG).
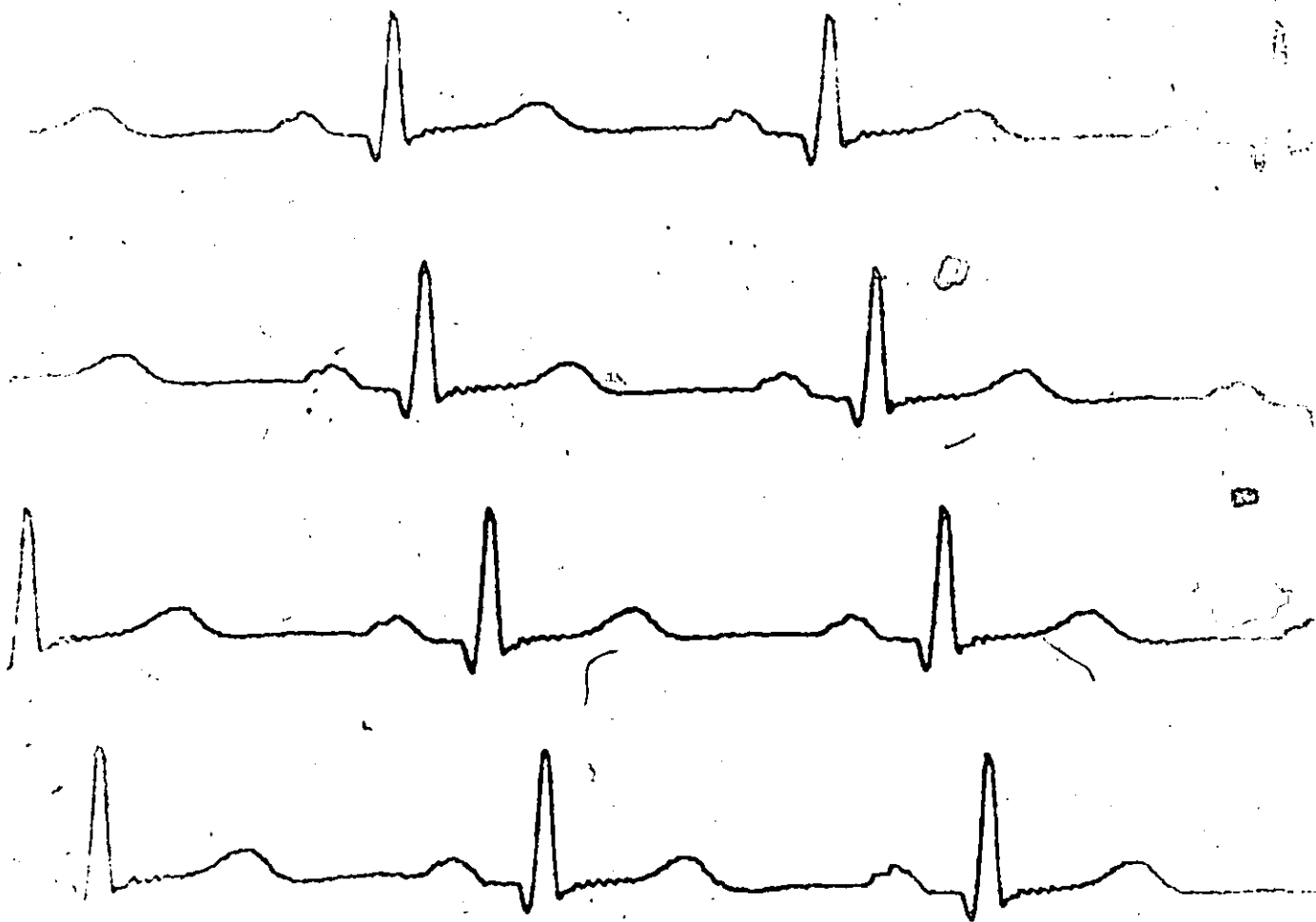
Figure 22a. Original ECG signal (2).
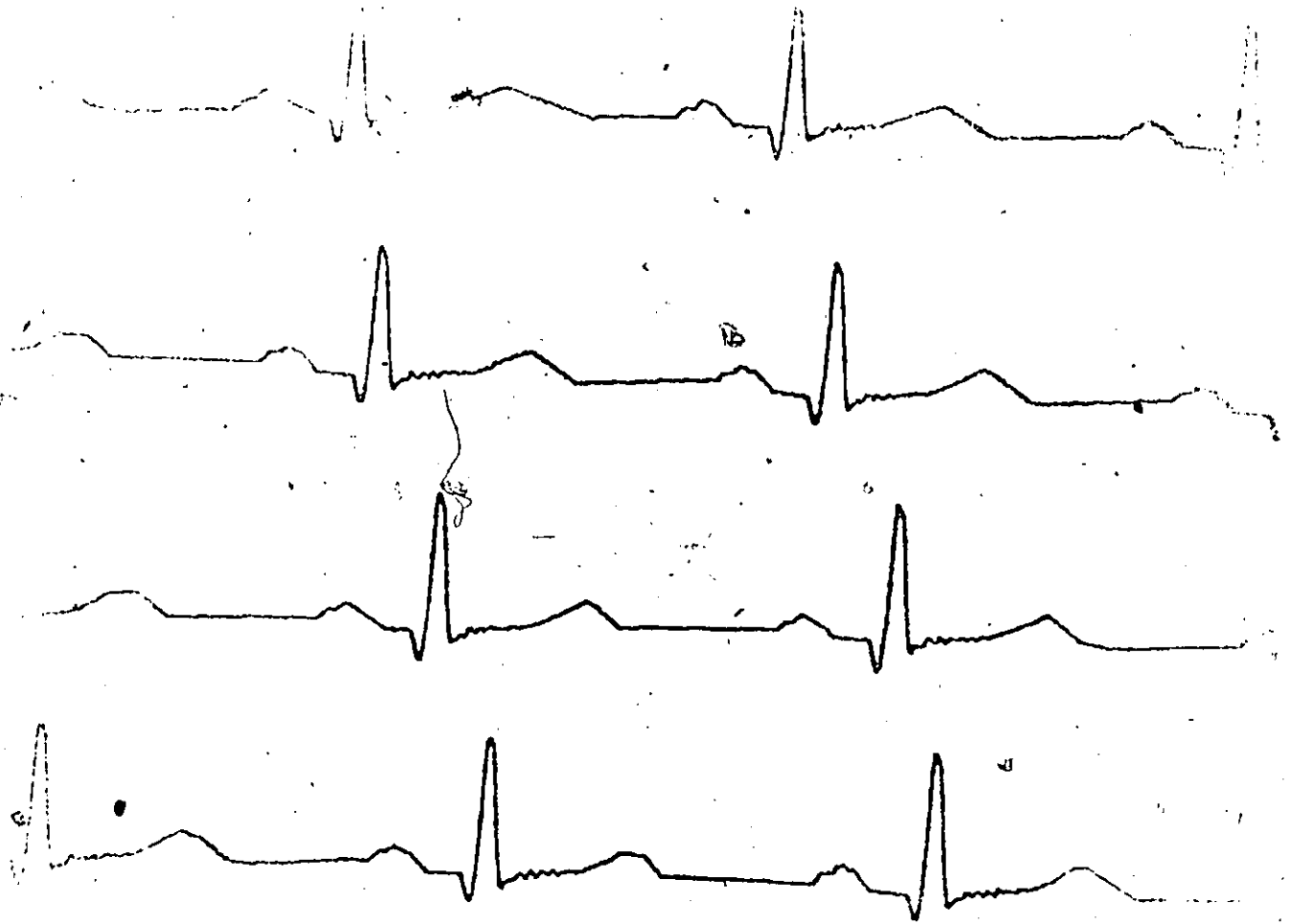
Figure 22b. Reconstruction with 2:1 data reduction (SCD-ORG).

Figure 22c. Reconstruction with 3:1 data reduction (SCD-ORG).
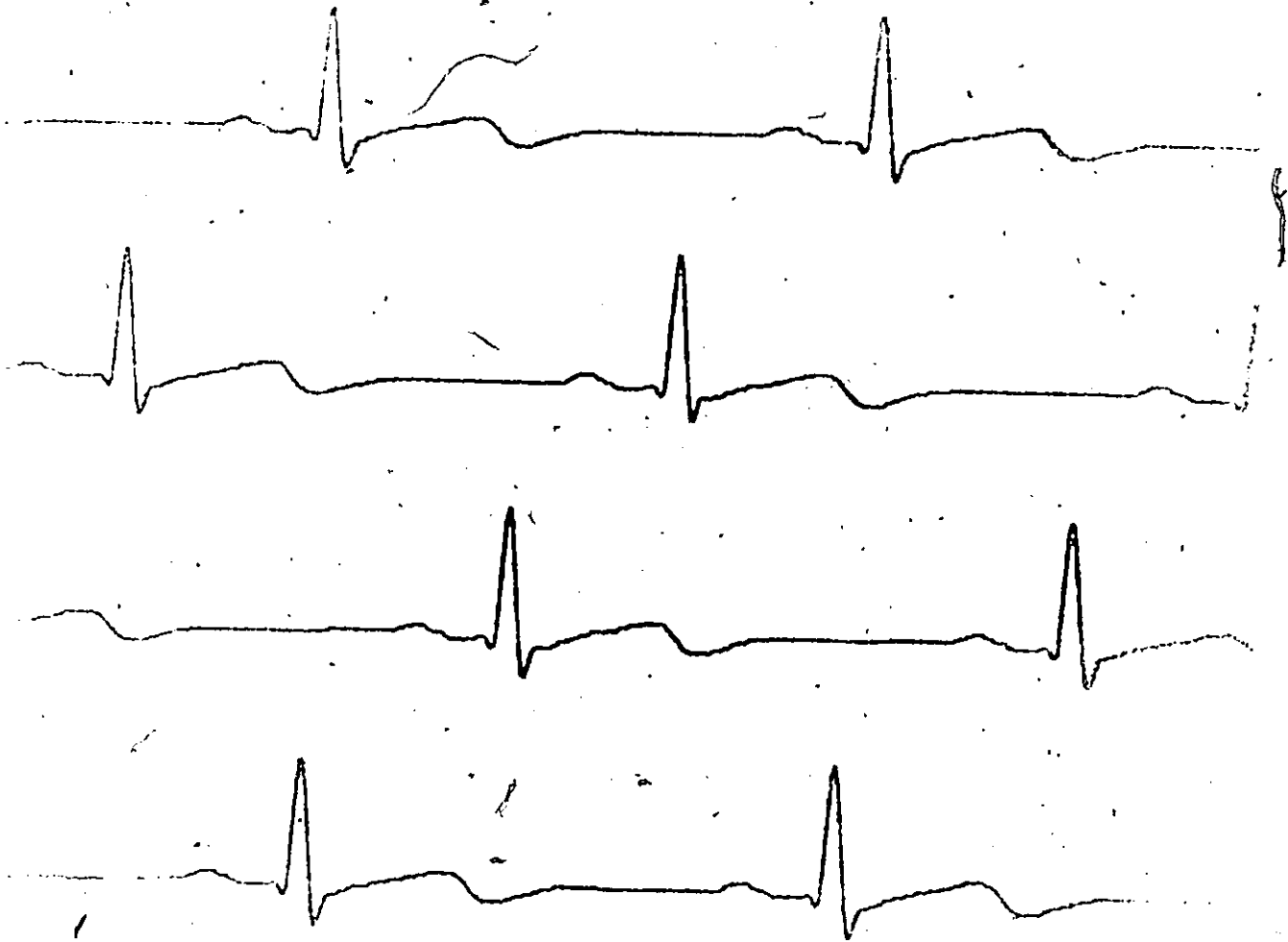
Figure 23a. Reconstruction With 2:1 data reduction (SCD-P).
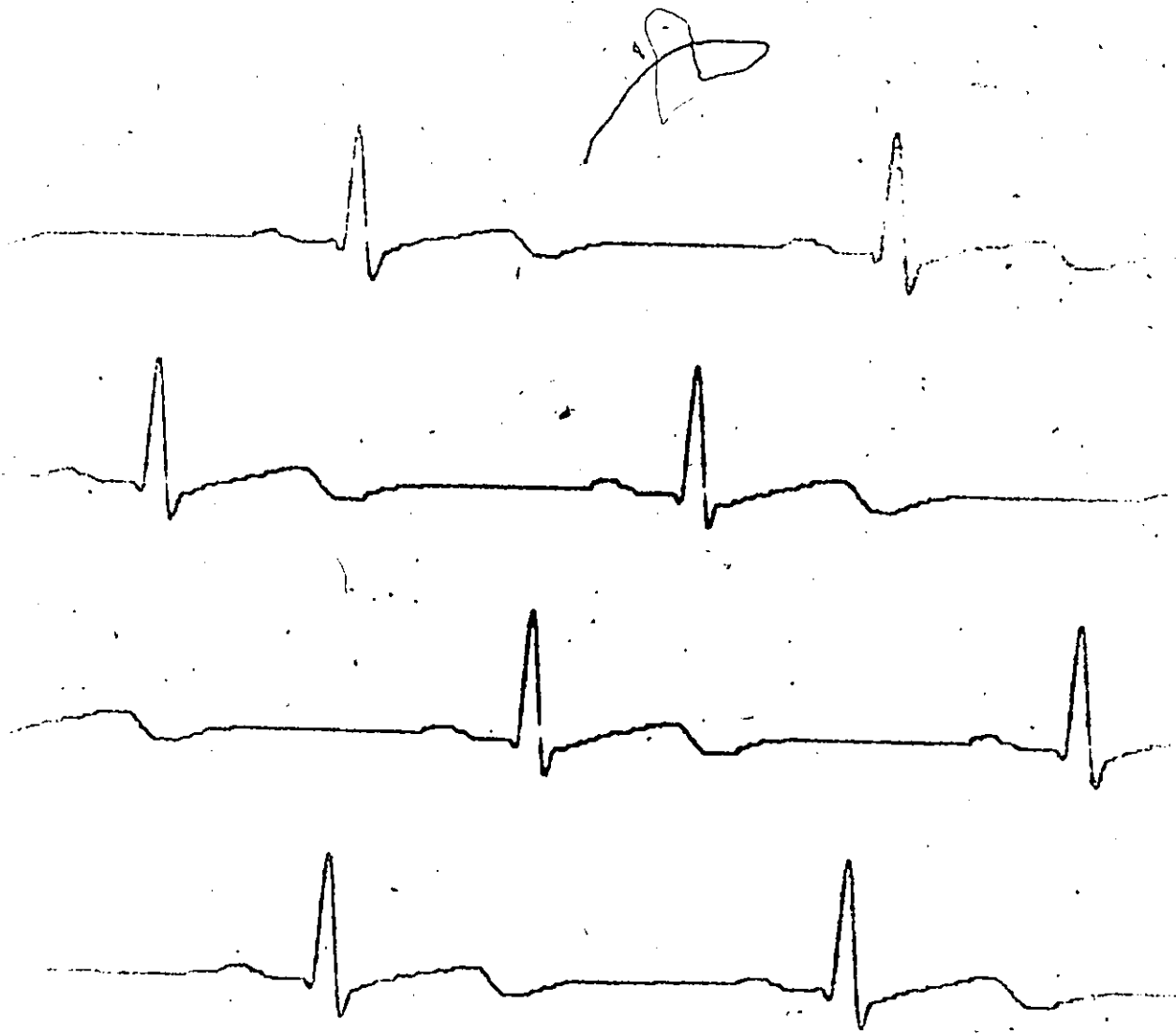
Figure 23b. Reconstruction with 3:1 data reduction (SCD-P).

88
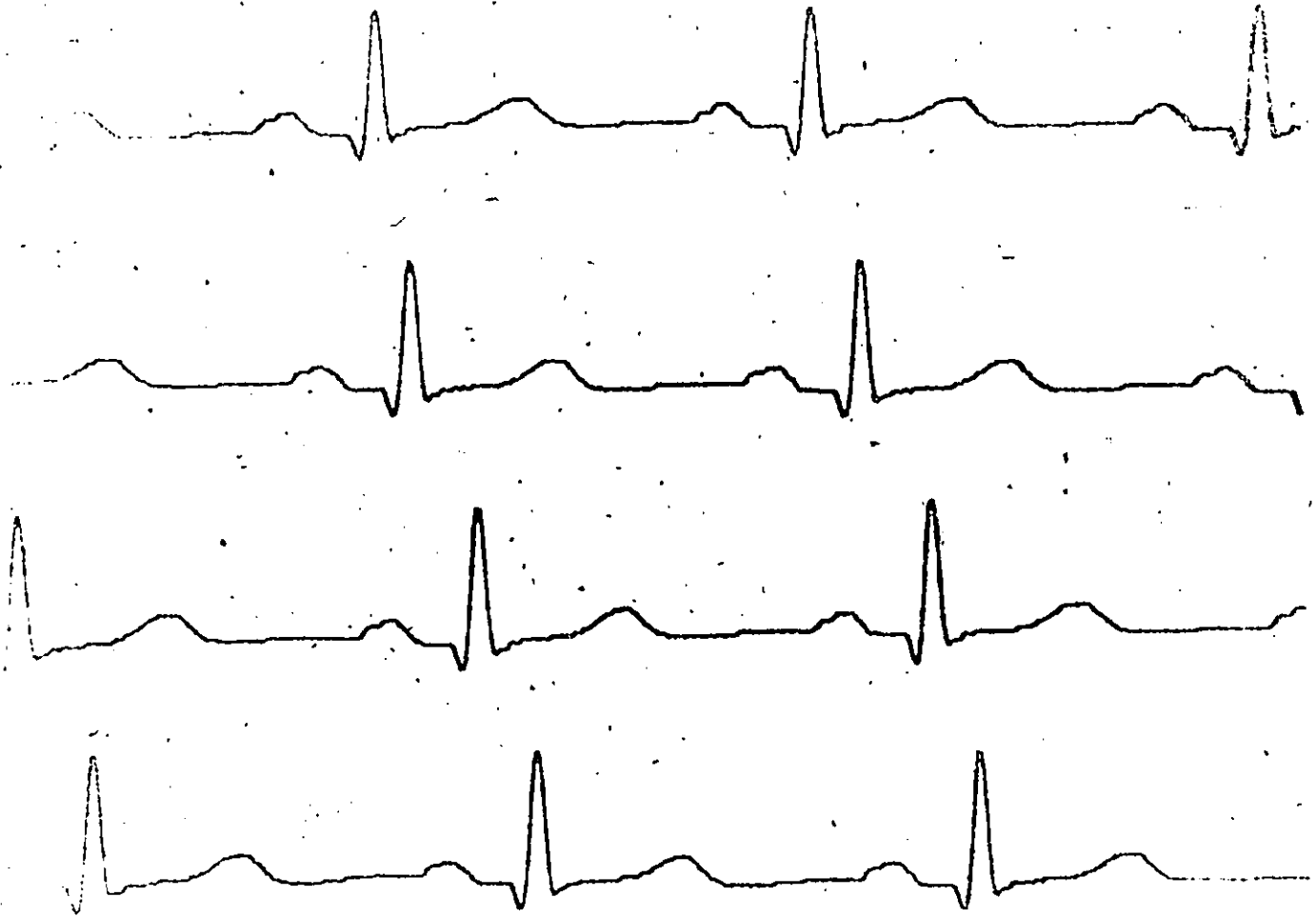
Figure 24a. Reconstruction with 2:1 data reduction (SCD-P).
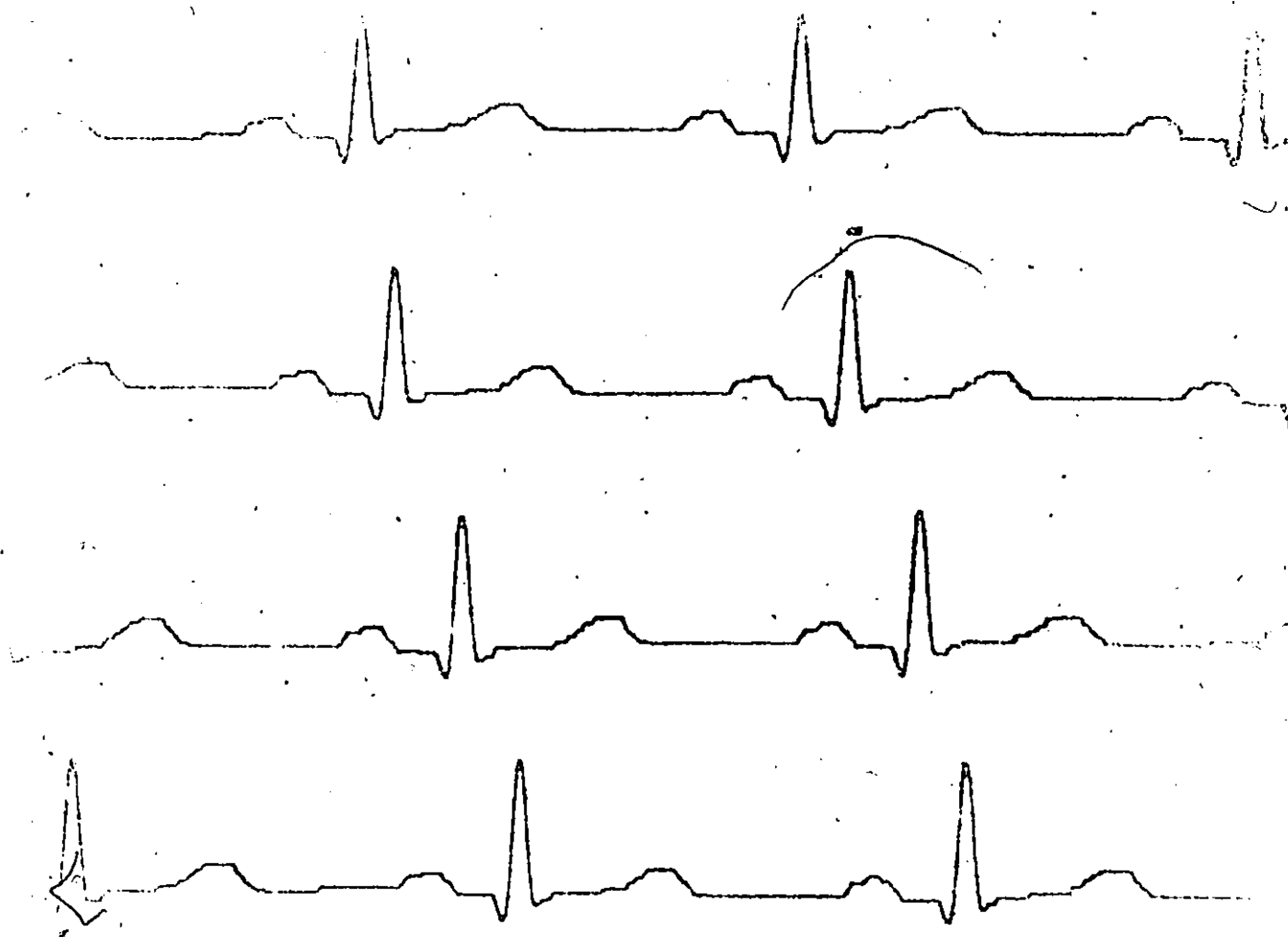
Figure 24b. Reconstruction with 3:1 data reduction (SCD-P).

CHAPTER IV

COMPARISON OF ORIGINAL AND RECONSTRUCTED SIGNALS

4.1 EVALUATION CRITERIA

The techniques investigated were compared on a
mean squared and peak error basis, as well as on a visual
basis. It was hoped to keep the mean squared and peak
errors within 1% and 5% respectively, since reproductions
with errors above these limits were normally visually
unacceptable. The mean squared error is calculated as
follows

$$e_m = \frac{1}{N} \sum_{n=1}^{N} (f_n - \hat{f}_n)^2 \qquad (4.1)$$

where f_n, n = 1,2,3,...,N   original sample sequence

$\hat{f}_n$, n = 1,2,3,...N   reconstructed sample sequence

For this analysis the percentage mean squared error in
the reconstruction was used rather than the mean squared
error described by Equation (4.1). The percentage mean
squared error was given by:

$$\% \, e_m = \frac{e_m}{\frac{1}{N} \sum_{n=1}^{N} f_n^2} \times 100 \qquad (4.2)$$

Since the percentage mean squared error, (% MSE),
is an average error figure, some reconstructions may have
relatively low % MSE values yet still exhibit large peak

errors over a small interval. Therefore, these large peak errors in the reconstructed waveform may cause the reconstruction to be unacceptable, if they occur at diagnostically critical points in the ECG waveform. Thus, it was decided to calculate the percentage peak error for each of the reconstructed waveforms. The percentage peak error is defined by

$$\% \ E_p = \frac{e_p}{f_{n_{max}} - f_{n_{min}}} \times 100 \ . \tag{4.3}$$

where $e_p = |f_n - f_n|_{max}$

and $\quad f_{n_{max}}$ = largest value in the sequence

$f_{n_{min}}$ = smallest value in the sequence

Since the ECG signal must be diagnosed on a visual basis, it is only natural that the final decision, as to whether the reconstructed waveform is acceptable or not, should be based on the visual fidelity of the reconstruction. One might find that a particular reconstruction is acceptable, while another is unacceptable, from the visual standpoint, yet they both may have similar % MSE and peak errors. It all depends on how well the diagnostically significant features are represented in the reconstruction.

4.2 ERROR ANALYSIS

Figures 25 and 26 show the % MSE and peak error versus reduction factor plots respectively, for all the techniques investigated. The reduction factors in this case are calculated as the total number of sample points versus the total number of model parameters needed to represent this data. It can be seen from Figure 25 that the slope change detection technique, applied to pre-filtered ECG data gives the best % MSE versus reduction factor for reduction factors above about 1.7. The linear prediction model proved to be very sensitive to the number of times the quantized average error was updated each cycle. This seemed to be due to the quazi-periodic nature of the signal. For each set of data a new optimal number of updates had to be found. It was also observed that certain cycles of a particular data set would be reconstructed relatively well, while other cycles were oscillatory. This was due to the period changes that occur within a set of sampled ECG data. This was evident in the reproductions shown in Figures 11b,c and 12b,c of the previous chapter. Therefore, Figure 25 shows that for one particular % MSE value one can get more than one reduction factor.

It can be seen in Figure 26 that the peak error for the slope change detection technique, as applied to prefiltered data, is below 5% for reduction factors up to about

Figure 25. %MSE versus reduction ratio curves.

* Linear Prediction
X Slope Technique (No Prefiltering)
O Spectral Technique
• Slope Technique With Prefiltering
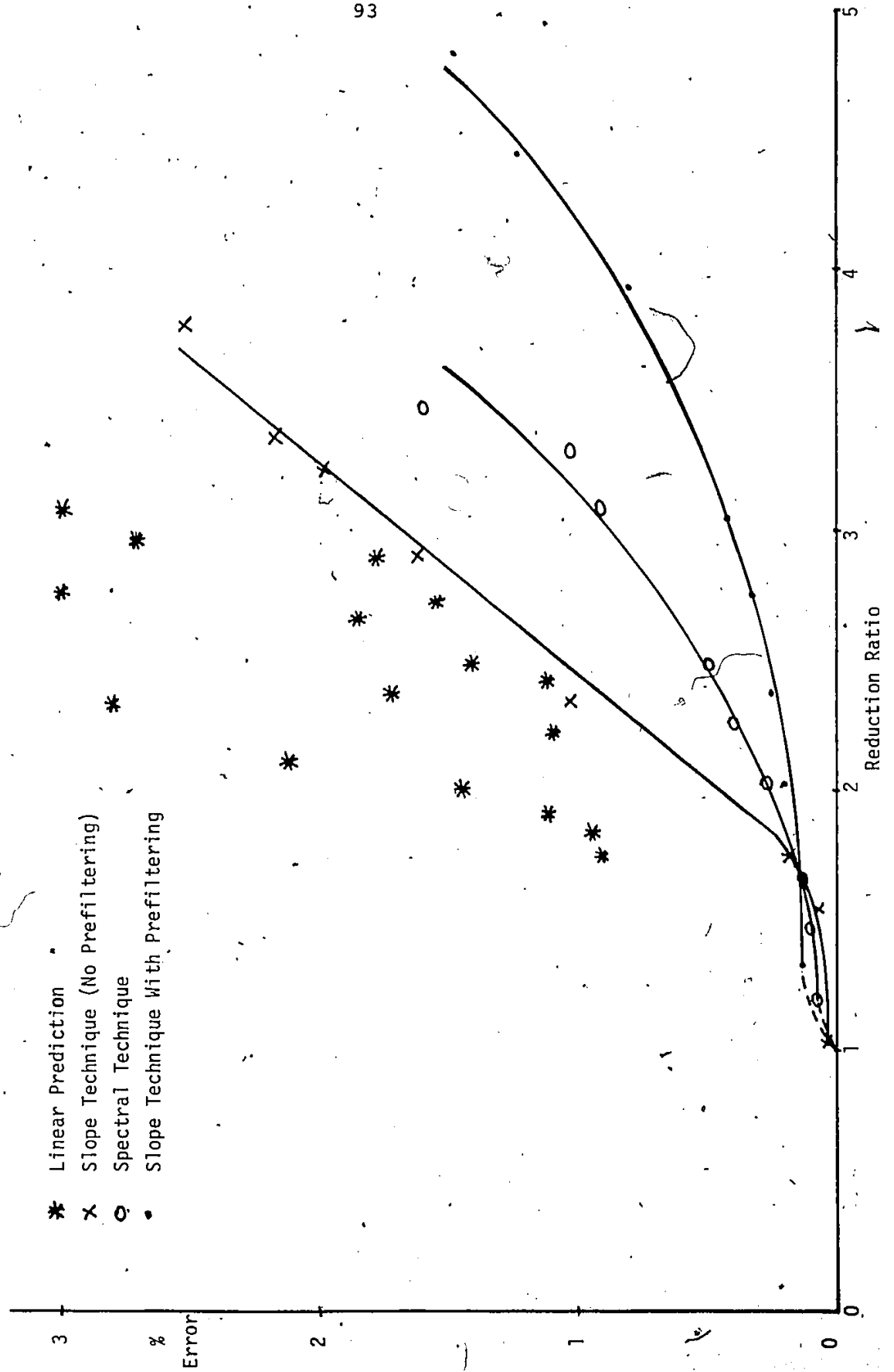
Figure 26. %Peak error versus reduction ratio curves.

x   Slope Technique (No Prefiltering)
o   Spectral Technique
·   Slope Technique With Prefiltering
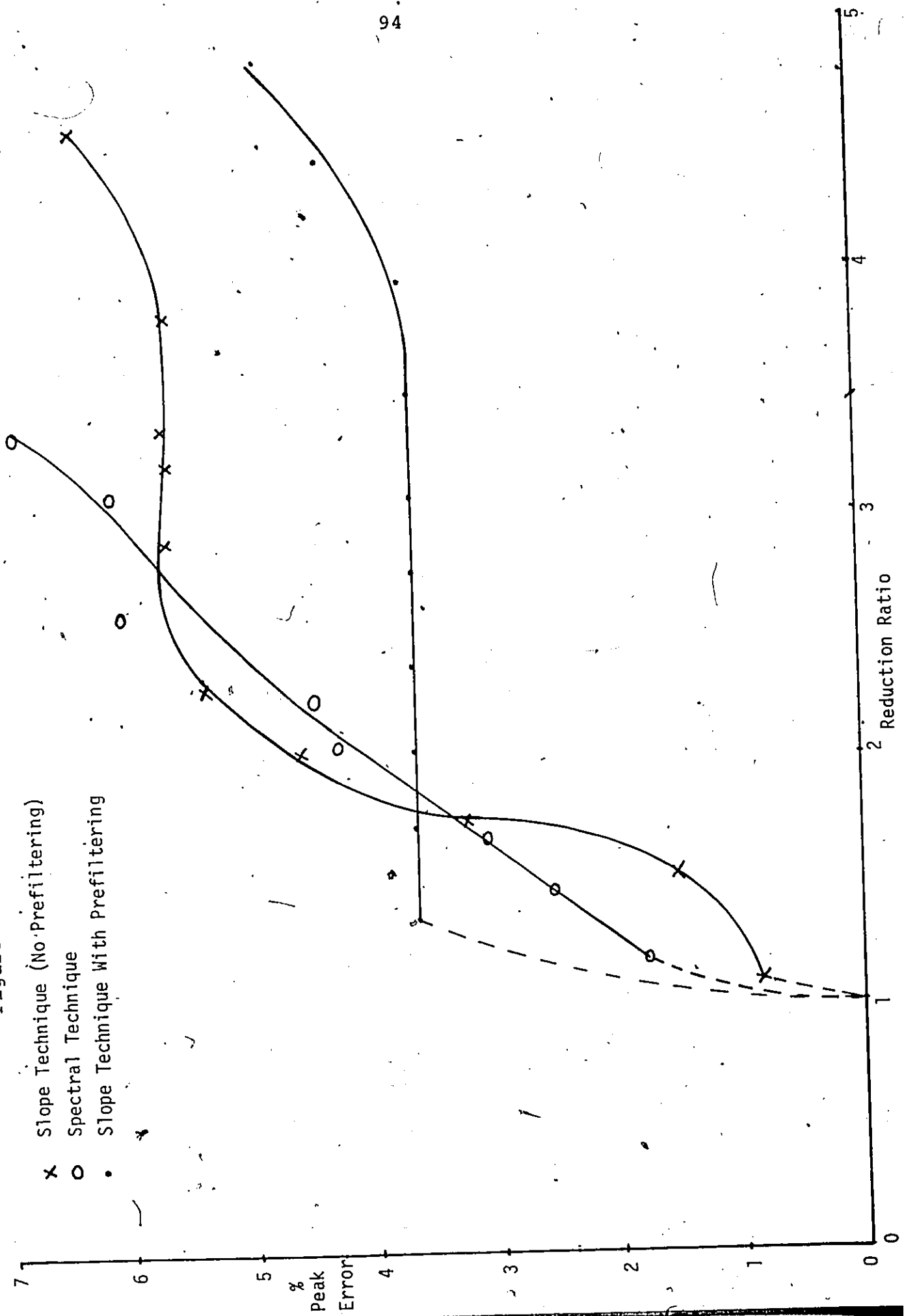
5. The peak error for lower reduction factors remained relatively constant. These peak errors were due to the error involved in numerically integrating the signal and also because of the averaging which takes place in the reconstruction process. These errors showed up as slight depressions of the Q, R and S wave, which were not evident until the plot was expanded to exaggerate these errors. The peak error curve for the slope change detection technique (without prefiltering) shows a fast rise in the peak error values for reduction factors between about 1.8 to 2.5. This is due to the approximations used between the end of the T-wave and the onset of the Q-wave.

Figures 27 and 28 compare the four main techniques with two original sets of data. For these reproductions the reduction factor is about 3. One finds that the linear prediction with DPCM and the spectral method reproductions are oscillatory in nature. These oscillations in the spectral technique reproductions are due to the absence of important frequency information. This problem can be corrected by lowering the threshold levels to include the missing frequency components. The oscillations in the linear prediction reproductions is caused mainly by the 1 bit error quantization scheme implemented. The slope change detection technique, as applied to the original ECG signal, represents the Q, R and S waves well but makes gross approximations in the T-P interval, for large threshold values. This error

Original Signal (1)

LP-DPCM

Spectral Technique

SCD-ORG

SCD-P

Figure 27. Original ECG signal (1) compared with the reconstructions
using the four techniques analyzed (3:1 data reduction).

Original Signal (2)

LP-DPCM

Spectral Technique

SCD-ORG

SCD-P

Figure 28 . Original ECG signal (2) compared with the reconstructions
using the four techniques analyzed (3:1 data reduction).

makes the onset of the P-wave impossible to determine to
any acceptable degree of accuracy. Also, when noise is
present in the signal, this technique tends to store
most of the noise samples which reduces the reduction
factors for a given threshold value. This is evident in
Figures 21a,b. The slope change detection technique as
applied to prefiltered data represents all portions of
the ECG waveform well. This technique is not sensitive
to noise components in the ECG signal. By approximating
the integrated version of the signal using the slope
change detection technique, one is filtering out the high
frequency noise.   This technique was applied to ECG data
with relatively high level noise and it was found that
for reduction factors above about 2 the reproductions
compared very close to those obtained using ECG signals
with relatively low noise components.

4.3   DISCUSSION

Overall, it was felt that the slope change
detection technique, as applied to the prefiltered data,
gave the best reconstructs of all the techniques inves-
tigated. All the ECG waves were well represented using
the slope technique with prefiltering, for reduction
factors below about 3. It was also found that this
technique tended to filter out noise components present
in the original sampled signal. The slope technique
also has the advantage that the analysis can be started

at any portion of the ECG signal, which was not the case
for the linear prediction or spectral technique. The
Q-wave of the ECG signal had to be detected before the
linear prediction or spectral technique could be applied.

The slope change detection technique, with pre-
filtering was compared to a straight piece wise
approximation of the ECG signals and it was found that
the errors were about 70% higher for the piece wise constant
approximation, for comparable reduction factors. This
was mainly due to the averaging which takes place in the
slope change detection technique with prefiltering, to
come up with the time representation.

Since the slope change detection technique, with
prefiltering, proved to be the best technique of the
one's investigated, it was decided to do a quantization
study of this technique. Now by quantizing the original
sample points, one can compare the slope change detection
technique, as applied to prefiltered data, with the
quantized original samples, on a bits/sample basis.

CHAPTER V

QUANTIZATION STUDY

It was found in Chapter IV that the slope change detection technique, as applied to prefiltered data gave the best data reduction of all the techniques studied. The reduction factors were based on the total number of model parameters needed to reconstruct a set number of original sample points. It was then decided to do a quantization study on the original sample points to see how many bits/sample are needed to represent this data in the sampled form. Now if the parameters of the slope change detection model are also quantized, one can compare the two reconstructions on a total bits or bits/sample basis. By doing a comparison on the bits/sample basis one has a true indication of the storage savings achieved. A technique may give good data reduction when compared on a number per number basis but may give very little data reduction when compared on a bit per bit basis, because the model parameters may be very sensitive to quantization.

5.1 QUANTIZATION SCHEME

There are two types of quantization schemes used, linear and non-linear. For this analysis only linear quantization schemes were used. By quantizing data, one is attempting to reduce the number of bits needed to represent the set of data points. Figure 29 shows an
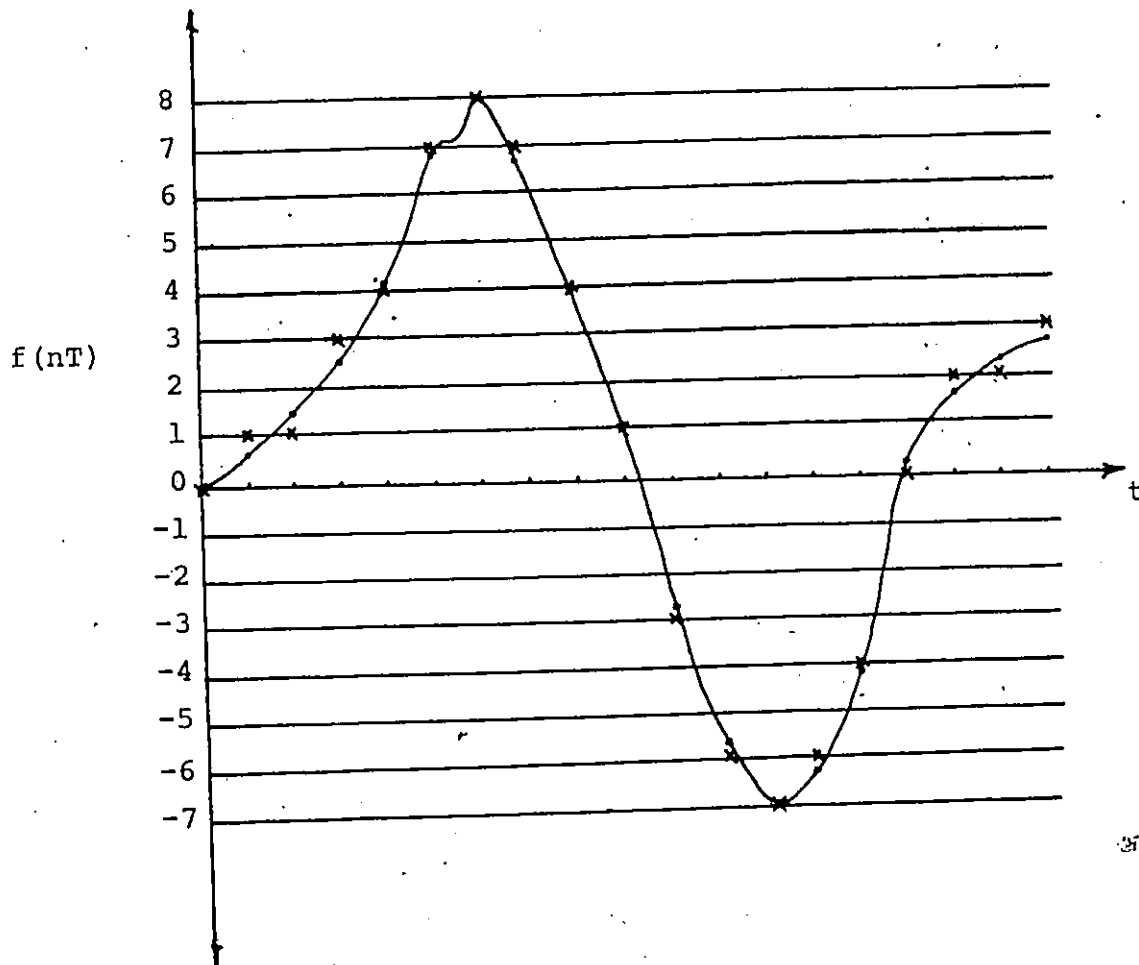
Figure 29. Original sampled waveform along with the quantized version (4 bits).

original sampled waveform along with the set of data points, after the data was quantized to 4 bits. The dots (·) represent the original sample points while the crosses (x) represent the data points after quantization. An N bit quantizer corresponds to 2^N levels, therefore, for a 4 bit quantizer there are $2^4 = 16$ levels. It can be seen, that the accuracy goes up as the number of bits for the quantization routine is increased.

The quantization method used in this analysis was as follows.

Let f_n, $n = 1,2,3,...,N$ sample sequence.

Now,

$$·f_n = \text{integer } (A·f_n + B + 0.5) \text{ , } n = 1,2,3,...,N \quad (5.1)$$

where f_n, $n = 1,2,3,...,N$ are the quantized sample points, and,

$$A = \frac{2^{NB} - 1}{f_{big} - f_{small}}$$

and,

$$B = 2^{NB}/2 - A·f_{big}$$

where NB = no. of quantization bits

f_{big} = largest magnitude of f_n

f_{small} = smallest magnitude of f_n.

Therefore, the largest value in the original same sequence is set equal to 2^{NB-1} while the smallest value is set equal to $-(2^{NB-1} - 1)$. Now the intermediate points are scaled accordingly, and are set equal to the

closest integer value. Therefore, after the scaling is complete, a value like 5.42 becomes simply 5, while a value like 6.77 becomes 7. For non-linear quantizers the levels are non-linearly spaced as opposed to the linear spacing of the levels shown in Figure 29.

5.2 QUANTIZATION OF THE ORIGINAL SAMPLED DATA

Since the A/D convertor used to sample these ECG signals was a 14 bit convertor, all the sample points are represented by 14 bits including the sign bit. Now these original sets of data were quantized to different levels (bits) to see its effect on the visual reproduction, as well as the mean squared error. There was no apparent visual distortion in the quantized data for a 7 bit representation. The 6 bit representation showed some visual distortion in the signal. Figures 30 and 31 show two original signals quantized to 6 bits. A staircasing effect can be observed in these two waveforms. This occurs because all sample values that lie within the same tolerance band of a particular quantizer level will all be set equal to that level value. Therefore, rising portions of the signal like the S-T interval will be represented by a staircase function while relatively constant portions like the T-P interval will be re-constructed as a straight line.

When this data was quantized to 5 bits, it was found that the reconstruction was unacceptable, because
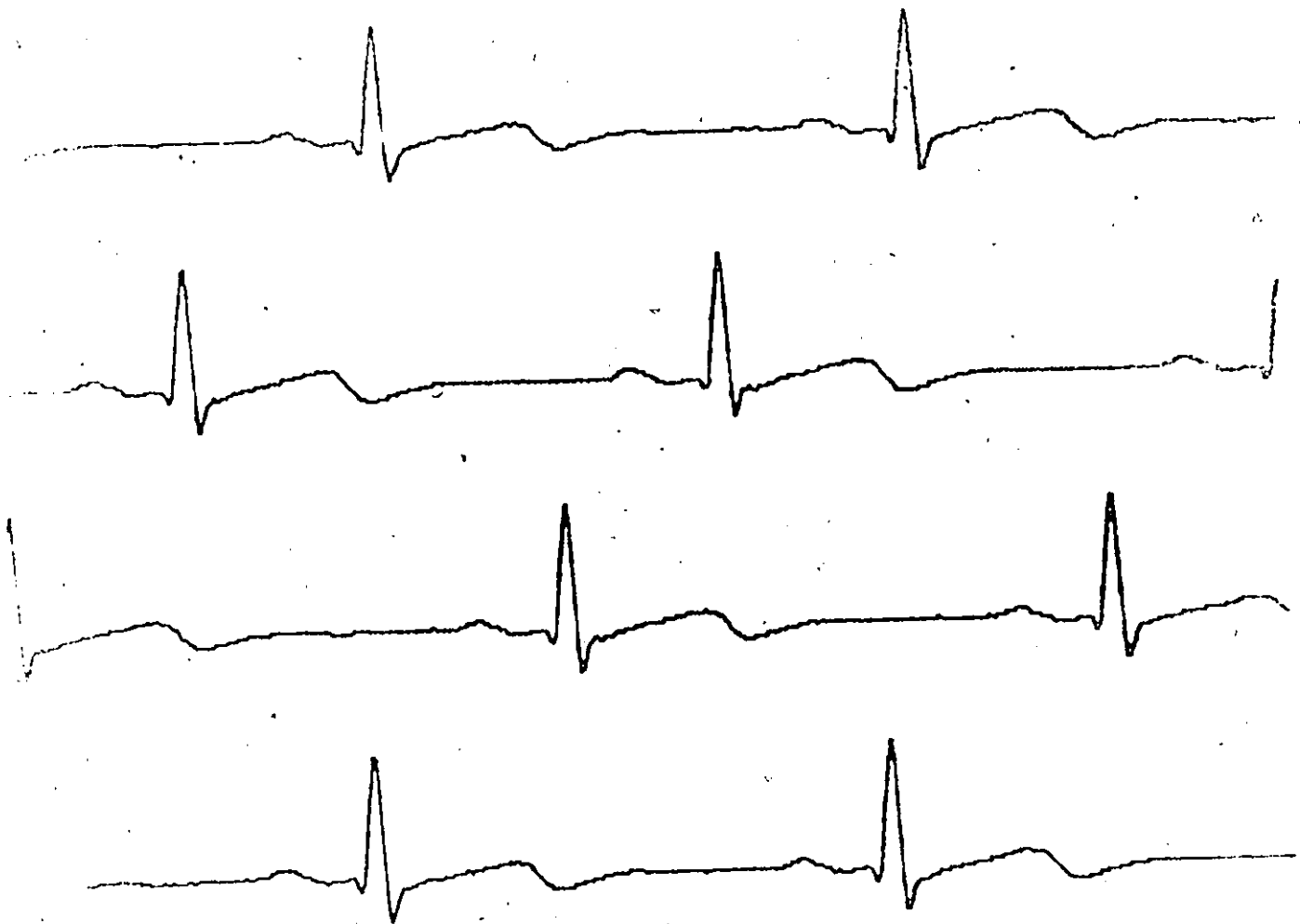
Figure 30. ECG signal (1) quantized to 6 bits.
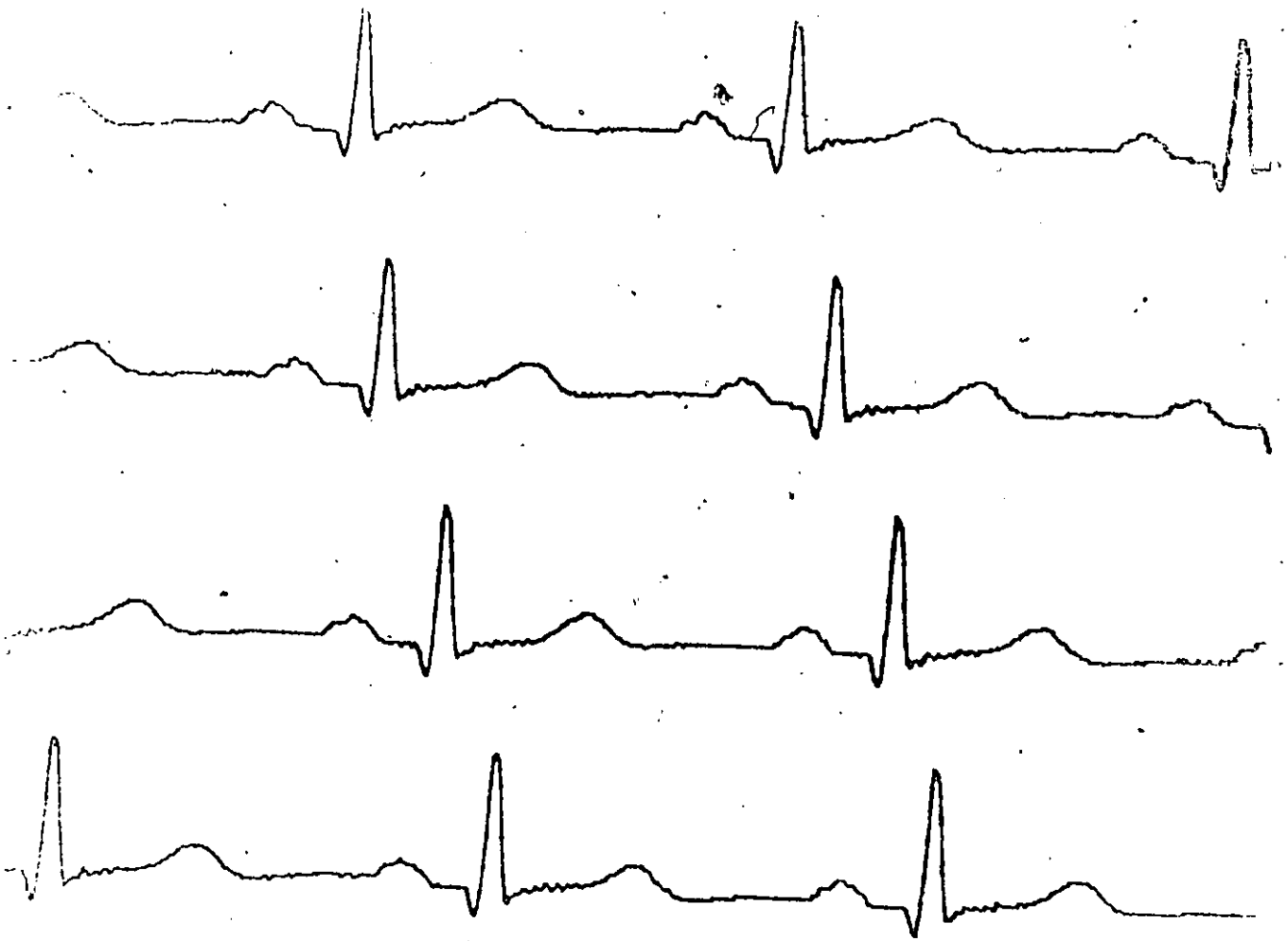
Figure 31. ECG signal (2) quantized to 6 bits.

of the relatively high distortion caused by the quantization noise. The P-wave was distorted so that the detection of the onset and end of the P-wave was impossible.

Therefore, it was decided that the ECG data under investigation could be directly quantized to 6 bits and still give a good representation of the ECG signal. The % MSE was less than 1% for all the data quantized to 6 bits. Therefore, the original sample points could be represented at a bit rate of 6 bits/sample.

5.3   QUANTIZATION OF THE MODEL PARAMETERS

Now the parameters of the slope change detection technique, with prefiltering, were quantized. Now by storing the time differences rather than the actual time values, one can store this time information using 7 bits. These time differences simply represent the number of sample intervals between each stored magnitude. Now the magnitude parameters were quantized to different levels (bits) and the reproductions were checked on a visual and % MSE error basis against the original data. It was found that these magnitude parameters could be quantized to 6 bits without significantly increasing the visual distortion over the unquantized results. Figure 32 shows the % MSE versus bits/sample for the slope change detection technique, (with prefiltering), with the time information represented by 7 bits and the magnitude information quantized to 6 bits. From this curve one

Figure 32. %MSE versus bits/sample for the slope change detection technique, with prefiltering.
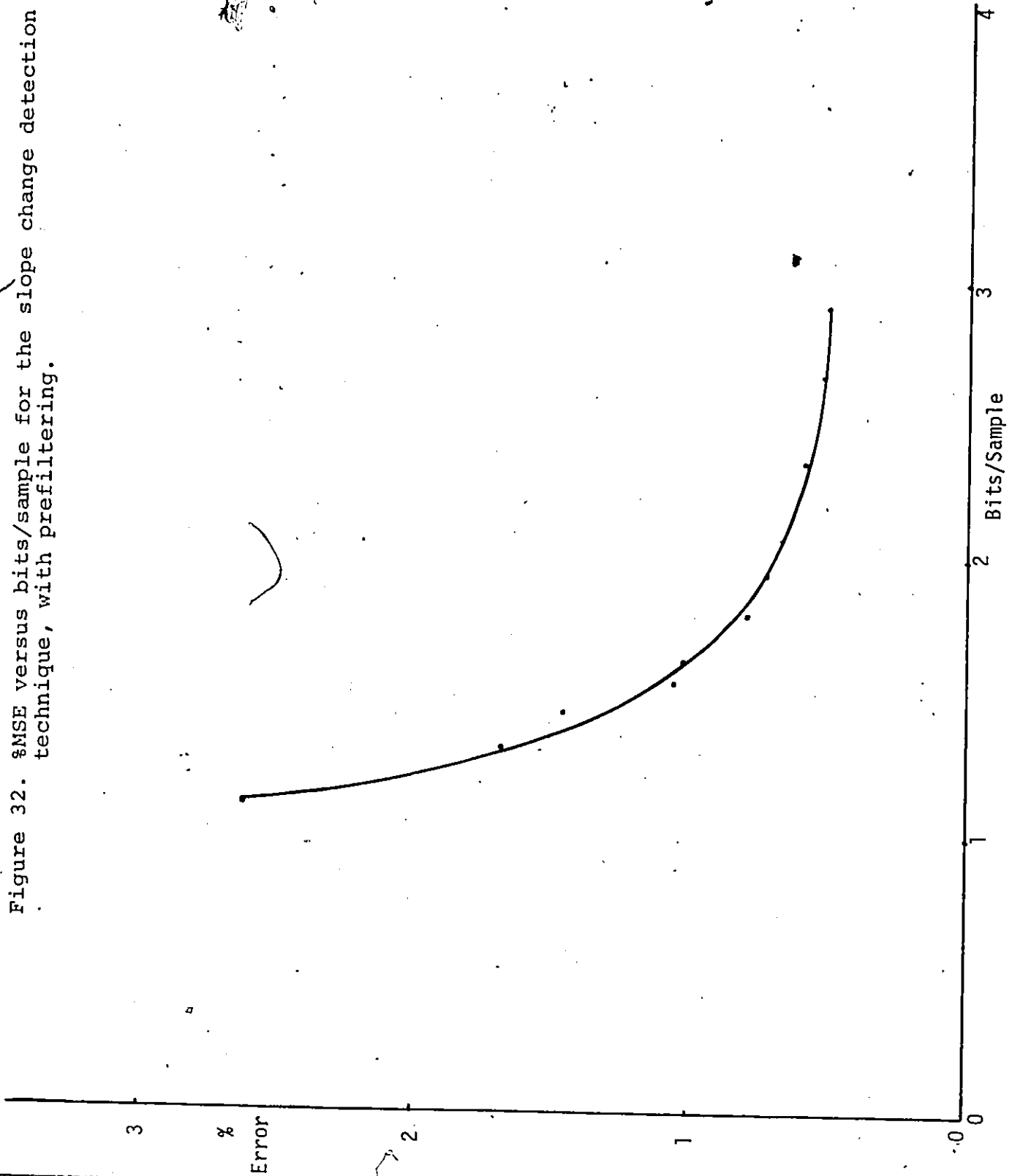
finds that the ECG data can be represented at a bit rate of 2 bits/sample with a % MSE below 1%. This was the case for all the data analyzed in this study. It was also found that the peak error was below 5% for all the 2 bit/ sample reconstructions.

5.4 SIMULATED ECG DATA

Figures 33a,b,c and 34a,b,c show the two original sets of ECG data along with two reconstructed waveforms using the slope change detection technique, applied to prefiltered data. The time information is represented in 7 bits while the magnitude information is quantized to 6 bits. Figure 33b and Figure 34b are the reconstructions with bit rates of approximately 3 bits/sample, therefore, an effective 2:1 reduction in data, while Figure 33c and Figure 34c show the reconstructions for a bit rate of 2 bits/sample, therefore, an effective 3:1 reduction of data. These reconstructions compare very closely to those achieved when the parameters were not quantized.

5.5 DIGITAL IMPLEMENTATION

Figure 35 shows a block diagram of the storage and retrieval procedures for the slope change detection technique, as applied to prefiltered data. First the signal is sampled at a rate of 250 Hz and the energy in the signal is equalized to a standard, so that a general threshold level can be established. The data is then
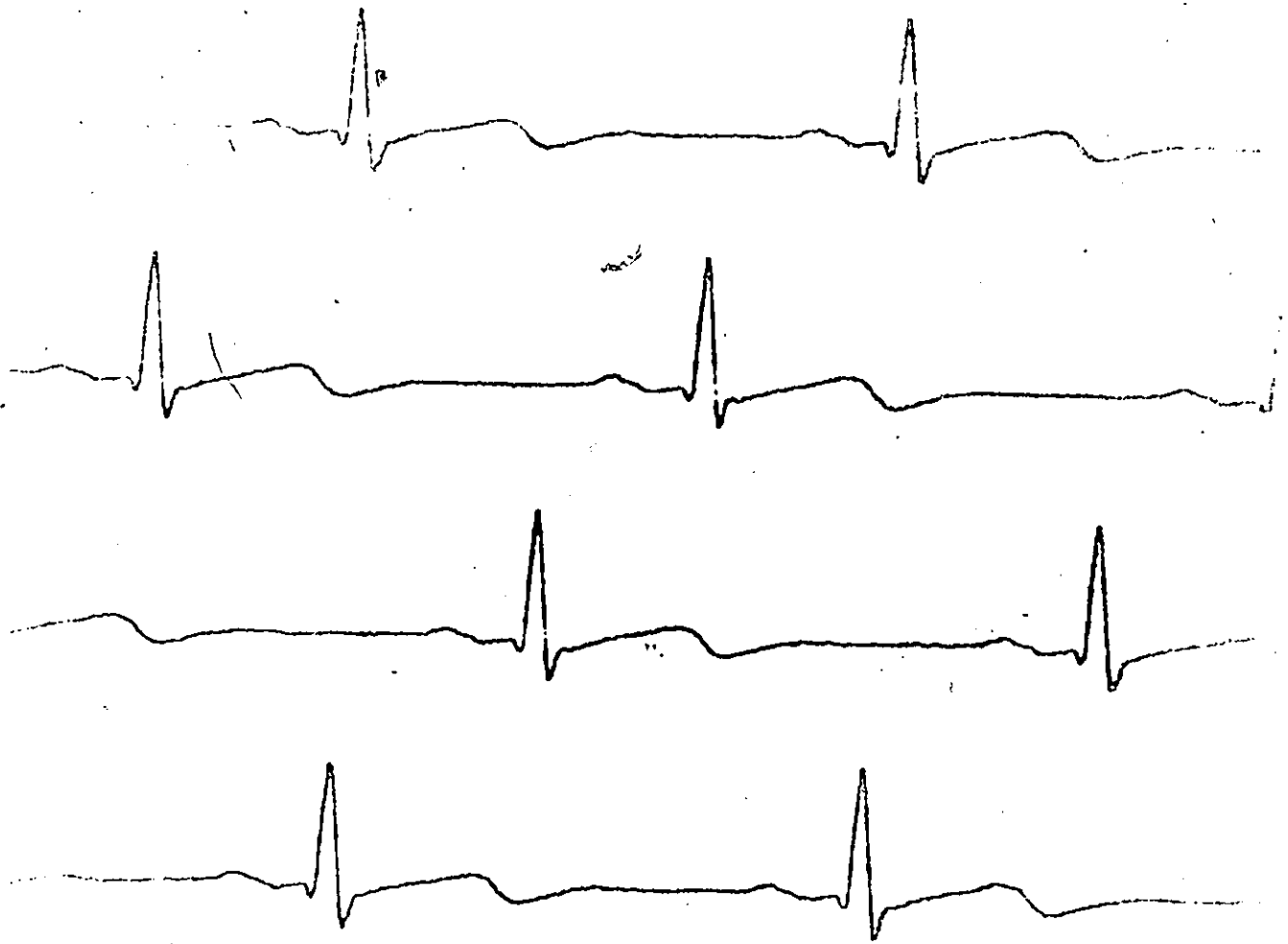
Figure 33a. Original ECG signal (1).
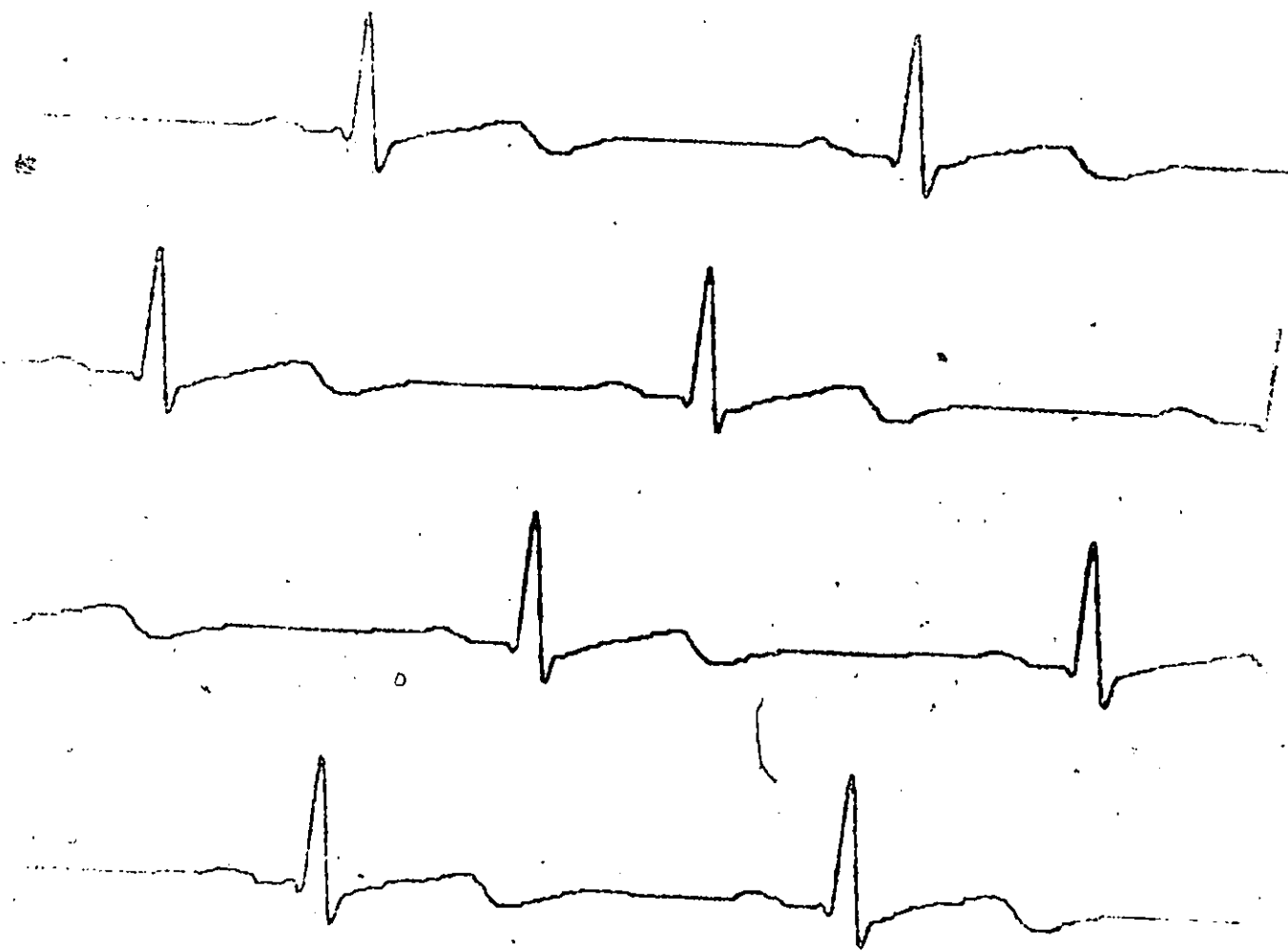
Figure 33b. Reconstruction with 2:1 data reduction (QSCD-P).
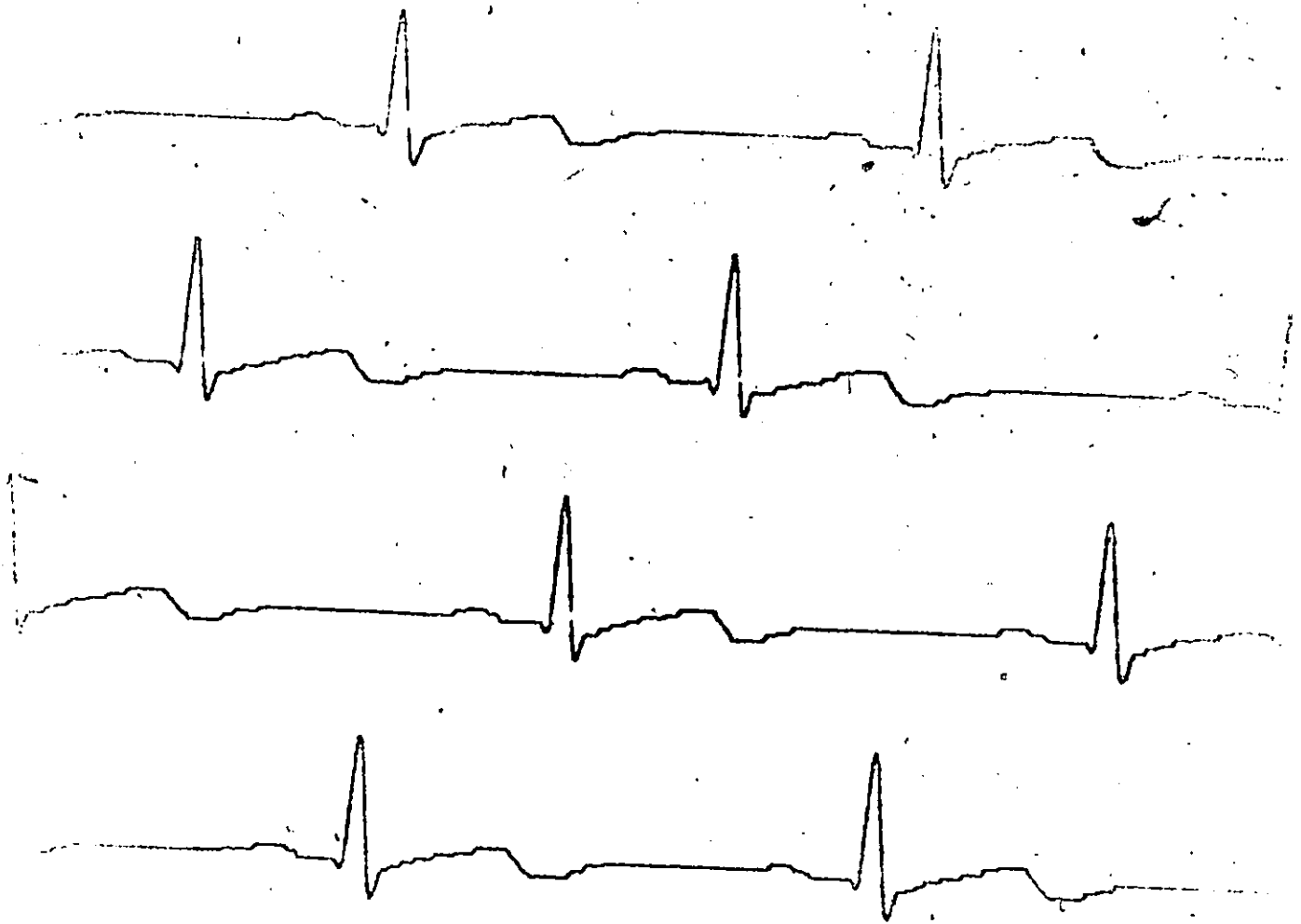
Figure 33c. Reconstruction with 3:1 data reduction (QSCD-P).
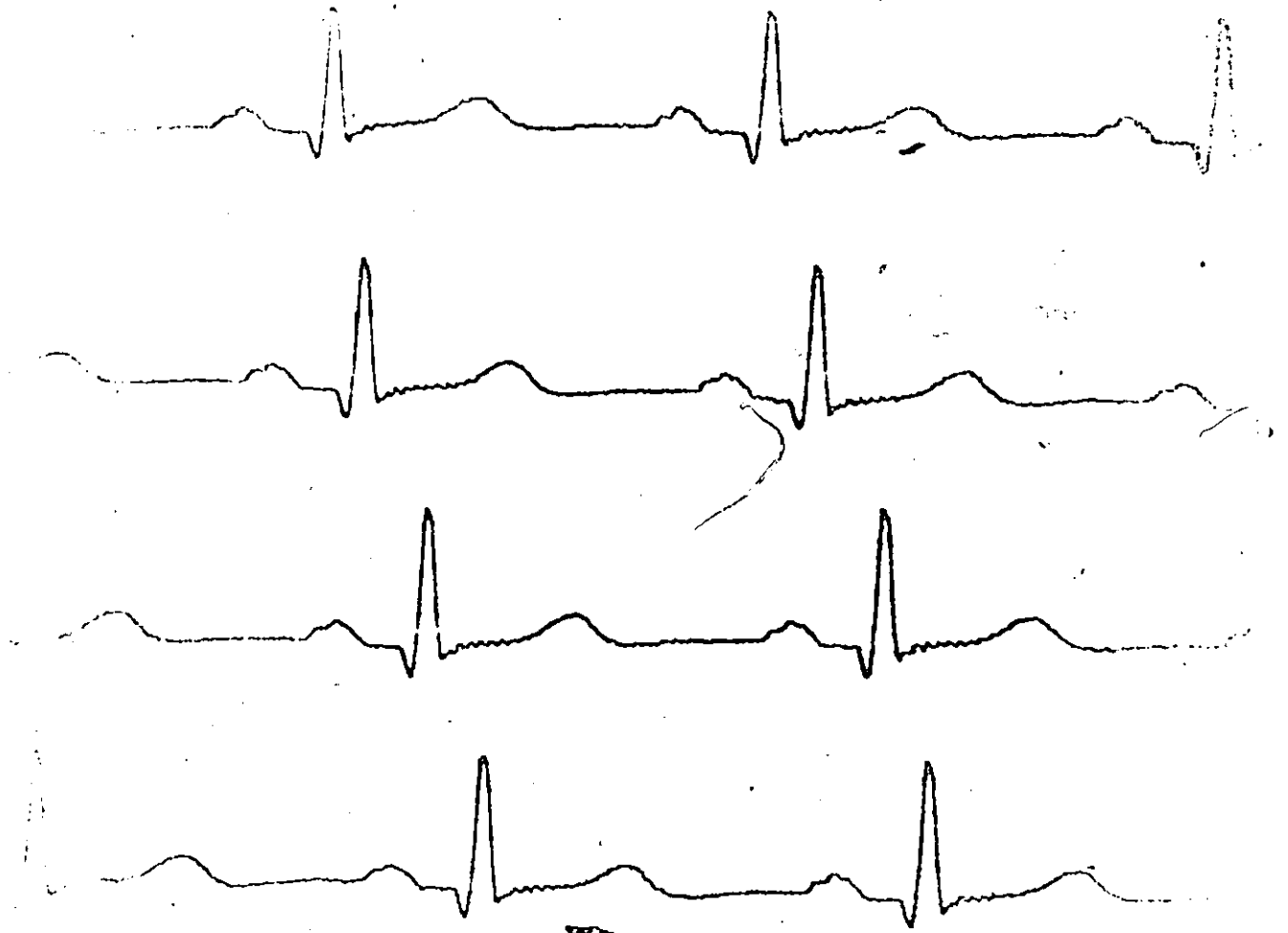
Figure 34a. Original ECG signal (2).
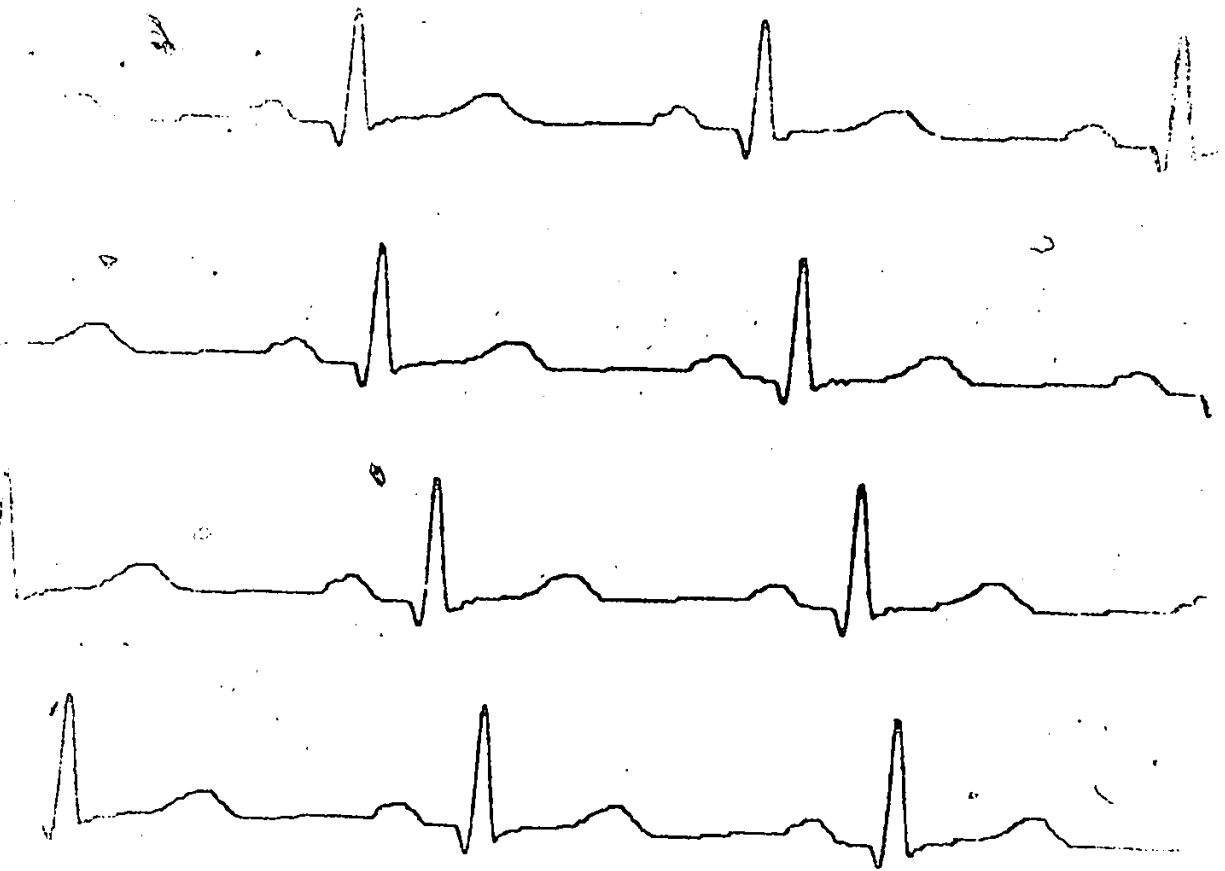
Figure 34b. Reconstruction with 2:1 data reduction (QSCD-P).
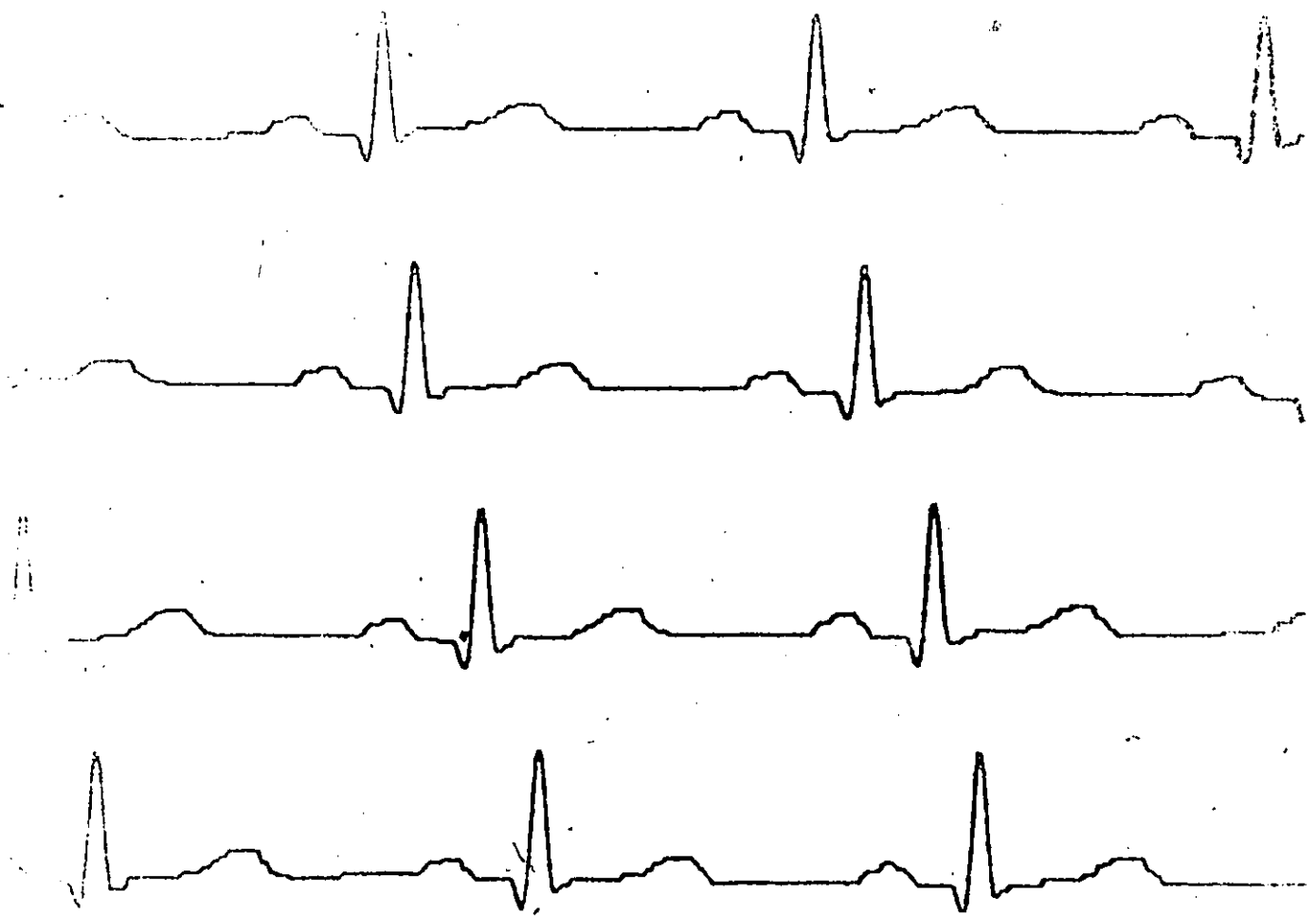
Figure 34c. Reconstruction with 3:1 data reduction (QSCD-P).

DATA STORAGE

DATA RETIEVAL
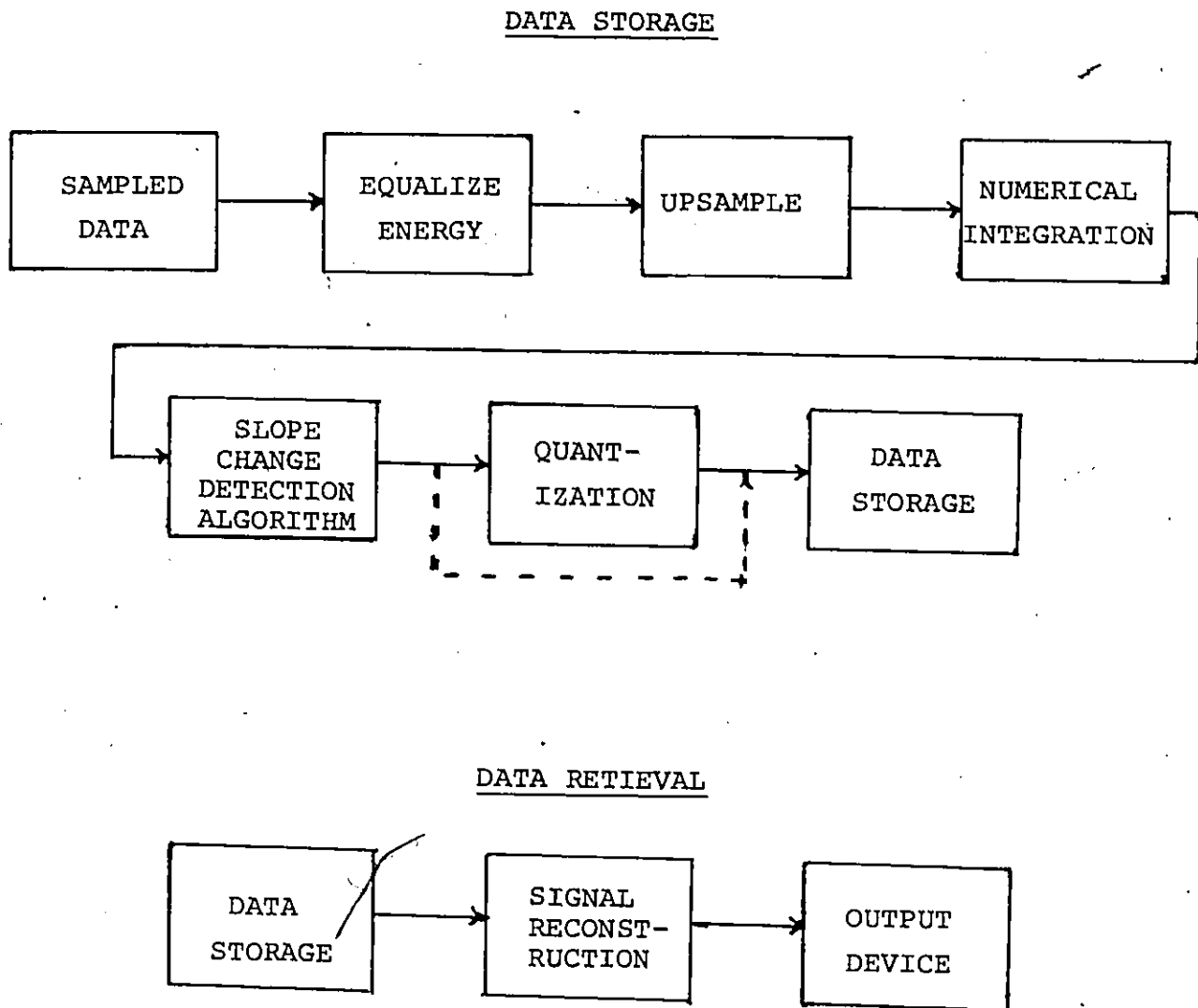
Figure 35. Block diagram of the storage and retrieval of data
using the slope change detection technique, with
prefiltering.

upsampled to 500 Hz so that the number of original and reconstructed samples are equal. Now the three point Simpson integration routine is used to integrate the ECG signal. The upsampling and integration steps could be eliminated if the original analog ECG signal is integrated by analog means before sampling the data. After integration, the slope change detection algorithm is applied to this data and the significant slopes and corresponding time information is picked out. Then the quantized slope information and corresponding time differences are stored.

The signal can now be reconstructed using the quantized slope values and the time difference values. The stored slopes represent points on the reconstructed signal and remain constant over the corresponding time differences. The point at the intersection of two constant slope values is calculated as the average of the two slopes.

5.6 DISCUSSION

It was found that the quantization of the slope change detection model parameters, to 6 bits, did not significantly effect the reproduction fidelity over that of the unquantized reproductions. This can be seen by comparing Figures 33b,c and 34b,c with Figures 26b,c and 27b,c. The % MSE errors and peak errors increased as the model parameters were quantized to fewer and fewer bits,

but for the 6 bit representations the % MSE and peak

errors were maintained below 1% and 5% respectively, for

a 2 bit/sample reconstruction. It was found that

general threshold levels could be established to achieve

different bit rates in the reconstructions. Therefore,

for a set threshold level the number of bits/sample in

the reconstruction will be similar for different sets of

ECG data.

It was felt that the slope change detection model,

as applied to prefiltered data, could be improved if two

ideas were implemented in the algorithm. First, if the

algorithm was modified so that the time difference would

not exceed 64, then the time information could be stored

in 6 bits rather than 7 bits. Therefore, if no slope

information was stored after 64 sample intervals, then

the algorithm would automatically store the value. This

situation would only arise during the T-P interval so

this would mean, on the average, that one extra slope

value and time difference value would be stored during

each ECG cycle. The other improvement would be in the

representation of the QRS complex of the ECG signal. It

was observed in Chapter III that the slope change

detection algorithm, as applied to the original time

signal, gave good reproductions of the QRS portion of the

waveform. Now if the QRS complex could be represented by

constant slopes rather than by constant levels, then this

portion of the signal could be represented more

efficiently. Therefore, by combining both these slope techniques into one algorithm, one should be able to obtain greater reduction of data.

Overall, it is felt that any technique for data reduction should be assessed on the basis of the number of bits/sample needed to represent the original data points. By using this criterion, one has a good indication of the savings in storage achieved by using a particular data reduction technique.

CHAPTER VI

CONCLUSIONS

The main conclusions of this research project are as follows:

1) It has been shown that of the techniques investigated, the slope change detection technique, as applied to prefiltered data yields the best reduction, when compared on a number per number basis.

2) It has been shown, also, that ECG data can be directly quantized to 6 bits for storage in a digital computer. Therefore, any data reduction technique must be able to represent a set of ECG data with a bit rate significantly lower than 6 bits/sample.

3) It was also found that by quantizing the parameters of the slope change detection technique, with prefiltering, one can reconstruct ECG data at a rate of 2 bits/sample, which is essentially a 3:1 reduction in storage. At this bit rate, the % MSE and peak errors are below 1% and 5% respectively.

APPENDIX A

MINNESOTA CODE

FOR ELECTROCARDIOGRAPHIC

CLASSIFICATION

APPENDIX A

MINNESOTA CODE

FOR ELECTROCARDIOGRAPHIC

CLASSIFICATION

The Minnesota Code is a systematic procedure for
coding different ECG waveform classifications. These
categories are based on a calibration of 1 cm deflection
on the ECG tracing corresponding to 1 millivolt. This
Code gives the reader an indication of the complexity
of ECG diagnosis.

Code for Resting Electrocardiograms

Punch	Category	Leads
0	Blank—no electrocardiogram available	
0	No herein reportable electrocardiographic items	
	Q and QS patterns (Q must be 1 mm. or more with associated R of 1 mm. or more)	
1	Class I (any of a through g)	
	a. Q/R=1/3 or more *and* Q duration=0.03 sec. or more	I, II, V_r-V_4
	b. Q duration=0.04 sec. or more	I, II, V_1-V_6
	c. Q duration=0.04 sec. or more *and* R amplitude 3 mm. or more	aV_L
	d. Q duration=0.05 sec. or more *and* a Q wave present in aV_F	III
	e. Q duration=0.05 sec. or more	aV_F
	f. QS pattern when R wave is present in adjacent precordial lead to the right	V_2-V_6
	g. QS pattern	V_1 through V_4 V_1 through V_3 V_1 through V_6
2	Class II (any of a through i)	
	a. Q/R=1/5 to 1/3 *and* Q duration=0.03 sec. or more	I, II, V_r-V_4
	b. Q duration=0.03 to 0.04	

Col.	Punch	Category	Leads
		sec.	I, II, V_r-V_4
		c. Q duration=0.03 to 0.04 sec. *and* R amplitude 3 mm. or more	aV_L
		d. Q duration=0.04 to 0.05 sec. *and* a Q wave present in aV_F	III
		e. Q duration=0.04 to 0.05 sec.	aV_F
		f. Q amplitude=5 mm. or more	III, aV_F
		g. QS pattern and absence of code VII_1	V_1 through V_2
		h. Decreasing absolute R amplitude *and* smallest R=2 mm. or less *and* absence of code III_1 or $VII_{2,3}$	V_1 through V_3, V_4
		i. Q duration=0.04 sec. or more or a QS pattern	(Ancillary leads, see text)
	3	Class III (any of a through c)	
		a. Q/R=1/3 or more *and* Q duration less than 0.03 sec.	I, II, V_r-V_4
		b. QS pattern *and* absence of code VII_1 or III_1	V_1 and V_2
		c. Q/R=1/5 to 1/3 *and* Q duration less than 0.03 sec.	I, II, V_r-V_4
II		*QRS axis deviation*	
	1	Left	
		QRS axis = −30° or greater	I, II, and III
	2	Right	
		QRS axis = +120° or greater	I, II, and III
		(The algebraic sum of major positive and major negative waves must be negative in I, positive in III, and in I must be one half or more of that in III)	
III		*High amplitude R waves*	
	1	Left	
		R more than 26 mm.	V_3, V_4
		R more than 20 mm.	I, II, III, aV_F
		R more than 12 mm.	aV_L
	2	Right	
		QRS duration less than 0.12 sec. *and* R amplitude=5 mm. or more *and* R/S ratio=1.0 or more *and* QRS transition zone or decreasing R/S to left of V_1. (Includes incomplete RBBB which meets above criteria)	V_1
IV		*S-T junction and segment* (Measured from preceding P-R interval at onset of QRS)	
		Depression:	
	1	S-T-J depression 1 mm. or more	I, II, aV_L, aV_F, V_1-V_6
	2	S-T-J depression 0.5-0.9 mm. *and* S-T segment horizontal or downward sloping	I, II, aV_L, aV_F, V_1-V_6
	3	No S-T-J depression as much as 0.5	

Punch	Category	Leads

mm. but S-T segment sloping down
and reaching 0.5 mm. or more below
P-R baseline.......I, II, aV$_L$, aV$_F$, V$_1$-V$_4$
Elevation: (Not routinely applied,
see text)

4   S-T segment elevation of
1.0 mm. or more .I, II, III, aV$_L$, aV$_F$, V$_3$, V$_4$
2.0 mm. or more..................V$_1$-V$_4$

T-wave items

1   T amplitude=minus 5 mm. or
more ....I, II, V$_2$-V$_4$
when R amplitude=5 mm. or more...aV$_L$
when QRS mainly upright..........aV$_F$

2   T amplitude=minus 1 to
5 mm. ....I, II, V$_2$-V$_4$
when R amplitude=5 mm. or more..aV$_L$
when QRS mainly upright..........aV$_F$

3   T wave flat or small diphasic (nega-
tive phase less than 1 mm.)...I, II, V$_3$-V$_4$
when R amplitude=5 mm. or more...aV$_L$
when QRS mainly upright..........aV$_F$

A-V conduction

1   Complete A-V block (permanent or
intermittent) ....any

2   Partial A-V block..................any

3   P-R interval over 0.21 sec. (*any*
heart rate) ....).I, II, III

4   Accelerated conduction ("Wolff-
Parkinson-White") ....any

Ventricular conduction

1   Left bundle-branch block (LBBB):
QRS duration 0.12 sec. or greater
in ....I, II, III
and R peak duration 0.06 sec. or
more in any of........I, II, aV$_L$, V$_5$, V$_6$

2   Complete right bundle-branch block
(RBBB):
QRS duration 0.12 sec. or greater
in ....I, II, III
and R prime greater than R in........V$_1$

3   Incomplete RBBB: R prime greater
than R *and* QRS duration less than
0.12 sec. ....V$_1$
(report under III$_3$ if those criteria
are met)

4   Intraventricular block: QRS 0.12
sec. or more *and* no LBBB or RBBB
pattern ....I, II, III

Arrhythmias

0   Any combination of arrhythmias below
(for punch card purposes)

1   Frequent (4 or more in 40 complexes)
premature atrial, nodal, or ventricular
beats

2   Ventricular tachycardia (over 100/min.)

Col.	Punch	Category	Leads

3   Atrial fibrillation or flutter

4   Supraventricular tachycardia

5   Ventricular (idioventricular) rhythm (up
to 100/min.)

6   A-V nodal rhythm (up to 100/min.)

7   Sinus tachycardia (over 100/min.)

8   Sinus bradycardia (under 50/min.)

9   Arrhythmias not mentioned above

IX   *Miscellaneous*

0   Combinations below of item 2 or 3 with
item 1, 2, 3, 4, 5, or 6 (for punch card
purposes)

1   Low QRS amplitude (in I, II, III no
positive or negative deflection over 5 mm.
or maximum QRS amplitude less than 10
mm. in V$_1$-V$_6$)

2   "Qualitative" T-wave findings including
"high" or peaked T, postextrasystolic T-
wave inversion, T notching, etc.

3   QRS findings not mentioned above includ-
ing notching, slurring, RR prime, rotation,
or others

4   Prolonged Q-T interval (evaluated from
kQT)

5   P wave findings including peaked, nega-
tive, 3 mm. amplitude or over, or others

6   Negative U wave in V$_2$-V$_4$

7   Other items not mentioned above

8   Questionable category due to technical im-
perfections in record or beat-to-beat varia-
bility of measurement

9   Combinations above of item 7 or 8 with
item 1, 2, 3, 4, 5, or 6 (for punch card
purposes)

Code for Postexercise Records

Col.	Punch	Category

X   *Exercise test*

1   No exercise test made

2   Exercise test stopped

3   Exercise test completed

XI   *S-T items postexercise*

1   Change from *no* coded S-T item at rest to
S-T item type IV, 1 postexercise

2   Change from *no* coded S-T item at rest to
S-T item type IV, 2 postexercise

3   Change from *no* coded S-T item at rest to
S-T item type IV, 3 postexercise

4   Change from one coded S-T item at rest
to a lower numerical S-T item postexercise
(IV, 3 to type IV, 1, etc.)

5   Change from one coded S-T item at rest
to a higher numerical item postexercise
(IV, 1 to type IV, 3, etc.)

6   No change from resting coded S-T item

7   Change from *any* coded S-T item at rest

Col. Punch   Category

         to *no* reportable S-T item postexercise

   8   Questionable S-T depression postexercise due to technical considerations

XII   *T items postexercise*

   1   Change from *no* coded T item at rest to T item type V, 1 postexercise

   2   Change from *no* coded T item at rest to T item type V, 2 postexercise

   3   Change from *no* coded T item at rest to T item type V, 3 postexercise

   4   Change from one coded T item at rest to a lower numerical T item postexercise (V, 3 to type V, 2, etc.)

   5   Change from one coded T item at rest to a higher numerical T item postexercise (V, 2 to type V, 3, etc.)

   6   No change from resting coded T item

   7   Change from *any* coded T item at rest to *no* reportable T item postexercise

   8   Questionable T item postexercise due to technical considerations

XIII   *A-V conduction, postexercise*

   1   Change from *no* coded A-V conduction item at rest to complete A-V block postexercise

   2   Change from *no* coded A-V conduction item at rest to partial A-V block postexercise

   3   Change from *no* coded A-V conduction item at rest to P-R interval more than 0.21 sec. postexercise

   4   Change from *no* coded A-V conduction item at rest to accelerated conduction

   5   Change from one coded A-V conduction item at rest (VI, 1-4) to another A-V conduction item postexercise

   6   No change from resting coded A-V conduction item

   7   Change from *any* A-V conduction item at rest to *no* A-V conduction item postexercise

XIV   *Ventricular conduction, postexercise*

   1   Change from *no* coded ventricular conduction item at rest to left bundle-branch block (LBBB)

   2   Change from *no* coded ventricular conduction item at rest to complete right bundle-branch block (RBBB)

   3   Change from *no* coded ventricular conduction item at rest to incomplete right bundle-branch block

   4   Change from *no* coded ventricular conduction item at rest to intraventricular block

   5   Change from one coded ventricular conduction item at rest (VII, 1-4) to another

Col. Punch   Category

         ventricular conduction item postexercise

   6   No change from resting coded ventricular conduction item

   7   Change from *any* ventricular conduction item at rest (VII, 1-4) to *no* ventricular conduction item postexercise

XV   *Arrhythmias, postexercise*

     (exclude VIII, 7-8, sinus tachycardia and bradycardia)

   1   Change from *no* coded arrhythmia at rest to *any* reportable arrhythmia postexercise

   2   Change from one coded arrhythmia at rest to another arrhythmia postexercise

   3   No change from coded resting arrhythmia

   4   Change from *any* arrhythmia at rest to *no* arrhythmia postexercise

XVI   *Miscellaneous, postexercise*

   1   Change postexercise to any item not mentioned above

Code for Serial Electrocardiograms

Serial electrocardiograms will rarely be available in ordinary cross-sectional surveys but their utilization in longitudinal studies must be considered. Major serial changes will be apparent by comparing the classification according to the present system from the same persons on different occasions. In order to note the findings in such serial comparisons, it is suggested to add another category, and column, for the punch code, as follows:

XVII   *Serial changes, general*

   1   Change from item I, 0 to *any* reportable item I-XVI

   2   Change in *any* reportable item I-XVI

   3   No change in coded item

   4   Change from *any* item I-XVI to *no* reportable item

   5   No serial comparison available

XVIII   *Q and QS items, serial changes*

   1   Change from one coded Q and QS item to a lower numerical Q and QS item (I, 3 to I, 2, etc.)

   2   Change from one coded Q and QS item to a higher numerical Q and QS item (I, 1 to I, 2, etc.)

   3   No change in coded Q and QS item

   4   Change from *no* coded Q and QS item to Q and QS item I, 1

   5   Change from *no* coded Q and QS item to Q and QS item I, 2

   6   Change from *no* coded Q and QS item to Q and QS item I, 3

   7   Change from *any* coded Q and QS item to *no* reportable Q and QS item

Col. Punch   Category

XIX   *S-T items, serial changes*

1 Change from one coded S-T item to a lower numerical S-T item (IV, 3 to IV, 1, XI, 3 to XI, 1, etc.)

2 Change from one coded S-T item to a higher numerical S-T item (IV, 1 to IV, 2, XI, 2 to XI, 3, etc.)

3 No change in coded S-T item

4 Change from *no* coded S-T item to S-T item type IV, 1, rest or postexercise

5 Change from *no* coded S-T item to S-T item type IV, 2, rest or postexercise

6 Change from *no* coded S-T item to S-T item type IV, 3, rest or postexercise

7 Change from *any* coded S-T item to *no* reportable S-T item

XX   *T items, serial changes*

1 Change from one coded T item to a lower numerical T item (V, 3 to V, 1, XII, 3 to XII, 1, etc.)

2 Change from one coded T item to a higher numerical T item (V, 2 to V, 3, XII, 2 to XII, 3, etc.)

3 No change in coded T item

4 Change from *no* coded T item to T item type V, 1, rest or postexercise

5 Change from *no* coded T item to T item type V, 2, rest or postexercise

6 Change from *no* coded T item to T item type V, 3, rest or postexercise

7 Change from *any* coded T item to *no* reportable T item

XXI   *Blocks, serial changes*

1 Change from *no* coded A-V block to *any* A-V block (VI, 1-4)

2 Change from *any* coded A-V block to *no* A-V block

3 No change in A-V block

4 Change from *no* coded ventricular conduction defect to *any* ventricular conduction defect (VII, 1-4)

5 Change from *any* coded ventricular conduction defect to *no* ventricular conduction defect

6 No change in ventricular conduction defect

XXII   *Arrhythmias, serial changes*
(exclude VIII, 7-8, sinus tachycardia and bradycardia)

1 Change from one coded arrhythmia to another (VII, 1-6)

2 Change from *no* coded arrhythmia to *any* reportable arrhythmia

3 No change in coded arrhythmia

4 Change from *any* coded arrhythmia to *no* reportable arrhythmia

APPENDIX B

COMPUTER PROGRAMS USED FOR

THE SLOPE CHANGE DETECTION TECHNIQUE

AS APPLIED TO PREFILTERED DATA

126

APPENDIX B

COMPUTER PROGRAMS USED FOR

THE SLOPE CHANGE DETECTION TECHNIQUE

AS APPLIED TO PREFILTERED DATA

This section contains all the programs used for the storage and retrieval of ECG data, using the slope change detection technique, as applied to prefiltered data.

127

```
       DIMENSION NAME(5),X(2048),Y(2048)
       ACCEPT "NO.  OF SAMPLES= ",N
1      FORMAT(5A2)
       TYPE "ORIGINAL FILENAME"
       READ(11,1)(NAME(I),I=1,N)
       OPEN 0,NAME
       READ(0)(Y(I),I=1,N)
       CLOSE 0
       OPEN 1,"NOTCHMS1
       READ(1)(X(I),I=1,N)
       CLOSE 1
       XENER=0.0
       YENER=0.0
       XSUM=0.0
       YSUM=0.0
       DO 2 I=1,N
       XSUM=XSUM+X(I)
       YSUM=YSUM+Y(I)
2      CONTINUE
       XSUM=XSUM/FLOAT(N)
       YSUM=YSUM/FLOAT(N)
       DO 3 I=1,N
       X(I)=X(I)-XSUM
       Y(I)=Y(I)-YSUM
3      CONTINUE
       DO 4 I=1,N
       XENER=XENER+X(I)**2
       YENER=YENER+Y(I)**2
4      CONTINUE
       RAT1=SQRT(YENER/XENER)
       DO 5 I=1,N
       Y(I)=RAT2*Y(I)
5      CONTINUE
       OPEN 3,"ORG"
       WRITE(3)(Y(I),I=1,N)
       CLOSE 3
       STOP
       END
```

```
      DIMENSION X(2048), Y(4096), NAME(5)
      ACCEPT "NO. OF INPUT SAMPLES=", N
      TYPE "INPUT FILENAME"
      READ(11, 1)(NAME(I), I=1, 5)
1     FORMAT(5A2)
      OPEN 0, NAME
      READ(0)(X(I), I=1, N)
      CLOSE 0
      TYPE "OUTPUT FILENAME"
      READ(11, 1)(NAME(I), I=1, 5)
      OPEN 1, NAME
      NN=N-1
      DO 2 I=1, NN
      Y(2*I-1)=X(I)
2     Y(2*I)=(X(I)+X(I+1))/2. 0
      Y(2*N-1)=X(N)
      NNN=2*N-1
      WRITE(1)(Y(I), I=1, NNN)
      CLOSE 1
      STOP
      END
```

```
      DIMENSION NAME(5), X(4096), Y(2048)
      ACCEPT "NO. OF INPUT SAMPLES= ", N
      TYPE "INPUT FILENAME"
      READ(11, 1)(NAME(I), I=1, 5)
1     FORMAT(5A2)
      OPEN 1, NAME
      READ(1)(X(I), I=1, N)
      TYPE "OUTPUT FILENAME"
      READ(11, 1)(NAME(I), I=1, 5)
      OPEN 0, NAME
      CLOSE 1
      Y(1)=0. 0
      XX=X(1)
      NN=(N-1)/2
      NNN=NN+1
      DO 2 I=1, NN
      YY=(XX+4*X(2*I)+X(2*I+1))/3.
      IF(I. EQ. 1)GO TO 3
      Y(I+1)=YY+Y(I)
      GO TO 4
3     Y(I+1)=YY
4     XX=X(2*I+1)
2     CONTINUE
      WRITE(0)(Y(J), J=1, NNN)
      CLOSE 0
      STOP
      END
```

```
      DIMENSION SLOP1(2),NAME(5),Y(2048),X(2048),IT(2048)
        DIMENSION XTRA(2048)
        ACCEPT "ERROR LIMIT   ",E
        ACCEPT "NO.  OF SAMPLE POINTS",NN
        TYPE "INPUT FILENAME"
        READ(11,11)(NAME(I),I=1,5)
11      FORMAT(5A2)
        OPEN 1,NAME
        READ(1)(Y(I),I=1,NN)
        CLOSE 1
        I=1
        ITI=0
        J=1
        X(1)=Y(1)
        IT(1)=0
        Y1=Y(I)
        GO TO 2
1       CONTINUE
        J=J+1
        IT(J)=ITI-1
        X(J)=Y(I-1)
        ITI=IT(J)
        I=I-1
        Y1=Y(I)
2       CONTINUE
        I=I+1
        ITI=ITI+1
        Y2=Y(I)
        SLOP1(1)=(Y2-Y1)
        DO 3 N=1,NN
        IF(I.GE.NN)GO TO 10
        I=I+1
        ITI=ITI+1
        Y1=Y2
        Y2=Y(I)
        SLOP1(2)=Y2-Y1
        IF(N.GE.NN)GO TO 10
        IF(ABS(SLOP1(1)-SLOP1(2)).GE.E)GO TO 1
3       CONTINUE
        GO TO 4
10      J=J+1
        IT(J)=ITI
        X(J)=Y(I)
4       CONTINUE
        WRITE(10,77)J
77      FORMAT('  ',2X,I5)
        JJ=(J+5)/6
        JJJ=JJ*6
        IF(JJJ.EQ.J)GO TO 58
        JT=J+1
```

```
         DO 57 I=JT,JJJ
         X(I)=0.0
57       CONTINUE
58       CONTINUE
         DO 59 I=1,JJ
         JK=6*(I-1)
         WRITE(10,60)JK,(X(K+JK),K=1,6)
60       FORMAT(I5,6(1X,F10.1))
59       CONTINUE
         NT1=0
         ACCEPT "IF QUANTIZATION DESIRED, TYPE 1, IF NOT TYPE 0",IQ
         IF(IQ.EQ.0)GOTO300
         ACCEPT "NO. OF BITS  ",NB
         CALL TUANT(X,J,NB)
300      CONTINUE
         BIG=0.0
         IBIG=0
         DO 20 I=2,J
         SLOP=(X(I)-X(I-1))/(IT(I)-IT(I-1))
         IF(IQ.EQ.0)GO TO 304
         IF(BIG.LE.X(I)-X(I-1))BIG=X(I)-X(I-1)
304      CONTINUE
         IF(IBIG.LE.ABS(IT(I)-IT(I-1)))IBIG=IT(I)-IT(I-1)
         NT=IT(I)-IT(I-1)+.5
         XTRA(1+NT1)=X(I-1)
         IF(NT.EQ.1)GOTO20
         DO 21 K=2,NT
21       XTRA(NT1+K)=X(I-1)+SLOP*(K-1.)
20       NT1=NT1+NT
         WRITE(10,302)IBIG
302      FORMAT(' ',2X,'MAXIMUM DIFFERENCE=',I3)
         IF(IQ.EQ.0)GO TO 305
         WRITE(10,303)BIG
303      FORMAT(' ',2X,'MAXIMUM DIFFERENCE DATA=',F5.1)
305      CONTINUE
         XTRA(NT1+1)=X(J)
         DO 7 I=2,J
         Y(I-1)=(X(I)-X(I-1))/(IT(I)-IT(I-1))
         JT=IT(I)-IT(I-1)
7        IT(I-1)=JT
         JI=J-1
         OPEN 2,'SLP'
         OPEN 3,'IDT'
         WRITE(2)(Y(I),I=1,JI)
         WRITE(3)(IT(I),I=1,JI)
         CLOSE 2
         CLOSE 3
         NN=NT1+1
         OPEN 1,'MSLOPE'
         WRITE(1)(XTRA(J),J=1,NN)
         CLOSE 1
         STOP
         END
```

```
      DIMENSION NAME(5), X(2048), IT(2048), XX(2048)
      ACCEPT "NO. OF STORED SLOPES = ", N
      OPEN 0, 'SLP'
      READ(0)(X(I), I=1, N)
      CLOSE 0
      OPEN 0, 'IDT'
      READ(0)(IT(I), I=1, N)
      CLOSE 0
      ACCEPT "NO. OF RECONSTRUCTED POINTS= ", NN
      ACCEPT "DO YOU WISH TO QUANTIZE? YES-1 NO-0 ", NQ
      IF(NQ. EQ. 0)GO TO 200
      ACCEPT "NO. OF BITS=", NB
      CALL TUANT(X, N, NB)
200   CONTINUE
      BIG=0. 0
      DO 6 I=2, N
6     IF(BIG. LE. ABS(X(I)-X(I-1)))BIG=ABS(X(I)-X(I-1))
      WRITE(10, 7)BIG
7     FORMAT(' ', 2X, 'MAXIMUM DIFFERENCE= ', F7. 1)
15    CONTINUE
      XX(1)=X(1)
      K=1
      DO 4 J=1, N
      Y=X(J)
      IIT=IT(J)-1
      IF(IIT. EQ. 0)GO TO 8
      DO 5 I=1, IIT
5     XX(K+I)=Y
8     IF(J. EQ. N)GO TO 11
      K=K+IIT+1
      XX(K)=(X(J)+X(J+1))/2. 0
4     CONTINUE
11    CONTINUE
      XX(NN)=X(N)
      OPEN 0, 'RCNT'
      WRITE(0)(XX(I), I=1, NN)
      CLOSE 0
      STOP
      END
```

```
      SUBROUTINE TURNT(X,N,NB)
      DIMENSION X(N)
      NL=2**NB
      BIG=X(1)
      SMALL=X(1)
      DO 2 J=1,N
      IF(SMALL. GT. X(J))SMALL=X(J)
      IF(BIG. LT. X(J))BIG=X(J)
2     CONTINUE
      A=(FLOAT(NL)-1. 0)/(BIG-SMALL)
      B=FLOAT(NL/2)-(A*BIG)
      DO 3 J=1,N
      IY=A*X(J)+B+. 5
      X(J)=IY
3     CONTINUE
      RETURN
      END
```

APPENDIX C

BITS/SAMPLE CRITERION

BITS/SAMPLE CRITERION

Let NP equal the total number of parameters needed to reconstruct N sample data points. NBP will equal the total number of bits needed to represent each parameter, while NBO equals the total number of bits needed to represent the original sample points. Therefore,

NTD = N · NBO

NTP = NP · NBT

where NTO represents the total number of bits needed to represent the data in its original sample form while NTP is the total number of bits needed to represent the N data points using the parametric representation. Therefore,

NBO = the number of bits/sample for the

original sample points

NTP/N = the number of bits/sample for the parametric representation

By comparing NTP/N and NBO one can come up with the effective reduction in storage.

REFERENCES

1. Zywietz, Chr, and Schneider, B., "Computer Application on ECG and VCG Analysis", American Elsevier, New York, 1973.

2. Andrews, C.A., Davies, J.M., and Schwarz, G.R., "Adaptive Data Compression", Proceedings of the IEEE, Vol. 55, No. 3, P.P. 267-277, March 1967.

3. Cox, J.R., Nolle, F.M., and Arthur, R.M., "Digital Analysis of the Electroencephalogram, The Blood Pressure Wave, and the Electrocardiogram", Proceedings of the IEEE, Vol. 60, No. 10, P.P. 1137-1164, October 1972.

4. Cornfield, J., Dunn, R.A., Barchlor, C.D., and Pipberger, H.V., "Multiground Diagnosis of Electrocardiograms", Computers and Biomedical Research, Vol. 6, No. 1, P.P. 97-120, February 1973.

5. Burton, C.E., Portnoy, W.M., and Dirilten, H., "An Algorithm for On-Line, Real-Time Computer Detection of ECG Changes", International Journal of Bio-Medical Computing, Vol. 6, No. 1, P.P. 23-32, January 1975.

6. Ahmed, N., Milne, P.J., and Harris, S.G., "Electro-cardiographic Data Compression Via Orthogonal Transforms", IEEE Transaction on Biomedical Engineering, Vol. BME 22, No. 6, P.P. 484-487, November 1975.

7. Young, T.Y., and Huggins, W.H., "On the Representation of Electrocardiograms", IEEE Transaction on Biomedical Electronics, P.O. 86-95, July 1963.

8. Kortman, C.M., "Redundancy Reduction - A Practical Method of Data Compression", Proceedings of the IEEE, Vol. 55, No. 3, P.P. 253-263, March 1967.

9. Swenne, C.A., Van Bemmel, J.H., Hengeveld, S.J., and Hermans, M., "Pattern Recognition for ECG - Monitoring: An Interactive Method for the Classification of Ventricular Complexes", Computers in Biomedical Research, Vol. 5, P.P. 150-160, 1973.

10. Golden, D.P., Wolthuis, R.A. and Hoffler, G.W., "A Spectral Analysis of the Normal Resting Electrocardiogram", IEEE Transaction on Biomedical Engineering, Vol. BME-20, No. 5, P.P. 366-371, September 1973.

11. Pipberger, H.V., "Recommendations for Standardization of Instruments in Electrocardiograph and Vectorcardiography", IEEE Transaction on Bio-Medical Engineering, Vol. BME-14, No. 1, P.P. 60-68, January 1967.

12. Robinson, E.A., "Statistical Communication and Detection with Special Reference to Digital Data Processing of Radar and Seismic Signals", Hafner Publishing, New York, P.P. 274-279, 1967.

13. Cirjanic, B., "Synthesis and Coding of Voice Signals", Dissertation, University of Windsor, 1973.

14. Bergland, G.D., "A Guided Tour of the Fast Fourier Transform", IEEE Spectrum, P.P. 41-52, July 1969.

15. Wartak, Josef, "Computers in Electrocardiography", Charles C. Thomas, Springfield, Illinois, 1970.

16. Golden, B., and Radar, C.M., "Digital Processing of Signals", McGraw Hill Book Co., New York, 1969.

17. Berne, R.M., and Levy, M.N., "Cardiovascular Physiology", C.V. Mosby W., St. Louis, 1967.

18. Hambley, A.R., Moruzzi, R.L., and Feldman, C.L., "The Use of Intrinsic Components in a ECG Filter", IEEE Transaction on Biomedical Engineering, Vol. BME-21, No. 6, November 1974.

19. McFee, R., and Baule, G.M., "Research in Electrocardiography and Magnetocardiography", Proceedings of the IEEE, Vol. 60, No. 3, March 1972.

VITA AUCTORIS

1950   Born on June 27, in Windsor, Ontario.

1970   Completed secondary education at Vincent Massey,
       Windsor, Ontario.

1972   Graduated from St. Clair College, Windsor, Ontario,
       with a diploma in Electrical Technology.

1974   Graduated from The University of Windsor, with the
       degree of B.A.Sc. in Electrical Engineering.

1976   Candidate for the degree of M.A.Sc. in Electrical
       Engineering at The University of Windsor.